VIBRATION ANALYSIS OF CRACKED ALUMINIUM PLATES

by

Asif Israr

THESIS SUBMITTED IN FULFILLMENT OF THE REQUIRMENTS
FOR THE DEGREE OF DOCTOR IN PHILOSOPHY
TO THE FACULTY OF ENGINEERING
DEPARTMENT OF MECHANICAL ENGINEERING
UNIVERSITY OF GLASGOW

June 2008

This thesis is produced under the accordance of British Standards BS 4821:1990

Dedication

To my parents and my family

AUTHOR'S DECLARATION

ABSTRACT

This research is concerned with analytical modelling of the effects of cracks in structural plates and panels within aerospace systems such as aeroplane fuselage, wing, and tail-plane structures, and, as such, is part of a larger body of research into damage detection methodologies in such systems. This study is based on generating a so-called reduced order analytical model of the behaviour of the plate panel, within which a crack with some arbitrary characteristics is present, and which is subjected to a force that causes it to vibrate. In practice such a scenario is potentially extremely dangerous as it can lead to failure, with obvious consequences. The equation that is obtained is in the form of the classical Duffing equation, in this case, the coefficients within the equation contain information about the geometrical and mass properties of the plate, the loading and boundary conditions, and the geometry, location, and potentially the orientation of the crack. This equation has been known for just over a century and has in the last few decades received very considerable attention from both the analytical dynamics community and also from the dynamical systems researchers, in particular the work of Ueda, Thompson, in the 1970s and 1980s, and Thomsen in the 1990s and beyond. An approximate analytical solution is obtained by means of the perturbation method of multiple scales. This powerful method was popularized in the 1970s by Ali H.Nayfeh, and discussed in his famous books, '*Perturbation Methods*' (1974) and '*Nonlinear Oscillations*' (1979, with D.T.Mook), and also by J.Murdock (1990), and M.P.Cartmell *et al*. (2003) and has been shown to be immensely useful for a wide range of nonlinear vibration problems. In this work it is shown that different boundary conditions can be admitted for the plate and that the modal natural frequencies are sensitive to the crack geometry. Bifurcatory behaviour of the cracked plate has then been examined numerically, for a range of parameters. The model has been tested against experimental work and against a Finite Element model, with good corroboration from both. In all events, this is a significant new result in the field and one that if implemented within a larger damage detection strategy, could be of considerable practical use.

ACKNOWLEDGEMENTS

I would like to express my gratitude to all those people who made this research possible and those who have made my experience in the University one that I will always remember fondly.

First and foremost I wish to thank my supervisor, **Matthew Phillip Cartmell**, James Watt Professor of Mechanical Engineering. He has been supportive since the days I began working on this research as a postgraduate. Ever since, Matthew has supported me not only by providing a research assistantship over almost one year, but also academically and emotionally through the rough road to finish this work. Thanks to him I had the opportunity to develop a new analytical model. His patience, stimulating suggestions and encouragement helped me in all the time of research for and writing of this thesis. He also gave me the moral support and the freedom I needed to move on.

I want to thank the Institute of Space Technology, Pakistan, who provided me with a scholarship for two years and the Goudie Bequest of the University of Glasgow, UK for their one year assistantship for this course of study. All the relevant facilities such as computing facilities, and laboratories associated with Department of Mechanical Engineering, University of Glasgow are greatly appreciated and acknowledged.

A special acknowledgement goes to **Mrs. Pat Duncan**, Secretary Faculty of Engineering office, and **Mrs. Avril MacGregor**, International Student Adviser for their full co-operation and my office-mate of three years: **Mr. Lawrence Atepor**. He was a good friend ever since we began to share an office in October 2005.

I greatly thank my late father and my mother, brothers and sisters for their affectionate support and love during this course of study. Last but not least, I want to thank my wife for all the support that she gave me during the years I have been working on this research, especially all the holidays that she arranged to give me time to write, to think and to talk to her about this

subject. Especially, I would like to give my special thanks to my lovely son Muhammad Rafae who made me laugh during critical circumstances, and enabled me to complete this work. Without them, I would not have been able to achieve what I have today.

A. Israr
April, 2008

LIST OF FIGURES

Figure 3-1: Isotropic plate loaded by uniform pressure and a small crack at the centre 41

Figure 3-2: In-plane forces and a crack of length 2*a* at the centre of the plate element 45

Figure 3-3: Two sided constraints and plate deformation having a part-through crack at the centre 46

Figure 3-4: Line Spring Model (LSM) representing the bending and tensile stresses for a part-through crack of length 2*a*, after Rice and Levy, 1972 48

Figure 3-5: Isotropic plate loaded by arbitrary located concentrated force and small crack at the centre, and parallel to the *x*-axis 52

Figure 3-6: Plate first mode natural frequency of aspect ratio 0.5/1 as a function of half-crack length.....61

Figure 3-7: Plate first mode natural frequency as a function of the thickness of the plate for the half-crack length of 0.01 m 62

Figure 4-1: Linear and nonlinear response curves for three different cases of boundary conditions and half-crack length of 0.01 m.....73

Figure 4-2: Comparison between linear and nonlinear model of the cracked rectangular plate and the boundary condition CCFF.....74

Figure 4-3: The amplitude of the response as a function of the detuning parameter, σ_{mn} [rad/s] and the point load at different locations [m] of the plate element 74

Figure 4-4: Nonlinear overhang in the form of the softening spring characteristic by the use of NDSolve within *Mathematica*™ for an aspect ratio of 0.5/1, and initial conditions zero.....76

Figure 4-5: Three modes of vibration for an aluminium plate without a crack ..80

Figure 4-6: Three modes of vibration for an aluminium plate of sides 0.5x1 m and a half-crack length of 0.01 m.....80

Figure 4-7: Three modes of vibration for an aluminium plate of sides 0.5x1 m and a half-crack length of 0.025 m.....80

Figure 5-1: *Dynamics 2* program code for the cracked plate model and a boundary condition SSSS.....88

Figure 5-2: Explanation of Lyapunov exponent.....89

Figure 5-3: Bifurcation diagrams for three different cases of boundary conditions and a half-crack length of 0.01 m for the normalised control parameter, ω.....93

Figure 5-4: Bifurcation diagrams for three different cases of boundary conditions and a half-crack length of 0.025 m for the normalised control parameter, ω.....93

Figure 5-5: Bifurcation diagrams for three different cases of boundary conditions and a half-crack length of 0.01 m for the normalised excitation acceleration in the *x*-direction.....97

Figure 5-6: Bifurcation diagrams for three different cases of boundary conditions and a half-crack length of 0.025 m for the normalised excitation acceleration in the *x*-direction.....98

Figure 5-7: Dynamical system analysis for a half-crack length of 0.01 m and the boundary condition SSSS.....102

Figure 5-8: Dynamical system analysis for a half-crack length of 0.01 m and the boundary condition CCSS.....103

Figure 5-9: Dynamical system analysis for a half-crack length of 0.025 m and the boundary condition SSSS.....104

Figure 5-10: Dynamical system analysis for a half-crack length of 0.025 m and the boundary condition CCSS.....105

Figure 5-11: Poincaré map for the three boundary condition cases and a half-crack length of 0.01 m from the use of specialised code written in *Mathematica*™.....106

Figure 5-12: Time plots, and phase planes for a half-crack length of 0.01 m by the use of specialised code written in *Mathematica*™ and the boundary condition SSSS.....107

Figure 5-13: Time plots, and phase planes for a half-crack length 0.01 m by the use of specialised code written in *Mathematica*™ and the boundary condition CCSS.....108

Figure 5-14: Time Plots, and phase planes for a half-crack length 0.01 m by the use of specialised code written in *Mathematica*™ and the boundary condition CCFF.....109

Figure 6-1: Simple layout of the experimental setup.....112

Figure 6-2: Aluminium plate with crack at the centre.....113

Figure 6-3: Complete assembly of the test rig.....114

Figure 6-4: First mode shape for an un-cracked aluminium plate of aspect ratio 0.5/1.....116

Figure 6-5: First mode shape for cracked aluminium plate of crack length 50 mm, and aspect ratio of the plate 0.5/1.....116

Figure 6-6: Amplitude responses (in terms of voltage signals) for first mode of an un-cracked (white mesh area) and cracked (coloured mesh area) aluminium plates of aspect ratio 0.5/1.....117

Figure 7-1: Comparison between method of multiple scales and that of numerical integration.....120

LIST OF TABLES

Table 3-1: Natural frequencies of the cracked plate model for different boundary conditions and aspect ratios 60

Table 3-2: Relative changes of the natural frequencies of the cracked simply supported plate for the first mode only.....63

Table 4-1: Peak amplitudes for three sets of boundary conditions and two sets of half-crack length for a plate aspect ratio of 0.5/1 75

Table 4-2: Finite element analysis results 81

Table 5-1: Data used for dynamical system analysis for various cases of boundary conditions and half-crack lengths.....87

Table 5-2: *Dynamics 2* command values for plotting.....91

Table 6-1: Experimental results of first mode of vibration for an un-cracked and cracked aluminium plates 117

TABLE OF CONTENTS

AUTHOR'S DECLARATION ..... **iii**

ABSTRACT ..... **iv**

ACKNOWLEDGEMENTS ..... **v**

LIST OF FIGURES ..... **vii**

LIST OF TABLES ..... **x**

TABLE OF CONTENTS ..... **xi**

NOMENCLATURE ..... **xiv**

Chapter 1 ..... **1**

INTRODUCTION **1**

1.1 Motivation **1**

1.2 Overview **2**

1.3 Research Objectives **4**

1.4 Outline and Methodology **5**

Chapter 2 ..... **7**

LITERATURE REVIEW **7**

2.1 Historical Background **7**

2.2 Nonlinear Deflection Theory **10**

2.3 Damage in Plate Structures **13**

2.4 Finite Element Approach in Cracked Plate Structures **21**

2.5 Damage Detection Methodologies in Plate Structures **23**

2.6 Damaged Plates of Various Sizes and Shapes **26**

2.7 Solution Methodologies **27**

2.7.1 Perturbation Theory 31

2.7.2 The Method of Multiple Scales 33

2.8 Dynamical Systems and Nonlinear Transitions to Chaos **36**

Chapter 3 ..... **39**

FORMULATION OF CRACKED PLATES **39**

3.1 Governing Equation of Cracked Rectangular Plate **39**

3.2 Addition of In-plane or Membrane Forces **44**

3.3 Crack Terms Formulation **47**

3.4 Galerkin's Method for a Vibrating Cracked Plate **51**

3.5 Linear Viscous Damping **58**

3.6 Investigation of Natural Frequencies for Cracked Plate Model **59**

Chapter 4 ..... **64**

APPROXIMATE ANALYTICAL TECHNIQUES **64**

4.1 The Method of Multiple Scales **65**

4.2 Analytical Results **72**

4.2.1 Linear and Nonlinear Response Curves 72

4.2.2 Comparison of Linear and Nonlinear Cracked Plate Model 73

4.2.3 Nonlinearity affects by changing the location of the Point Load 74

4.2.4 Damping Coefficient influences Nonlinearity 75

4.2.5 Peak Amplitude 75

4.3 Direct Integration – NDSolve within *Mathematica*™ **75**

4.4 Finite Element (FE) Technique – ABAQUS/CAE 6.7-1 ..... **76**

4.4.1 Steps Taken to Perform FE Analysis 77

4.4.2 ABAQUS/CAE Results 79

Chapter 5 ..... **82**

DYNAMICAL SYSTEM ANALYSIS **82**

5.1 Dynamical System Theory **83**

5.2 A Model of the Cracked Plate for Dynamical System Analysis **85**

5.2.1 Nondimensionalisation 85

5.3 *Dynamics 2* - A Tool for Bifurcation Analysis **87**

5.3.1 Bifurcation Analysis 89

5.3.2 Lyapunov Exponents....89

5.3.3 Amplitude of response, *x*, as a function of normalised excitation frequency, *ω* and the Lyapunov exponent....91

5.3.4 Amplitude of response, *x*, as a function of normalised excitation acceleration and the Lyapunov exponent....94

5.3.5 Time plots, Phase planes, and Poincaré maps 99

5.4 Specialised Numerical Calculation Code written in *Mathematica*™ 106

Chapter 6 111

EXPERIMENTAL INVESTIGATIONS 111

6.1 Instrumentation 111

6.2 Machining Procedure of the Crack in the Aluminium Plate 112

6.3 Test Setup 113

6.4 Experimental Results 115

Chapter 7 118

RESULTS AND DISCUSSION 118

7.1 Analytical Results 118

7.2 Numerical Results 121

7.3 Experimental Results 123

7.4 Conclusions 124

Chapter 8 125

CONCLUSIONS AND FUTURE RECOMMENDATIONS 125

8.1 Summary 125

8.2 Future Recommendations 128

LIST OF REFERENCES 129

PUBLICATIONS 150

LIST OF FIGURES IN APPENDICES A-1

CONTENT OF APPENDICES A-2

NOMENCLATURE

Symbols	Description	Units
D	Flexural rigidity	N-m
E	Modulus of Elasticity	Kg-m^{-2}
υ	Poisson's ratio	-
w	Transverse deflection	m
n_x , n_y , n_{xy} , n_{rs}	In-plane or Membrane forces per unit length	N-m^{-1}
h	Thickness of the plate	m
Q_x , Q_y	forces per unit length acting on the plate element	N-m^{-1}
P_z	Load per unit area	N-m^{-2}
$\bar{P}_z$	Point load	N
M_x , M_y , M_{xy} , M_{rs}	Bending moments per unit length	N-m-m^{-1}
σ_x , σ_y , τ_{xy}	Bending and shear stresses	N-m^{-2}
$\bar{M}_y$	Bending moment due to crack per unit length	N-m-m^{-1}
$\bar{n}_y$	In-plane force due to crack per unit length	N-m^{-1}
$\bar{\sigma}_{rs}$ and $\bar{m}_{rs}$	Nominal tensile and bending stresses at the	N-m^{-2}

	crack location	
σ_{rs} and m_{rs}	Nominal tensile and bending stresses at the far sides of the plate	N-m^{-2}
a	Half crack length	m
$\alpha^o_{bb}, \alpha^o_{tt}, \alpha^o_{bt} = \alpha^o_{tb}$	Nondimensional bending, stretching and stretching-bending compliance coefficients	-
X_m, Y_n	Characteristic or modal functions of the cracked plate	m
A_{mn}	Arbitrary amplitude	m
$\psi_{mn}(t)$	Time dependent modal coordinate	m
l_1, l_2	Lengths of the sides of the plate	m
$\lambda_{m,n}$, $\gamma_{m,n}$	Mode shape constants	-
m, n	Mode numbers	-
ε_x, ε_y	Middle surface strains	-
F_{1mn}, F_{2mn}	Complex in-plane force functions	m^{-4}
M_{mn}	Complex modal component-1	s^{-2}
K_{mn}	Complex modal component-2	-
G_{mn}	Complex modal component-3	m^{-2}
P_{mn}	Complex modal component-4	m

ω_{mn}	Natural frequency of the cracked plate	rad-s^{-1}
β_{mn} , C_3	Nonlinear cubic spring stiffness	m^{-2}-s^{-2}
$P_o(t)$	Harmonic or periodic Load	N
μ , C_1	Damping coefficient	N-s-m^{-1}
Ω_{mn}	Excitation frequency	rad-s^{-1}
ε	Perturbation parameter for the method of multiple scales	-
$T_n = \varepsilon^n t$	n=0: fast time scales; n=1: slow time scale	s
$\varepsilon\sigma_{mn}$	Detuning parameter	rad-s^{-1}
b	Real amplitude	m
α	Phase angle	radians
b_p	Peak amplitude	m
λ	Lyapunov exponent	-

CCFF	Clamped-clamped-free-free
CCSS	Clamped-clamped-simply supported-simply supported
SSSS	All sides simply supported
FEM	Finite element method

LSM	Line spring model
BIFD	No. of iterates for each bifurcation parameter
BIFPI	Pre-iterates for each bifurcation parameter
BIFV	No. of parameter values in bifurcation diagram
CON	Connect consecutive dots of trajectories
IPP	No. of iterates per plots

Chapter 1

INTRODUCTION

1.1 Motivation

Nonlinearity in plate structures has been of general interest to the scientific and engineering communities for many years. These structures have multitude of applications in almost every industry. The aircraft industry has shown much interest in this, some of the early solutions were motivated by this industry [Trendafilova, 2005]. In electrical engineering, nonlinear behaviour is quite evident in Micro-Electro-Mechanical-Systems (MEMS) [Wei *et al.*, 2005]. In civil engineering, this is also of interest and was illustrated in regard to the behaviour of window glass plating [Wang, 1948]. The current application which is being worked on at University of Glasgow is to predict the nonlinear behaviour of parametrically excited beams, rotor dynamics, and momentum exchange tethers for space vehicle propulsion. Therefore, studying the dynamic response, both theoretically and experimentally, of plate structures with minor cracks under various loading conditions would help in understanding and explaining the behaviour of more complex, real structures under similar loading.

In this research, an approximate analytical model of a cracked plate is developed, and a study, both theoretically and experimentally of the nonlinear vibrations of a plate with a crack at the centre consisting of continuous line under transverse harmonic excitations with three sets of boundary conditions has been undertaken. In addition, the bifurcatory behaviour within this system has been investigated for a nonlinear transition to chaos through the use of available software such as *Dynamics 2* and by means of code written in *Mathematica*™. Therefore, the eventual goal is to

provide an understanding of vibration and dynamic system analysis of plate structures associated with a centrally located crack.

1.2 Overview

Plate and beam structures are fundamental elements in engineering and are used in a variety of structural applications. Structures like aircraft wings, satellites, ships, steel bridges, sea platforms, helicopter rotor blades, spacecraft antennae, and subsystems of more complex structures can be modelled as isotropic plate elements. In this dissertation, only aircraft wing structures modelled as an isotropic plate are discussed. The plate panels on the tips of aircraft wings are mainly under transverse pressure, and are often subjected to normal and shear forces which act in the plane of the plate. The plate panels may not behave as intended if they contain even a small crack, or form of damage, and such small disturbances can create a complete loss of equilibrium and cause failure.

Interesting physical phenomena occur in structures in the presence of nonlinearities which cannot be explained by linear models. These phenomena include jumps, saturation, sub-harmonic, super-harmonic, and combination resonances, self-excited oscillations, modal interactions, periodic doubling, and chaos. These various phenomena have been discussed in most of the literature to date. In reality, no physical system is strictly linear and hence linear models of physical systems have limitations of their own. In general, linear models are applicable only in a very restrictive domain such as when the vibration amplitude is very small. Thus, to accurately identify and understand the dynamic behaviour of a structural system under general loading conditions, it is essential that nonlinearities present in the system also be modelled and studied. Nayfeh and Mook (1979), Moon (1987), Cartmell (1990), Strogatz (1994), Thomsen (1997), Sathyamoorthy (1998) and Murdock (1999) explain various types of nonlinearities in detail, along with examples. Here, some of these nonlinearities are briefly described which can be broadly classified into two main categories i.e. geometric nonlinearity and material nonlinearity. The accurate representation of displacement may involve geometric nonlinearity. Geometric nonlinear problems may arise because of

two reasons (a) the nonlinear strain–displacement relationship; (b) the nonlinearity in the governing differential equation due to the coupling of in-plane and transverse displacement fields. As the deflection of the plate increases, the stretching effect becomes more pronounced than the bending effect, particularly when the edges of the plate are restrained. These types of problems are also referred to as large deflection problems which result in nonlinear equations. There is another class of problem, where the stress strain relationship of the material of the structure is not linear. In the case of steel, linearity occurs up to the yield point, but beyond that it deviates from linear to nonlinear. Therefore it involves nonlinear material behaviour. Many other types of nonlinearities exist in structures such as inertia, impacts, backlash, boundary conditions, fluid effects and damping.

Plate structures undergoing transverse deflection can be classified into numerous regimes that describe the nature of their behaviour and thus the characteristics of the mathematical problem. This behaviour can generally be classified in the literature by carefully observation of the amount of deflection in comparison to the plate dimensions. These regimes include (a) small deflection theory (Linear) which can typically be used for deflections less than twenty percent of the thickness, (b) moderately large deflection theory (Nonlinear) is applied when the deflection is a multiple of the plate thickness but much less than the plate side length, (c) and very large deflection theory (Highly Nonlinear) is applied when the deflection of the plate is similar in magnitude to the plate side length. These large deformations occur in structures subjected to shock loads, and can not be adequately analysed by linear theory since the deflection of the panels does not remain small in comparison with the thickness. Depending on the plate classification the solution to these problems can be relatively simple or highly complex, and typically impossible without the implementation of approximating techniques. In this literature review, discussion will only be made of linear and moderately nonlinear systems, very large deflection is currently not pertinent to this work and subsequently will not be covered. Interestingly, the majority of physical systems appear to belong to the class of weakly nonlinear or quasi-linear systems. For certain phenomena, these systems exhibit behaviour only slightly different from that of their linear

counterpart. In addition, they can also exhibit phenomena which do not exist in the linear domain. Therefore, for weakly nonlinear structures, the usual starting point is still the identification of the linear natural frequencies and mode shapes. Then, in the analysis, the dynamic response is usually described in terms of the linear natural frequencies and mode shapes. The effect of small nonlinearities is seen in the equations governing the amplitude and phase of the structure's response. Weak nonlinearity can be seen for example in wave drift forces, whereby waves generate steady forces on floating bodies. Wave drift forces are typically proportional to the square of the wave height, and can be analysed with a perturbation scheme. Whereas, strong or highly nonlinear systems can not be analysed with a perturbation scheme.

At the turn of the 20th century, Henri Poincare made one of the first predictions of the existence of chaos, of what is prosaically now called the butterfly effect. These chaotic or nonlinear systems exhibit surprising and complex effects that would never be anticipated by someone trained only in linear techniques. Nonlinearity has its most profound effects on dynamical systems and can be found in much of the literature.

1.3 Research Objectives

This research proposes a new analytical model for the nonlinear vibration analysis of an aircraft panel structure modelled as an isotropic cracked plate and based on classical plate theory with different possible boundary conditions including clamped – clamped – free – free (CCFF), clamped – clamped - simply supported – simply supported (CCSS), and all sides simply supported (SSSS), and subjected to transverse harmonic excitation. A crack is arbitrarily located at the centre of the plate, consisting of a continuous line. This model is developed by assuming that the effects of rotary inertial and through thickness stresses are negligible. The emphasis, however, is to develop an approximate analytical model of the cracked plate, which is in the form of single-degree-of-freedom system. Secondly, an approximate solution technique is proposed by use of the method of multiple scales, and in addition, direct integration and finite element analysis in ABAQUS are also employed for comparison. This model can also be studied for the nonlinear

vibration analysis of the plate without the application of the transverse harmonic excitation. Thirdly, dynamical systems analysis is performed by the use of commercially available software *Dynamics 2* and *Mathematica*™ and generates interestingly complex phenomena from the nonlinear transitions to chaos. Finally the results are verified via experimental investigations followed by useful results and conclusions.

1.4 Outline and Methodology

In Chapter 2 an extensive literature review is presented that is related to the present work.

The equations of motion governing the nonlinear vibrations of isotropic plates are derived with possible boundary conditions, using the equilibrium principle based on classical plate theory, in Chapter 3. An arbitrary located crack at the centre of the plate is defined by a continuous line. Assumptions used in this derivation are also elaborated. The derived equations are used in the theoretical analysis which is explained in subsequent chapters. Furthermore, the governing partial differential equation is converted into the time domain by defining the characteristic or modal functions depending upon the boundary conditions, using Galerkin's method[1].

In Chapter 4, an approximate analytical solution is proposed via the method of multiple scales for the governing differential equation of the cracked plate subjected to transverse loading, for studying the effect of nonlinearity caused by the crack within plate structures. Similarly, solution of the problem is also obtained by direct integration and finite element analysis in ABAQUS.

In Chapter 5, the bifurcatory behaviour of the proposed cracked plate model is discussed to analyse the nonlinear transition to chaos through the use of

[1] Galerkin's method is used to reduce the set of partial differential equations to a set of ordinary differential equations, and then it is possible to study linear, nonlinear, and chaotic behaviour of the system. It uses the shape or characteristic functions which depend upon the boundary condition of the system. Galerkin's method can be divided into two main categories such as Petrov-Galerkin method and Ritz-Galerkin method. In the Ritz-Galerkin method the solution is expended in terms of a series with unknown coefficients which depend on time and satisfy the given boundary conditions. In the Petrov-Galerkin method the residual be orthogonal to each of the expansion functions, one may define a different set of test functions and require the residual to be orthogonal to each of these test functions.

Dynamics 2 and *Mathematica*™. In this chapter, we briefly introduce the chaos and some important properties of chaotic systems including time plots, phase planes, Poincaré maps, bifurcation diagrams, and the Lyapunov exponent.

An experimental study of the response of rectangular, aluminium CCFF cracked and un-cracked plates to transverse harmonic excitations is presented in Chapter 6.

In Chapter 7, results and discussions are presented and show that a model of the cracked plate with different boundary conditions can exhibit a multitude of nonlinear dynamical phenomena, followed by conclusions and future recommendations in Chapter 8.

Chapter 2

LITERATURE REVIEW

To cover some general historical background, we begin with a discussion of linear homogenous beams and plates. This is followed by nonlinear aspects of plates, brief coverage of damage in plate structures, solution methodologies, and finally an introduction to nonlinear transitions to chaos.

2.1 Historical Background

Plate theory, and its behaviour in the dynamic and static domains has been applied to reduce vibration and noise in structures since the end of the 19th century where it began with the work of German physicist Chladni (1827) who discovered various modes of free vibrations experimentally [Szilard, 2004]. Since then it has developed into an escalating and expansive field with a wide variety of theoretical and empirical techniques, dealing with increasingly complicated problems. The first mathematical solutions to the free vibration problem of the membrane theory of plates were formulated by Euler in 1766 and his student Bernoulli in 1789. Lagrange developed the first correct governing equation for the free vibration of plates in 1813 [Szilard, 2004]. The plate problem has progressed through history to the present, where it is commonly analyzed using the finite element method and other rigorously applied computational methods that are capable of accommodating many different geometries and ranges of parameters. Navier can be credited with developing the first correct differential equation of plates subjected to distributed static lateral loads in 1836 followed by Kirchhoff who derived the same differential equation through the use of a different energy approach in 1887. The first correct statement of the differential equation governing plate vibrations is attributed by Rayleigh to Sophie German in the early 19th century. In 1877, Rayleigh published the first edition of his famous book

Theory of Sound and the second edition appeared in 1945, in which he proposed seminal methods for determining natural frequencies of vibration.

Tomotica presented work on the vibrations of square plates in 1936. In 1950, Young adopted the Ritz method to approximate the first six natural frequencies for clamped square plates, and in 1954, Warburton proposed the first comprehensive collection of solutions for rectangular plates. He used Rayleigh's method to obtain the approximate frequency expressions for plates with a series of different boundary conditions. In addition to that a useful discussion on the mode shapes of rectangular plates, and the method for obtaining the mode shapes, were also a part of this paper. The frequency equation was not fully explored until seven years later by Mindlin in 1960. To extend the range of applicability of classical theories to higher frequencies, refined dynamic theories of beams and plates were introduced by Timoshenko in 1921, and by Mindlin in 1951, respectively, and included the effects of transverse shear and rotary inertia. Mindlin not only generalised the Timoshenko beam theory to the plate, but also compared and coordinated the results of his plate theory with those derived by Lord Rayleigh from elasticity theory. This was one of the first attempts to establish a connection between the exact dynamic elasticity theory and an approximate plate theory, by means of which the shear factor introduced in Mindlin's theory could be determined.

Small deflection vibrations in plates have been widely studied due to the relative ease of obtaining solutions in these cases. Therefore a variety of literature is available concerning such linear vibration problems. A monograph on the vibration of plates was published by Leissa in 1969, reprinted in 1993; in which he reviewed the contemporary literature on plate vibrations. Later, in 1973, this author presented a review paper on free vibrations of rectangular plates, and comparisons were made with Warburton's useful approximate formulas of 1954. One of the classical references for plate problems is *Theory of Plates and Shells* by Timoshenko, 1940, which provides an expansive amount of information on plates and derivative systems. Szilard, in 2004, also provides an excellent overview of the linear plate problem with an emphasis on finite difference techniques. Laura and Duran, in 1975, used the simple polynomial approximation and Galerkin's method to determine the

response of a clamped plate subjected to a harmonic excitation. The results were presented in terms of amplitudes and bending moments as a function of the relative frequency (ratio of the frequencies) for different aspect ratios for simply supported and clamped rectangular plates. For simply supported rectangular plates the agreement of the approximate solution with the exact solution for the relative frequency of 0.30 and aspect ratios of 1 and 2, were quite reasonable, while for clamped rectangular plates the results were in good agreement for a zero relative frequency. Jones and Milne applied an extended Kantorovich method in 1976, as proposed by Kerr in 1968 for the evaluation of the eigen frequencies of vibration of clamped rectangular plates in detail, and this was also applied for the cases of clamped – clamped – simply supported - simply supported (CCSS) and clamped – clamped – clamped - simply supported (CCCS) sets of boundary conditions. The results were compared with those of Leissa from 1973, and a very close agreement was found. Bhat investigated the vibration problem of rectangular plates with different boundary conditions in 1985 by using a set of characteristic orthogonal polynomials in the Rayleigh-Ritz method. The result when compared with the published literature yielded good agreement for the lower modes only. Some developments in the finite element method have been led by Han and Petyt *et al*. in 1996(a) leading to a new approach now known as the hierarchical finite element method (HFEM) for the study of linear vibrations of symmetrically laminated rectangular plates with clamped boundary conditions. The results showed that the solutions converged rapidly with the increase in the number of polynomials used, which resulted in far fewer degree of freedom than those when used the conventional finite element method. These authors further investigated the same problem in 1996(b), however at this time they considered the analysis of forced vibration. The loads considered were harmonic acoustic plane waves impinging on the plate surface in a normal direction and at grazing incidence. These authors obtained the natural frequencies of five layer symmetrically laminated rectangular plates for different grazing incidents and found a decreasing trend of frequencies with the increase of incident. Furthermore, they found that the maximum surface bending strains might not occur at the middle of the edges due to the distorted mode shapes.

Fan, in 2001, analyzed the transient vibration and sound radiation of a rectangular plate with visco-elastic boundary supports subjected to an impact loading and obtained the sound radiation pressure in the time and frequency domain by means of the Rayleigh integral. Au and Wang, in 2005, studied the dynamic responses in terms of sound radiation from the forced vibration of an orthotropic plate with the effects of moving mass, damping coefficient, and boundary conditions. Yagiz and Sakman, in 2006, observed the dynamic response of a bridge modelled as an isotropic plate under the effect of a moving load with all sides simply supported. They considered a vehicle with seven degrees of freedom system as the moving load. A mathematical model was obtained by the use of Lagrange's formulation, and used to investigate the dynamic response of the bridge and vehicle.

2.2 Nonlinear Deflection Theory

Many formulations for nonlinear deflection theory have been proposed and tested to give a closed-form solution to the problem. Higher deflections, of the order of approximately a tenth the thickness of the plate, can cause stiffening of the structure that cannot be predicted by linear theory. The credit for uncovering the nonlinear theory that satisfactorily accounts for both bending and stretching of the plate is given to G. Kirchhoff (1824–1887). The final form of the nonlinear differential equations governing the moderately large deflection behaviour of a statically deflected plate was published by Von Karman in 1910. A review concerning the nonlinear vibration analysis of plates and shells was presented by Leissa in 1984, followed by Sathyamoorthy in 1988, and who summarised work on nonlinear vibrations of plates from 1983 to 1986, including 99 published references. The nonlinear analysis of plates has led to the production of famous reference books such as *Non-linear Analysis of Plates* by Chia, 1980, and *Nonlinear Oscillations* by Nayfeh and Mook in 1979.

One of the first studies dealing with the problem of nonlinear plate vibrations was due to Chu and Hermann in 1956. They obtained a solution for the nonlinear free vibrations of rectangular elastic plates with fixed and hinged edges through the use of a perturbation method and the principle of

conservation of energy. Later, in 1961, Yamaki used a Galerkin approach to obtain the solutions for rectangular plates simply supported on all edges and clamped on all edges. Berger, in 1955, derived a simplified set of equations describing the large deflection of plates. He solved several static problems and concluded that his simplified theory gave results in substantial agreement with more elaborate methods. Wah, in 1963, employed an approximate formulation based on Berger's hypothesis of 1955 for the numerical solution of rectangular plates with various boundary conditions for large vibration amplitudes. He plotted his results for relative time period and bending stresses as a function of the ratio of the amplitude and thickness of the plate for various values of the aspect ratios. Srinivasan, in 1965, used the Ritz–Galerkin method to study the case of hinged-hinged beams and circular plates with different boundary conditions at large vibration amplitudes. Stanišić and Payne introduced a technique in 1968 which was based on the Galerkin approach for determining the natural frequencies of rectangular plates with discrete masses added for simply supported and clamped boundary conditions. Their results indicated the expected trend that natural frequencies decreased with the added mass whereas the deflections and stresses of the plate increased. Rehfield, in 1973, developed an approach for analysing the nonlinear free vibrations of elastic structures by the use of Hamilton's principle and a perturbation procedure, and this was extended to the case of forced vibration of beams and rectangular plates. Mei applied the finite element method in 1973 for the prediction of large amplitude free flexural vibrations of beams and plates with various boundary conditions. The nonlinearity considered was due to large deflections, and not due to nonlinear stress-strain relationships, and the results showed the hard spring nonlinear characteristics as the dimensionless amplitude increased. Various analytical formulations of the problem of large-amplitude free vibration behaviour of simply supported beams with immovable ends based on the Rayleigh–Ritz technique were formulated by Singh *et al*. in 1990. At the same period, another model based on Hamilton's principle and spectral analysis was proposed for nonlinear free vibrations of thin straight structures by Benamar *et al*. in 1990; this was applied to clamped-clamped beams, homogeneous and symmetrically laminated fully clamped rectangular plates in 1991, and further extended to fully clamped thin plates in 1993. These studies showed that the

mode shapes were amplitude dependent. The general trends of the mode shape change were an increase of the displacement, or curvature, near the edges, and flattening near the centre of the beam or plate. However, the theoretical models employed in these studies considered transverse displacements only and neglected the effects of in-plane displacements. At the start of the 21st century, this model has been extended and improved to determine the geometrically nonlinear free and forced vibrations of clamped - clamped and simply supported beams by El Kadiri *et al.* in 2002(a). In this model, the nonlinear free vibration problem was reduced to the solution of a set of nonlinear algebraic equations, which was performed numerically using appropriate algorithms in order to obtain a set of nonlinear mode shapes for the structure. They were considered in each case with the corresponding amplitude-dependent nonlinear frequencies. This approach was also applied in order to determine the amplitude-dependent deflection shapes associated with the nonlinear steady-state periodic forced response. The authors applied the same procedure for determining the first and second nonlinear mode shapes of fully clamped rectangular plates in 2002(b), and in 2003 they proposed an improved form for determining the geometrically nonlinear response of rectangular plates which were excited by concentrated, or distributed harmonic forces. This approach was applied to the cases of fully clamped (CCCC), simply supported and clamped - clamped - simply supported (SCCS) rectangular plates. Similarly, these studies showed that the relative frequency was a function of the ratio of the amplitude and thickness of the plate. Further studies showed that El Bikri *et al.* extended Benamar's model in 2003 to determine the fundamental nonlinear mode shape, the associated amplitude dependent natural frequencies, and the flexural stress distribution of a clamped – clamped - simply supported - simply supported (CCSS) rectangular plate. Later, Beidouri *et al.* extended this model in 2006 to the cases of clamped - simply supported – clamped - simply supported (CSCS) and clamped - simply supported - simply supported - simply supported (CSSS) rectangular plates and determined iteratively the amplitude dependence of the first nonlinear mode shapes for aspect ratios of 0.66 and 1.5, and for various vibration amplitudes. Han and Petyt in 1997(a) developed the HFEM for the geometrically nonlinear vibration analysis of thin laminated rectangular plates with clamped boundary conditions to study the variation of

the natural frequencies and the mode shapes with the change of vibrational amplitude. They observed the hardening spring effect for the fundamental mode of rectangular isotropic plates and compared the nonlinear frequency ratios for the first and higher modes with fully clamped boundary conditions with, without in-plane displacements and with the average of in-plane strains. The first and higher modes of isotropic and laminated plates were also reported in 1997(b).

The large deflection theory for the Mindlin plate was employed by Wang and Kuo in 1999 for the examination of the nonlinear vibration of the plate induced by the coupling of moving loads with the weight of the plate. In the initial part of the studies one of the equations of static equilibrium due to the weight of the plate was derived and secondly, static responses of the plate were accounted for in deriving the equations of motion of the plate. Static and dynamic findings were presented for a simply supported square plate of length 20 m and thickness of 10 cm. Static results showed that the deviation in amplitude between the large deflection theory and the small deflection theory increased as the thickness decreased, and similarly it increased with the area of the plate. Results also showed that changes in dynamic transverse deflection and dynamic bending moment between the large deflection theory and the small deflection theory are significant for thin plates with large area.

2.3 Damage in Plate Structures

Cracks present a serious threat to the performance of structures. Most failures are due to material fatigue. It is for this reason that methods allowing early detection and localisation of cracks are of the utmost necessity for smooth running and longevity of machines and structures. The dynamic responses of rectangular plates with cracks, or minor irregularities under different loading conditions, have been investigated in the past by many researchers for different boundaries conditions, and various methods have been proposed to deal with the problem. Nevertheless fewer material has been published on the vibration analysis of cracked plates. Dimarogonas, in 1996, reported a comprehensive review of the vibration of cracked structures. This author covered a wide variety of areas that included cracked beams, coupled

systems, flexible rotors, shafts, turbine rotors and blades, pipes and shells, empirical diagnoses of machinery cracks, and bars and plates with a significant collection of references. Irwin, in 1962, examined a part-through crack in a plate subjected to tension and derived a relation for the crack stress-field parameter and the crack extension force at the boundaries of a flat elliptical crack. Gross *et al.*, in 1964, described in their technical report that stress intensity factors can be obtained by a boundary value collocation procedure applied to the Williams stress function for a single edge notch tension specimen. The results were presented in terms of non-dimensionalised stress intensity factors and ratio of the crack length to the specimen width, and this showed an increasing trend with the increase of crack ratio. Moreover, at small ratios of crack length to specimen width (0.15-0.40) the results were in good agreement with other authors' results, and above 0.40 differences in their results were implicitly due to bending, which was not taken into account in their analytical solutions.

The vibrations of a cracked rectangular plate were first investigated by Lynn and Kumbasar in 1967, who used a Green's function approach to obtain a homogenous Fredholm integral equation of the first kind which satisfied the mixed edge condition along a fictitious line partially formed by the crack. Lynn and Kumbasar used the Krylov and Bogolivbov method to solve the integral equation for narrow cracks, and for a simply supported plate on all sides. The result was presented in terms of variations of frequencies with respect to different crack lengths, and the relative moment distributions along the un-cracked segments. The dynamic characteristics of centrally located cracked plates in tension were analyzed by Petyt in 1968 by the use of the finite element displacement method. In addition, the effect of an increase in the width of the plate was described and this showed the decrease in amplitude in the area of the crack and the increase in the curvature of the plate in the region of the crack tip. The results were presented in terms of frequencies vs. crack length, and stresses and defections vs. length of the plate. Okamura *et al.*, in 1969, obtained the lateral deflection, the load carrying capacity, and the stress intensity factor of a rectangular cross-section single-edge cracked column with hinged ends under compression. They compared an un-cracked column with a cracked column, and examined

the effect of a crack on load carrying capacity and deflections, with the ratio of crack length to column width, and the ratio of column width to column length as important parameters. In particular these authors considered the effect of compliance due to bending, and ignored the effect of compliance due to rotation induced by the axial load. Stahl and Keer, in 1972, as well as Aggarwala and Ariel, in 1981, solved the eigenproblem of simply supported plates by using homogeneous Fredholm integral equations of the second kind by taking the stress singularity at the crack tips into account. These authors presented methods which were limited to crack locations that allowed the problem to be reduced to a dual series equation, however the procedure of the model involved lots of computation. Aggarwala and Ariel pointed out that the frequency appeared to be higher when the cracks started from outside of the plate as compared to the case when cracks started from inside. The reason for this discrepancy was explained for the cracks starting from the outside, that in the limiting case when they reached the centre, on account of symmetry the condition $\partial w/\partial x$ (where w is the transverse displacement of the plate) must be satisfied at the centre, which was not applicable when the cracks started from the centre. Rice and Levy, in 1972, introduced the line spring model that reduced the truly three dimensional problem to one using two dimensional plate or shell theory. This approach is computationally inexpensive compared to full three dimensional models, and, within certain restrictions, provides acceptable accuracy. They employed two dimensional generalised plane stresses, and used Kirchhoff's plate bending theories with a continuously distributed line spring to represent a part-through crack, and also chose compliance coefficients to match those of an edge-cracked strip in plane strain. The line of discontinuity was of length $2a$ and the plate was subjected to remote uniform stretching and bending loads along the far sides of the plate. These authors computed the force and moment across the cracked section to determine the stress intensity factor, and the solution to the problem was characterised in terms of the Airy stress function. Their results showed that $K_{rs}/\bar{K}_{rs}$ (where K_{rs} is the stress intensity factor for an all-over crack, and $\bar{K}_{rs}$ is the stress intensity factor of an edge crack in plane strain for the same relative depth l_o/h, and for remote tensile or bending load) approaches unity with an increase in the ratio of crack length to plate

thickness $2a/h$. Furthermore, at small values of relative depth l_o/h, the ratio $K_{rs}/\bar{K}_{rs}$ approaches unity for small values of $2a/h$. Moreover Rice and Levy, 1972, pointed out that the line spring approximation appears to be most appropriate along regions where the crack depth varies slowly. Hirano and Okazaki, in 1980, and Nezu, in 1982, applied a finite Fourier transform to the differential equations governing the problem of the plates in which one pair of simply supported edges was perpendicular to the line of the crack. They obtained a system of integral equations which possessed the unknown discontinuities of the deflection and slope across the crack. These unknown quantities were expanded into a Fourier series. The results were presented for symmetric and anti-symmetric cases of their proposed models with excellent conclusions.

Bending of a cracked rectangular plate was first investigated by Keer and Sve in 1970. Their analysis was limited to such a location of the crack that allowed reduction of the problem to a dual series equation. Hence the crack was confined to a position along the symmetry axis. They formulated the problem as dual series equations and used a modification of the technique proposed by Westmann and Yang in 1967 to obtain a solution in terms of a Fredholm integral equation of the second kind. Keer and Sve studied three cases comprising two collinear external cracks of equal length, an internal centrally located crack, and a single external crack. In all these cases the two plate boundaries perpendicular to the line of the crack were simply supported and clamped. The authors found that there was a change in strain energy due to the crack for both support cases, and for different aspect ratios of the plate. By comparing the two support conditions it was concluded that the clamping will tend to decrease the possibility of fracture since the strain energy release rate is smaller. An analogous method was applied by Stahl and Keer in 1972 for the analysis of natural vibration and stability of rectangular plates and was bounded by the similar limitations encountered by Keer and Sve in 1970. Solecki, in 1975, attempted to remove existing restrictions by developing a method that would allow the study of rectangular plates with arbitrarily located cracks. Solecki, in 1983, extended this work and developed a method to study the natural flexural vibration of simply supported rectangular plates with an arbitrarily located crack parallel to one edge, and

the method was based on the combination of finite Fourier transformation and of the generalized Green-Gauss theorem. A simply supported rectangular plate with a centrally located, and off-centre, crack was discussed as one of the examples. Numerical data was not obtained however, partially because the singularity of the curvature at the tips was not explicitly isolated. Rossmanith, in 1985, used the Westergaard stress function approach and solved for the stress intensity factor of associated, centrally located, cracked plate bending problems.

Rectangular plates with cut-outs are frequently found in engineering structures and these cut-outs are principally made for saving weight, for venting, for altering the natural frequencies and for providing accessibility to other parts of the structures. Many authors have investigated these types of structures and a few of them are mentioned here. Ali and Atwal, in 1980, used Rayleigh's method to study the natural vibration of rectangular plates with cut-outs. A comparison of the results obtained from Rayleigh's method and those obtained from the finite element method indicated that the maximum discrepancy between the two results was of the order of 10-11% for the first mode, and increased as the mode number increased. To reduce the percentage discrepancies in their results they proposed a correction factor depending on the cut-out size, and modified the deflection shape function which reduced the values from the corresponding finite element results to below 5%. Similarly, Lee *et al.*, in 1990, proposed an alternate method for the prediction of natural frequencies of rectangular plates with an arbitrarily located rectangular cut-out, and the plate was simply supported along one pair of opposite edges with any other boundary conditions in force at the remaining edges. The deflection function was chosen to satisfy all, or part of, the internal free edge conditions along the four edges of the cut-out, whereas the deflection function assumed by Ali and Atwal, 1980, was continuous throughout the whole domain of the plate, including the cut-out. Symmetric and anti-symmetric modes of vibration were considered in order to formulate the problem, and the results compared with those from finite element.

The Line Spring Model (LSM) has been rigorously treated by many researchers since it was initially proposed by Rice and Levy in 1972. Wen and Zhixe, in 1987, suggested a modified line spring model by taking into account the non-

local effect of the deformation for the line spring for the fracture analysis of part-through and slender cracks under tension and shearing. These authors investigated the accuracy and the relationship of the LSM between Reissner's theory of plates and shells and Kirchoff's theory, and calculated the stress intensity factors under different loading conditions and geometry of the cracked body. Two sets of problems were discussed; an infinite plate with an embedded symmetric elliptical crack under tension, and a rectangular surface crack under uniform shearing, and it was found that the relative error increased with the increase of the ratio of crack depth to plate thickness. Oliveira *et al.*, in 1991, described the Integrated Line Spring Element, which was designed to be associated with Semiloof shell elements for the simulation of the structural behaviour of the remaining ligament in a part-through crack in a thin shell. This shell element was used to determine the stress intensity factor for internal and external semi-elliptical cracks in arbitrary shells under mode I, II and III load conditions. Liu *et al.*, in 1999, obtained a three dimensional boundary element method with mixed boundary conditions for a nonlinear surface crack analysis, and used the LSM for the formulation of the problem and studied the fracture parameter *J* integral of a nonlinear surface crack. They also presented a predictor-corrector method for the nonlinear compliance matrix of the mixed boundary condition. The authors gave examples to illustrate their proposed method, in the first case a thick plate with a semi-elliptical surface crack with maximum crack depth of 0.6 was considered and the results showed that the plastic *J* integral appeared at around a normalised load of 0.6, and after 0.9 the results seemed to show a big difference, as compared with existing solutions, whereas in the case of the second example in which a hollow cylinder contained a circumferential external crack of constant depth, plastic behaviour was observed around a normalised load of 0.65, and uncertainty occurred after 0.85. Therefore, it was concluded that this method was not suitable for a surface crack problem with large scale plastic deformation. Zeng *et al.*, in 1993, developed a new LSM based on the boundary element method to find the surface flaws in the plate in the form of crack. The virtual crack extension technique was employed to obtain the stress intensity factor at the intersection of the crack front and free surface. These authors found by detail investigations that the stress intensity factor at the crack front-free surface intersection was barely

acceptable. Cordes and Joseph, in 1995, analyzed the LSM and used it to determine the stress intensity factors for the surface and internal cracks in a Reissner plate that contained residual stresses. Such stresses are usually caused by intentional or unintentional activities during manufacturing and installation, and need to be determined to ensure that the material responds in a safe, predictable manner during its lifetime. These authors presented a series of results for different crack length and depth, and compared their results with the LSM classical theory (the Irwin model of 1962) and the finite element model, which showed that the current model results ranged from 0.6-0.8% higher, whereas the average percentage difference was found to be 4.2%. The discrepancy increased slightly as the order of the loading increased. Goncalves and Castro reviewed the LSM in 1999, and its implementation in the finite element program i.e. ABAQUS. Some part-through crack configurations in plates were studied and these authors obtained the stress intensity factors for the case of pure tension and pure bending. It was pointed out that the LSM does not take into account the curvature of the crack front and is not a good approximation near the ends where the crack intersects the free surface and in cases where the crack depth varies rapidly.

Liew *et al.*, in 1994, employed the decomposition method to determine the vibration frequencies of cracked plates with any combination of boundary conditions. They assumed the cracked plate domain to be an assemblage of small sub-domains and used the appropriate functions to obtain a governing eigenvalue equation. The results were plotted and compared with those of other authors for a symmetric and anti-symmetric plate mode, for two sets of crack locations. Ramamurti and Neogy, in 1998, applied the generalized Rayleigh–Ritz method to determine the natural frequency of a cracked blade of a turbo-machine, modelled as a cracked non-rotating cantilevered plate. It was found through their results that the cracked frequencies were lower than the corresponding un-cracked frequencies, although the authors were not satisfied with these findings and argued that the natural frequency is not a good criterion for damage detection. Similarly Neogy and Ramamurti, in 1997, proposed a model of a damaged blade, and the damage was in the form of non-propagated crack for determining the natural frequency, however at this time they modelled a blade as a rotating shell. In their findings, they

observed that the effect of rotation in the first mode was very pronounced but the effect of the crack was marginal, and so rotation failed to alter considerably the pattern of frequency reduction. In the case of the second and third modes both the crack and the rotation produced noticeable effects and the relatively larger effect of rotation to the decrease in frequency was observed. Therefore, it was concluded from these results that the small cracks in turbine blades, when modelled as a cantilevered plate, cannot easily be detected by the natural frequency criterion.

At the start of the 21st century, Khadem and Rezaee, in 2000(a), introduced a new technique for the vibration analysis of cracked plates and considered the effect of compliance due to bending only. Later in 2000(b), they established an analytical approach for damage in the form of a crack in a rectangular plate using the application of external load for different boundary conditions. They concluded from their results that the presence of a crack at a specific depth and location would affect each of the natural frequencies differently. Wang *et al.*, in 2003, extended a boundary collocation method based on complex variable theory which was proposed for calculating the stress intensity factors of cracks in a finite plate. Five examples including a rectangular/circular plate with a central crack, a rectangular plate with a slanted crack, a simply supported plate with a central crack and a plate with two cracks were discussed, and it was concluded that good agreement for short cracks was evident with those obtained by other methods. Wu and Shih, in 2005, theoretically analyzed the dynamic instability and nonlinear response of simply supported cracked plates subjected to a periodic in-plane load. The incremental harmonic balance method was applied to solve the nonlinear temporal model. Their results indicated that the stability behaviour and the response of the system were governed by the crack location of the plate, the aspect ratio, conditions of in-plane loading, and the amplitude of vibration. They also explained that increasing the crack ratio i.e. the ratio of the crack length to the length of the edge where the crack lies or/and the static component of the in-plane load decreases the natural frequency of the system. Purbolaksona *et al.*, in 2006, proposed a dual boundary element method for the geometrically nonlinear analysis of a square cracked plate with fully clamped and simply supported boundary conditions. The results

showed that the normalised stress intensity factors in the membrane of the plate increase significantly after a few increments of the load. However, in bending the normalised stress intensity factors decrease if compared with the linear results.

2.4 Finite Element Approach in Cracked Plate Structures

The Finite Element Method (FEM) has also been employed for the study of the vibration of cracked structures and is very useful in analysing real engineering constructions. Cracked plates can be modelled in many ways using FEM. Circular or penny-shaped cracks and an elliptical crack completely embedded in a finite thickness plate subjected to uniform tension were analyzed by Raju and Newman in 1979 using a three dimensional FE model. Isoparametric and singular elements were used in combinations to model elastic bodies with cracks. The calculated stress intensity factors for these crack configurations were compared with the exact solutions to verify the validity of the FEM as used, and concluded that the stress intensity factors for embedded circular and elliptical cracks were generally about 0.4-1% below the exact solutions. However, for the elliptical crack the calculated stress intensity factors in the region of the sharpest curvature of the ellipse were about 3% higher than the exact solution.

Markström and Storàkers, in 1980, obtained a solution which was based on separating the nodes of the elements on both sides of the crack. The buckling characteristics of cracked elastic plates subjected to uni-axial tensile loads were analyzed by the aid of a FEM which was based upon linear bifurcation theory. Centrally cracked plates and some edge cracked members were tested in detail and the results were presented for the symmetric and anti-symmetric mode of cracked plates. In 1983, Alwar and Nambissan proposed that stress intensity factors can be obtained for finite rectangular plates by the use of FE techniques. Three dimensional isoparametric singular brick elements were used to analyse the bending of plates with cracks. This analysis showed the values of stress intensity factor to be about 5-10% higher than the two dimensional analysis and these authors found that the stress intensity factor varied in a nonlinear fashion across the plate thickness.

Qian *et al.*, in 1991, built a FEM of cracked plates using the integral of the stress intensity factor, and used this to solve the vibration problem of a damaged plate, one with a crack at the centre of a simply supported and a cantilever type square plate. In these cases mesh subdivision in the neighbourhood of the crack tip was unnecessary, and the time of the numerical computations was short. These authors compared their results with the model of Solecki (1983) with good agreement. Krawczuk, in 1993, presented a FE model based on the stiffness matrix for a rectangular plate and shell consisting of a through, non-propagating, open crack. He studied the effects of the crack length and location on the changes of the eigenfrequencies of the simply supported and cantilever rectangular plate. The centre of the crack was located in the middle of the span of the element and assumed a linear normal stress and constant shear stress distribution across the crack element. It can be concluded from this work that decreasing natural frequencies are a function of the length and location of the crack, the modes shape, and the boundary conditions of the plate. Later, in 1994 similar findings were obtained except that Krawczuk showed the influence of the crack length and its location upon the amplitudes of the transverse forced vibration for aluminium cantilevered cracked plates and beams, and found that an increase in the transverse forced vibration amplitude of the cracked plate was a function of the crack location and its length. Further studies show that Krawczuk *et al.* introduced elasto-plastic properties into cracked plates in 2001. Su *et al.*, in 1998, extended the fractal two level finite element method (F2LFEM) to analyze the free vibration of a thin cracked plate with arbitrary boundary conditions. The results for a simply supported centre cracked square plate subjected to edge moments for three modes of vibrations were compared with the model of Stahl and Keer (1972).

Saavedra and Cuitino suggested in 2002 an improved FE model for studying the dynamic behaviour of a test rotor affected by the presence of a crack in the shaft. The results indicated that changes in the shaft orbits with rotational speed were the indication of crack identification. It was also observed that at a sub-harmonic resonance experienced a peak when the rotating speed coincided with half of the first natural frequency of the system. Furthermore, these authors observed another characteristic that was an important

indication of the existence of a crack in the case of low rotational speed when the unbalance effects were negligible, and found that the vibration at the excitation frequency was due to the crack. Numerical results were in good agreement between the analytical model and the experimental work. Fujimoto *et al.*, in 2003, reported a vibration analysis of rectangular plates subjected to a tensile load and containing a centrally located crack along the line of symmetry perpendicular to the direction of the tensile load. These authors used the FEM for finding the eigenvalue analysis, and the body force method was implemented for in-plane stress analysis associated with the eigenvalue analysis. Their numerical and experimental results confirmed that the natural frequencies of all vibration modes increased monotonously with increase in tensile load, whereas the rate of increasing frequency depended upon the mode shapes. It was also observed that this method was well suited to the plate with a long crack and that this showed noticeable variations of mode shapes for a small range of tensile load. Failure assessment of a cracked plate subjected to biaxial loading was presented by Kim *et al*. in 2004. Their analyses were based on two dimensional and three dimensional elastic-plastic finite element analysis, while the through thickness and semi elliptical surface crack was considered in the plate. It was found that the effect of biaxiality on crack tip stress triaxiality was more pronounced for a thicker plate and in the case of semi elliptical surface cracks, the crack aspect ratio was found to be more important than the relative crack depth, and the effect of biaxiality on crack tip stress triaxiality was found to be more pronounced near the surface points along the crack front.

2.5 Damage Detection Methodologies in Plate Structures

The field of damage detection has received considerable attention during the past few years and a major collection of literature is now available. Cawley and Adams, in 1979(a), proposed a method which described a non-destructive assessment of the integrity of structures using measurement of the structural natural frequencies. This model was based on reducing the elastic coefficients of the element at the crack location. The main disadvantage of this method was that the reduced elastic coefficients were not related to the real dimensions of the crack. It was shown how measurements made at a single

point in the structure could be used to detect, locate and roughly to quantify damage in a wide variety of one and two dimensional structures. In 1979(b) these authors developed an experimental method to estimate the location and depth of the damage from the changes in the natural frequencies. Cornwell *et al.*, in 1999, used a strain energy method to detect and locate damage in plate-like structures. This method required the mode shapes of the structure before and after damage. The algorithm was found to be effective in locating areas with stiffness reductions as low as 10% using relatively few modes.

In 2002, Yan and Yam detected damages in composite plates by using wavelet analysis to decompose the dynamic responses. An application of spatial wavelet theory to damage identification in structures was initially proposed by Liew and Wang in 1998. The damage was in the form of crack and considered a simply supported beam with a transverse on-edge non-propagating open crack for modelling the problem. They calculated the wavelets along the length of the beam based on the numerical solution for the deflection of the beam. The damage location was then indicated by a peak in the variations of some of the wavelets along the length of the beam. Krawczuk *et al.*, in 2003, and later in 2004, applied a versatile numerical approach for the analysis of wave propagation and damage detection within cracked plates. They considered the spectral plate element as a tool for the investigation of such phenomena and showed that when a propagating wave runs to the crack location of the plate it divides itself into two signals, which show an indication of the damage section. Chang and Chen, in 2004, presented a spatial wavelet approach for damage detection in a rectangular plate with clamped edges on four sides. In this method the only need was for spatially distributed signals in terms of displacement, or mode shapes of the rectangular plate after damage. These spatially distributed signals can be obtained by FEM and can then be analysed by wavelet transformation. The results showed that the distributions of the wavelet coefficients can identify damage position by showing a peak at this location. However, some indications of damage were also observed at the clamped edges of the rectangular plate. Therefore, it was concluded that it was very hard to detect the crack position at the edges. In 2004, Epureanu and Yin monitored

structural health while employed vibration based damage detection. They investigated a panel excited by flow induced loads and considered the nonlinearity resulted from the stretching and bending of the panel. The panel was modelled as a one dimensional, homogenous, isotropic and elastic thin plate with spring-supported end points. This method used probability density functions for determining the structural response. These authors argued that nonlinearities interfered with linear behaviour, and small parameter variations were difficult to detect using linear methods, and that this lack of sensitivity arose from the fact that linear methods minimized the influence of nonlinearities. Vibration based damage detection and location in an aircraft wing scaled model was studied by Trendafilova in 2005. In this study localised and distributed damage was considered, and a simplified FEM in ANSYS was used to model the problem for the vibration response. The wing was split into five volumes for the purpose of analysing the damage detection for the first ten natural frequencies. It was shown that the cracks of length less than half of the wing width are undetectable in the case of localised damage, whilst in the case of distributed damage damage less than 30% in any of the volumes was not detectable using natural frequencies. The author proposed in her concluding remarks that changes in the lower modal frequencies were affected by damage close to the wing root, and their changes decreased when the damage moved towards the wing tip, or conversely the higher frequencies were more affected by damage close to the wing tip and their changes increased when damage moved from the wing root towards the tip. Later in 2006, Trendafilova *et al.* applied a similar technique for vibration based damage detection in aircraft panels modelled as isotropic plates with a crack at some specified location, and they obtained extremely good results.

The modal frequencies are often used as a principal parameter for determining how a structure will respond to a known dynamic forcing, or, as the main parameter for vibration health monitoring of structures. In this connection, Gorman *et al.*, in 2006, used the modal frequencies approach for the vibration health monitoring of a coupled plate/fluid interacting system. A theoretical-analytical method based on the Galerkin method was developed for the frequency–modal analysis and the theory was further extended to

describe the natural coupled modes in terms of the relative energy associated with each of the two sub-systems of the plate and the fluid.

2.6 Damaged Plates of Various Sizes and Shapes

The past literature covers different types of plate structures from rectangular to circular shapes for the analysis of damage detection. Shawki *et al.*, in 1989, formulated the power-law line spring model for deep cracks in a fully-plastic semi-infinite body subjected to remote tension and bending to find the stress intensity factors and they implemented the model within the ABAQUS FE program. These authors also applied the LSM to three dimensional structural problems with semi-elliptical surface cracks which revealed the shifting of the loading axis with increasing loads and indicated the change in the local ratio of bending to tension. Lee, in 1992, introduced a method based on Rayleigh's principle and the sub-sectioning of plate domains for the determination of the fundamental frequency of annular plates. This method can be applied to annular plates with various boundary conditions, however, only the first natural frequency of the plate can be determined. The results showed that the fundamental frequency increases when the crack is located near one of the two edges and on the other hand the fundamental frequency decreases with increasing crack length for a crack located near the centre between the two edges. The determination of the dynamic stress intensity factor (DSIF) in structures having a stationary crack can provide information about crack propagation as reported by Polyzos *et al.* in 1994. They employed a frequency-domain boundary element method for the computation of the DSIF for cracked viscoelastic plates in conjunction with the numerical Laplace transform and the corresponding principle of linear viscoelasticity along with quarter-point boundary elements. Their results showed that viscoelasticity generally reduced the plate response.

Lele and Maiti, in 2002, extended the work of crack location detection in short beams based on frequency measurement by taking into account the effects of rotational inertia and shear deformation. A series of case studies was presented to justify this work for different locations of the crack in the short beam. The results presented in this paper were not so encouraging due

to the fact that the errors in the natural frequencies were in a reasonable range for first mode, whilst the error increased for second and third modes of vibration. Bamnios *et al.*, in 2002, investigated the influence of a transverse open crack in beams using mechanical impedance under different boundary conditions, both analytically and experimentally. These authors modelled the crack by an appropriate equivalent spring connecting the two segments of the beam. The results of this work showed that the mechanical impedance of the beam strongly depends on the size and location of the crack. The location of the crack was found by the indication of jumps in the slope of the response curve depending upon the crack's depth. The proposed method lacked accuracy for small cracks of $a/w < 0.20$ (a is the depth of the crack and w is the amplitude). Horibe and Watanabe, in 2006, proposed an inverse method that used a genetic algorithm (GA) for the identification of width and position of the cracks derived from changes in the natural frequencies in plate structures. In this method, the natural frequencies were calculated by FEM which was based on the Bogner, Fox and Schmidt model and employed the response surface method (RSM) for minimising the processing time. They discussed two types of crack in the analysis comprised internal and edge cracks for a cantilever, and a plate with two ends clamped. The results showed that the proposed method provides satisfactory identification of cracks in plates and explained the fact that the problem within the approximation accuracy of the interpolation function, and rapid changes in natural frequency could not be resolved due to coarse lattice-point intervals.

2.7 Solution Methodologies

Differential equation solution for beams and plates is a vast topic with many variations, although there is a consistent stream of more popular methods. These can be broken down into two solution groups the first being exact analytical solutions and the second being approximate solutions. A limited number of exact solutions exist and these are for fairly specific conditions. There are 21 independent boundary conditions that can be applied to rectangular plates. Leissa, in 1973, detailed these boundary conditions for rectangular plates, pointing out that the only exact solutions known were for the six cases of plates with simply supported opposite edges. Later, Leissa, in

1993, studied a wide range of plates and explained how to obtain the mode shapes and natural frequencies. Navier also proposed an exact method to solve these equations using a double Fourier series [Szilard, 2004]. Navier's solution, or Levy's solution, is valid for plates with simply supported edges and still remains the basic approach for the solution of plates. In methods for the solution of plate problems which are not based on differential equations, the beam function with free edges can be successfully applied, however, where the solution is based on differential equations of the plate, the beam function for free edges will give incorrect results, as discussed by Mukhopadhyay in 1979, who presented a numerical method for the solution of rectangular plates having different edge conditions and loading.

The most common and readily available solutions are those of the approximate techniques. These range from the familiar Rayleigh-Ritz technique [Warburton, 1954] to the hierarchical finite element technique [Han and Petyt, 1996]. In the case of Warburton's and Leissa's analysis they used the Rayleigh-Ritz technique in conjunction with beam functions to obtain approximate solutions for the remaining 15 boundary conditions [Leissa, 1973]. This technique is still widely used and can be found in a large assortment of the literature, referenced in Leissa's monograph (1993). Similarly, the Ritz method was applied by Young in 1950, and investigated the set of functions defining the normal modes of vibration of a uniform beam, and this author obtained a solution for the plate problem with more than one set of boundary conditions. Nagaraja and Rao, in 1953, and Stanišić, in 1957, obtained an approximate solution to the dynamical behaviour of rectangular plates for different boundary conditions. In these studies the Rayleigh-Ritz and Galerkin methods were adopted for the analysis.

The wide use of the finite difference technique to obtain solutions to problems of mathematical physics is also evident in the beam and plate literature. Szilard, in 2004, details this technique for multiple plate applications in his famous book, *Theories and Applications of Plate Analysis*, in order to develop this technique to plates with irregular boundaries and also plates with orthotropic properties. In the 1970s and early 1980s nonlinear plate elements were being developed using the FE techniques. The finite element technique is currently a popular technique within the field of

numerical solutions. One of the more recent finite element solution techniques for the linear plate problem is the hierarchical finite element method (HFEM) [Han & Petyt, 1996, and Ribeiro & Petyt, 1999]. These authors showed that this technique can be advantageous in that it reduces the number of degrees of freedom that must be used to yield an accurate result, when compared with the linear finite element method. They also used the harmonic balance method in conjunction with HFEM. The HFEM, which uses high-order polynomial displacement functions, allows the entire plate to be modelled with one element. This technique is illustrated for both isotropic and laminated plates by Han and Petyt in 1997. Later, Leung and Zhu, in 2004, applied the same technique for the analysis of nonlinear free and forced vibration of skew and trapezoidal Mindlin plates.

Prabhakara and Chia, in 1977, used the method of Fourier cosine series and applied it to analyze the dynamic of von Karman-type equations of the plate with all clamped and all simply supported stress free edges. These results showed that the nonlinear frequency increased with its amplitude and hence only a hardening type of nonlinearity was observed.

Wykes, in 1982, used Electronic Speckle Pattern Interferometry methods (ESPI) to measure the dynamic surface displacement followed by Wang *et al.*, in 1996, who used ESPI technique for vibration measurement, and compared three image processing methods based on time averaged techniques comprised the video-signal addition method, the video-signal-subtraction method, and the amplitude-fluctuation method, and found that amplitude-fluctuation method produced the best visibility. Liu and Lam, in 1994, provided a valuable technique for detecting horizontal cracks and determined both the length and depth of the crack by exciting the anisotropic laminated plate with harmonic loads moved along the plate surface. Numerical experiments were undertaken by using the strip element method.

Solutions for the nonlinear equations have been examined extensively in the literature. These solutions are substantially more complicated in the geometrically nonlinear case than those discussed for the linear problem. However, some of the same solution techniques are applied in the nonlinear case as applied in the linear variant, with little modification. Exact solutions

to the nonlinear plate are obviously difficult to obtain. To the author's best knowledge, no exact solutions exist for the dynamic behaviour of nonlinearly deflecting rectangular plates, but approximate solution techniques exist for some nonlinear plate problems. Generally these solutions either use approximating functions, or these assume certain terms to be negligible, or these use some form of finite discretisation method. Chia, in 1980, published an excellent compilation of information on nonlinear plates, and many of the methods needed to solve different plate problems, in his book, *Nonlinear Analysis of Plates*. One of the very prominent techniques found in the literature is attributed to Berger, in 1955, and consequently referred to as Berger's formulation. Writing the standard energy expression at the mid-plane of the plate, Berger assumed that the second strain invariant is negligible. This then results in decoupling and linearisation of the governing equations. Although, the caveat with this assumption is that there is no direct physical interpretation of the validity of the assumption used. Many other authors use the Berger technique in their analysis of a multitude of plate problems. In Leissa's monograph (1993) other techniques are illustrated which extend the Berger technique to include the vibrational behaviour of these nonlinear plates. Part of this approach is to assume a solution based on the spatial modes and on some function in time. This has been shown, in this thesis, to reduce to the well known Duffing oscillator problem.

Another very popular technique is the double series, typically a Fourier series, although in some cases a one term or single-mode solution is used for the transverse deflection [Han and Petyt, 1997]. Teng *et al.*, in 1999, used a Fourier series to obtain a governing equation for nonlinear plates that is exactly the well known Duffing equation. Lighthill's extension of the perturbation method was then used and a transient solution for rectangular plates under blast loading was obtained.

Hamilton's principle has also been applied by Benamar *et al.* (1990) to examine the changes in mode shapes and frequencies of vibration in nonlinear clamped plates and beams. A dependence on mode shapes and frequencies was found, curvatures near the clamped edge increased as the deflection increased. Also spatial distortion was analysed and it was found that there is an interaction at large deflection between the first and higher order odd

symmetric modes. This technique was also applied to symmetrically laminated rectangular plates by Beidouri (2006), and by El Bikri (2003) to rectangular plates with a combination of simply supported and clamped boundary conditions.

Vibration solutions for damaged plates have been investigated using various methods in the past, as has already been discussed in detail in section 2.3. Each solution technique is of some form of special relevance and treatment involves some particular type of approximations. A brief introduction to the methods used follows on. The finite displacement method was used by Petyt (1968) and the finite Fourier transform was used by Hirno and Okazaki (1980), Nezu (1982) and Solecki (1975) for their analyses. Ali and Atwal (1980) used Rayleigh's method for studying the natural vibration of rectangular plates with cut-outs, followed by the work of Ramamurti and Neogy (1998) who applied the Rayleigh-Ritz method for damaged plate structures. The finite element method is a fast growing technique which has also been applied to cracked plates by many researchers, such as Raju and Newman (1979), Markström and Storàkers (1980), Qian *et al*. (1991), Krawczuk (1992), Su *et al*. (1998), Saavedra and Cuitino (2002), and Fujimoto (2003) etc.

The method to be applied in this dissertation is the perturbation method of multiple scales. It has been previously applied in linear case of parametrically excited systems, and nonlinear cases for different structures. However, no literature has been found for its use in the case of damage in the form of cracks in plates. Comparisons are made with other papers and experimental results, and some reasonable agreement between the solutions has been found, which is discussed further.

2.7.1 Perturbation Theory

The development of basic perturbation theory for differential equations was fairly complete by the middle of the 19th century, when the French astronomer, mathematician and physicist Pierre Simon Laplace (1749–1827) was the first to use perturbation methods to solve the problem of equilibrium of a large weightless drop on a plane. It was at that time that Charles-Eugène Delaunay (1816–1872) was studying the perturbative expansion for the Earth-

Moon-Sun system, and discovered the so-called problem of small denominators.

The perturbation method is only capable of treating problems with weak nonlinearity, and quickly becomes difficult to work with when calculating higher order approximations, therefore other techniques must be explored in order to obtain results for stronger nonlinearity. Many perturbation methods have been envisaged in the resolution of nonlinear problems. These include such well established methods as Incremental Harmonic Balance (IHB), Averaging, Krylov-Bogolioubov (KB), Krylov-Bogolioubov-Mitropolski (KBM), Lindstedt-Poincaré (LP) and the Method of Multiple Scales (MS).

Many authors such as Lau and Cheung (1981), Lau *et al.* (1984), and Pierre and Dowell (1985) have all applied the IHB method to various problems in nonlinear dynamics. In addition, Pierre *et al.*, in 1985, proposed a multi-harmonic analysis of a dry, friction damped system using the IHB method, where they found that the IHB method can yield very accurate results over the time domain methods. Ferri, in 1986, showed the equivalence of the IHB method and the harmonic balance Newton Raphson method. Cheung and Lu, in 1988, presented a development of a simple algorithm for the implementation of the harmonic balance method for solving a nonlinear dynamic system. The versatility of this algorithm is demonstrated for a variety of nonlinear vibration responses, namely, the combination resonances of hinged-clamped beam, the nonlinear effect on the degenerate vibration modes of a square plate and the nonlinear oscillation of thin rings. Jezequel *et al.* in 1990, proposed a nonlinear synthesis in the frequency domain by using the Ritz-Galerkin-Newton-Raphson method in conjunction with IHB method.

A perturbation solution has also been investigated by Chu and Herrmann (1956) where the dynamic *w-F* formulation (*w* and *F* are the deflection and stress functions respectively) was used. A double sine series was used for the deflection term and a double cosine series was used for the stress function term, but only the first mode shape was accounted for. Lynn and Kumbasar (1967) used the Krylov and Bogoliubov method to solve the integral equation for the vibration analysis of cracked rectangular plates. Rehfield (1973)

applied Hamilton's principle and a perturbation procedure for the nonlinear free vibrations of beams and rectangular plates. Nayfeh (1979) used the perturbation method of multiple scales to solve the differential equations for symmetrically excited circular and rectangular plates, and documented this in the famous book *Nonlinear Oscillations*. Niyogi and Meyers, in 1981, applied the perturbation technique to the nonlinear dynamic response of orthotropic plates and found good agreement with other available numerical results of the time. Chati *et al.*, in 1997, used the perturbation method to predict the nonlinear normal modes of vibration and the associated period of the motion in a cracked beam. Teng *et al.*, in 1999, used the Lindstedt-Poincaré perturbation method and the Fourier series method for analysing the nonlinear dynamics of a square plate subjected to blast loading. Results were plotted for an exponentially decaying load function at various times, and central deflection and bending moments were noted. Wu and Shih (2005) analyzed the dynamic instability and nonlinear response of simply supported cracked plates subjected to periodic in-plane load by the use of the IHB.

2.7.2 The Method of Multiple Scales

The history of multiple scales is more difficult to chronicle than, say boundary layer theory. This is because the method is so general that many apparently unrelated approximation procedures are special cases of it. One might argue that the procedure got its start in the first half of the 19th century. For example, Stokes, in 1843, used a type of coordinate expansion in his calculations of fluid flow around an elliptic cylinder. Most of these early efforts were limited, and it was not until the later half of the 19th century that Poincaré, in 1886, basing his idea on the work of Lindstedt (1882), made more extensive use of the ideas underlying multiple scales in his investigations into the periodic motion of planets. He found that the approximation obtained from a regular expansion accurately described the motion for only a few revolutions of the planet, after which the approximation was incorrect. The error was due, in part, to the contributions of the second term of the expansion. He referred to this difficulty as the presence of a secular term. To remedy the situation, he expanded the independent variable with the intention of making the approximation uniformly valid by removing the

secular term. This idea is also at the heart of the modern version of the method. What Poincaré was missing was the introduction of multiple independent variables based on the expansion parameter [Holmes, 1995].

Various similar methods were later rediscovered by such workers as Whittaker (1914), Schrödinger (1926), and Lighthill (1949) in the contexts of various different applications. Several variants of the method of Lindstedt and Poincaré have been widely used formally in the applied literature since the early 1950s. The books by Nayfeh (1973), Nayfeh and Mook (1979), and Kevorkian and Cole (1981) contain numerous references to this literature. Particular note can be made of the work of Sturrock (1957), Kuzmak (1959), Cole and Kevorkian (1963), Cole (1968), and Levey and Mahony (1968), in which multiscale methods were used in the study of various important oscillation problems, although error estimates are not included in these references. Morrison (1966) and Perko (1969) proved a certain equivalence between the two-variable method of Kevorkian and Cole and the averaging method of Krylov, Bogoliubov, and Mitropolsky, thereby providing such error estimates indirectly, because such estimates had been given for the averaging method in Bogoliubov and Mitropolsky (1961) and Perko (1968) [Smith, 1985]. Classical perturbation methods generally break down because of resonances that lead to what are called secular terms. The first scheme to address this problem is what van Dyke (1975) refers to as the method of strained coordinates. Nayfeh (1986) gave an overview of the perturbation methods used to obtain analytical solutions of nonlinear dynamical systems.

In terms of useful, generic, engineering applications, the method of multiple scales is used to study the local dynamics of weakly nonlinear systems about an equilibrium state. To obtain an approximate analytical solution of a weakly nonlinear continuous system, one can either directly apply a perturbation method to the governing partial differential equations of motion and boundary conditions, or first discretise the partial differential system to obtain a reduced-order model and then apply a perturbation method to the nonlinear ordinary differential equations of the reduced order model. The former procedure is usually referred to as the direct approach. Application of the method of multiple scales, or any other perturbation method, to the reduced-order model, obtained by the Galerkin, or other discretisation

procedures, of a weakly nonlinear continuous system with quadratic nonlinearities can lead to both quantitative and qualitative erroneous results. This is primarily associated with the names of Pakdemirli, Nayfeh S., and Nayfeh (1995), Nayfeh and Lacarbonara (1997), Alhazza and Nayfeh (2001), Emam and Nayfeh (2002), and Nayfeh and Arafat (2002). The direct approach is completely devoid of this problem. Also, such a problem does not exist for systems with just cubic nonlinearities. Lacarbonara, in 1999, showed that quadratic nonlinearities produce a second-order contribution from all of the modes to the system response in the case of a primary resonance. Hence, reduced-order discretisation models may be inadequate to describe the dynamics of the original continuous system in the presence of quadratic nonlinearities. Nayfeh, in 1998, proposed a method for constructing reduced-order models of continuous systems with weak quadratic and cubic nonlinearities that overcomes this shortcoming of the discretisation procedures. Application of the method of multiple scales to dynamical systems expressed in second-order form can lead to modulation equations that cannot be derived from a Lagrangian in the absence of dissipation and external excitation, which is contrary to the conservative character of these dynamical systems. More specifically, this problem is encountered while determining approximate solutions of nonlinear systems possessing internal resonances to orders higher than the order at which the influence of the internal resonance first appears, as associated with the work of Rega *et al.*, (1999). Interestingly, transforming the second-order governing equations into a system of first-order equations and then treating them with the method of multiple scales yields modulation equations derivable from a Lagrangian, and is presented in Nayfeh (2000) and Nayfeh and Chin (1999), and Malatkar (2003).

According to Nayfeh (1973), 'the method of multiple scales is so popular that it is being rediscovered just about every 6 months'. Yasuda and Torii, in 1987, also used multiple scales to obtain the oscillation characteristics of a square membrane near a primary resonance with one nodal line and showed that this method matched experiment results. Although to simplify the analysis, mode shapes composed of a multiple of two sine functions were used and only the (1,2) and (2,1) modes were accounted for. Lee and Park, in 1999, investigated

a weakly nonlinear, harmonically excited, spring pendulum system, which is known to be a good model for a variety of engineering systems. Rahman and Burton, in 1989, proposed a version of the method of multiple scales which can be used to determine the periodic, steady state, primary response of a single degree of freedom, lightly damped, weakly nonlinear, forced oscillator. A comprehensive review of the method of multiple scales has been compiled by Cartmell *et al.*, in 2003, in which they examined the role of term ordering, the integration of the small perturbation parameter within system constants, non-dimensionalisation and time-scaling, series truncation, inclusion and exclusion of higher order nonlinearities, and typical problems in the handling of secular terms. These authors showed in a comparative example that the form of the adopted power series and the ordering terms can have a major bearing on the structure of the solution, with clear suggestion for accuracy and physical relevance. They then gave suggestions on how one can deal with ordering by basing it on some sort of physical appreciation of the problem in terms of hard and soft or strong and weak quantities within the equation of motion such as damping mechanisms, excitation amplitudes, and the coefficients of nonlinear terms. At present, the method of multiple scales has been computerised by means of specialised packages within *Mathematica*™ code constructed by Khanin and Cartmell (1999), Khanin *et al.* (2000) and Khanin and Cartmell (2001) with parallelisation strategies introduced for reasons of optimisation.

2.8 Dynamical Systems and Nonlinear Transitions to Chaos

Chaos theory began as a field of physics and mathematics dealing with the structure of turbulence and the self-similar forms of fractal geometry. It stems, in part, from the work of Edward Lorenz, in 1960, of MIT, a meteorologist, who simulated weather patterns on a computer. The theory of chaos brings the principles of quantum physics to the pragmatic world. At present, it is relatively easy to map chaotic behaviour by the use of various available software. The newly discovered underlying order to chaos sparked new interest and inspired more research in the field of chaos theory. The recent focus of most of the research on chaos theory is specifically on non-

equilibrium statistical mechanics and its applications to quantum systems, and in particular to nano-systems.

The founder of geometric dynamics is universally acknowledge to be Henri Poincaré (1854–1912), who alone among his contemporaries saw the usefulness of studying topological structure in the phase space of dynamical trajectories. The theoretical foundations laid by Poincaré were strengthened by G. D. Birkhoff (1844–1944); but, apart from a few instances such as the stability analysis of Lyapunov, Poincaré's ideas seemed to have had little impact on applied dynamics for almost half a century. In 1927, Van der Pol and Van der Mark reported irregular noise in experiments with an electronic oscillator. It has been well mentioned that chaotic vibrations occur when some strong nonlinearity exits. Some examples of nonlinearities that can be observed in many physical systems are; nonlinear elastic or spring elements, damping, boundary conditions etc. In mechanical continua, nonlinear effects arise from a number of different sources which includes kinematics, constitutive relations, boundary conditions, nonlinear body forces, geometric nonlinearities associated with large deformations in structural solids. [Thompson (1986), and Moon (1987)]

Wolf *et al.*, in 1985, presented a technique which estimated the non-negative Lyapunov exponents from experimental data. Lyapunov exponents are the average exponential rates of divergence or convergence of nearby orbits in phase space. They are positive for chaos, zero for a marginally stable orbit, and negative for a periodic orbit. It means that an attractor for a dissipative system with one or more positive Lyapunov exponents is said to be strange or chaotic. Wolf *et al.* tested this method on famous model systems such as those of Hénon (1976), Rössler (1976), Lorenz (1989), the Rössler-hyperchaos (1979) problem and MacKey-Glass (1997) with known Lyapunov spectra and observed that deterministic chaos can be distinguished in some cases from external noise and topological complexity.

The work by Maestrello, Frendi and Brown in 1992 demonstrated the nonlinear vibration and nonlinear acoustic radiation of a typical aircraft fuselage panel forced by plane acoustic waves at normal incidence, and investigated their finding both experimentally and numerically. Numerically, the nonlinear plate

equations were integrated through the use of an approximate method. The motion normally starts periodically and eventually becomes chaotic with time by the increase of the pressure level. A good agreement between the experimental and numerical results were obtained, which showed that when a panel is excited at a resonant frequency by plane acoustic waves, linear, nonlinear and chaotic responses can be obtained by changing the intensity of the loading. Guitiérrez and Iglesias, in 1998, introduced a *Mathematica*™ package for analyzing discrete and continuous systems, and much of the attention was focused on controlling the chaotic behaviour of these systems. This program is capable of obtaining the periodic points and the stability regions of nonlinear systems, as well as bifurcatory analysis and Lyapunov exponents. These author's results showed a good numerical results for the logistic and Hénon maps as well as for the Duffing and Rössler systems. Alighanbari and Hashemi, in 2003, reformulated the integro-differential aeroelastic equations of motion for an airfoil in an investigation of the potential nonlinear dynamical behaviour of the model. The bifurcation analysis was performed for the airfoil containing a cubic nonlinearity in the pitch stiffness under the action of a two dimensional incompressible flow. An approximate technique in the form of the Defect-Controlled Method and AUTO software package were employed for the analysis. Lyapunov spectra were also calculated to predict and confirm the chaotic behaviour of the airfoil. The result showed good agreement between two methods. Xiao *et al.*, in 2006, derived the nonlinear equations of motion based on Reissner plate theory and the Hamilton variational principle for moderate thickness rectangular plates with transverse surface penetrating cracks on an elastic foundation, under the action of external excitation and from these they investigated the bifurcations and chaotic motion. These nonlinear equations were solved by the use of the Galerkin and the Runge-Kutta integration techniques. It was seen from these results that the plate's motion bifurcated and then moved to more complex motions with the increase of external excitation amplitude. The Poincaré maps showed a double period motion for a nondimensionalised crack position of 0.1 and crack depth of 0.3, and this turned into chaotic motion with the increase in nondimensionalised crack position.

Chapter 3

FORMULATION OF CRACKED PLATES

In this chapter, we derive the equation of motion for a given set of boundary conditions governing the nonlinear vibrations of an isotropic plate with an arbitrarily located part-through crack at the centre of the plate, consisting of a continuous line. The equilibrium principle is followed to derive the governing equation of motion in order to get a tractable solution to the vibration problem. Principally, the effects of rotary inertia and through-thickness shear stress are neglected. Galerkin's method is applied to reformulate the governing equation of the cracked plates into time dependent modal coordinates. The simplifying assumptions, and their validity, are described as and when they are made during the derivation of the equations. Berger's formulation is used to generate the form for the in-plane forces and make the model differential equation of motion nonlinear.

3.1 Governing Equation of Cracked Rectangular Plate

The classical form of the governing equation of rectangular plate is rigorously treated by Timoshenko (1940), Leissa (1993), and Szilard (2004), and so, by neglecting the effect of rotary inertia and through-thickness shear forces, it can be stated that:

$$D\left(\frac{\partial^4 w}{\partial x^4}+2\frac{\partial^4 w}{\partial x^2\partial y^2}+\frac{\partial^4 w}{\partial y^4}\right)=-\rho h\frac{\partial^2 w}{\partial t^2}+n_x\frac{\partial^2 w}{\partial x^2}+n_y\frac{\partial^2 w}{\partial y^2}+2n_{xy}\frac{\partial^2 w}{\partial x\partial y}+P_z. \quad \textbf{(3.1-1)}$$

where w is the transverse deflection, P_z is the load per unit area acting at the surface, ρ is the density, h is the thickness of the plate and n_x, n_y, n_{xy} are the in-plane or membrane forces per unit length. D is the flexural rigidity

and can be defined as $D = Eh^3/12(1-\upsilon^2)$; E is the modulus of elasticity, and υ is the Poisson's ratio.

Initially, the derivation of the governing equation of the plate having a part-through crack consisting of a continuous line of length 2*a* which is located at the centre and parallel to the ***x***-direction of the plate as depicted in Figure 3-1 is performed by considering that the cracked plate is linear with the following basic assumptions. Later, the governing equation of the cracked plate transforms into nonlinear form by the application of Berger's formulation.

1. The plate is made of a perfectly elastic, homogeneous, isotropic material and has a uniform thickness *h* which is considered small in comparison with its other dimensions.

2. All strain components are small enough to allow Hooke's law to hold.

3. The normal stress component in the direction transverse to the plate surface is small compared with other stress components, and is neglected in the stress-strain relationship.

4. Shear deformation is neglected in this case and it is assumed that sections taken normal to the middle surface before deformation remain plane and normal to the deflected middle surface of the plate.

5. The effect of the rotary inertia, shear forces and in-plane force in the y-direction i.e. n_y and n_{xy} are neglected mainly to make the problem more tractable.

For relatively thick plates $\left(\frac{h}{l} > 20\right)$, where *h* is the plate thickness and *l* is an average length in its plane, the effects of shear deformation and rotary inertia become significant, as explained by Leissa (1978). Moreover, in vibration problems, the effect of rotary inertia and shear deformation corresponding to higher modes are more pronounced than on those corresponding to lower modes, and also yields mathematical complexity. In

the present model, the first mode is discussed in more detail, therefore the assumption made that the effect of the rotary inertia, and shear forces are both negligible is applicable in the subsequent derivation.

The equilibrium equations are obtained by resolving the forces in the *z*-direction and taking moments about the *x* and *y*-axes. The forces acting on the plate element are shown in Figure 3-1.

Summing the forces along the *z*-axis leads to,

$$\sum F_z = 0; \quad -Q_x dy + (Q_x + \frac{\partial Q_x}{\partial x} dx)dy - Q_y dx + (Q_y + \frac{\partial Q_y}{\partial y} dy)dx + P_z dxdy = \rho h \frac{\partial^2 w}{\partial t^2} dxdy, \tag{3.1-2}$$

where Q_x and Q_y are the forces per unit length which are projected along z direction, ρ is the density, h is the thickness and P_z is the load per unit area acting over the surface of the plate.

Later, this P_z is replaced by a point load $\bar{P}_z$ based on the application of the appropriate delta function in equation (3.4-8) to make it compatible with the experimental configuration. Furthermore, in practice, it is straightforward to implement this type of loading.

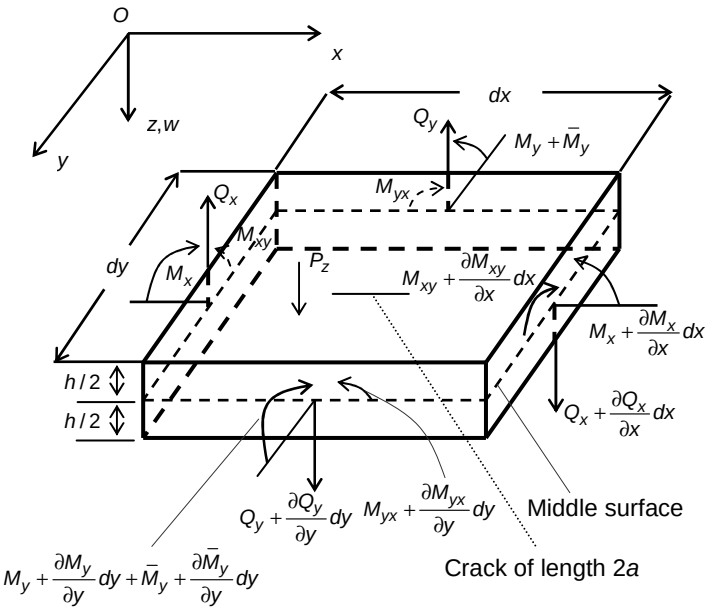

Figure 3-1: Isotropic plate loaded by uniform pressure and a small crack at the centre

Therefore,

$$\frac{\partial Q_x}{\partial x}+\frac{\partial Q_y}{\partial y}=\rho h\frac{\partial^2 w}{\partial t^2}-P_z. \tag{3.1-3}$$

The moment equilibrium about the *y*-axis gives,

$$\begin{aligned}\sum M_y=0;\quad & -M_x dy+(M_x+\frac{\partial M_x}{\partial x}dx)dy-M_{yx}dx+(M_{yx}+\frac{\partial M_{yx}}{\partial y}dy)dx\\ & -(Q_x+\frac{\partial Q_x}{\partial x}dx)\frac{dx}{2}dy-Q_x dy\frac{dx}{2}=0.\end{aligned} \tag{3.1-4}$$

After simplification, the term containing $\frac{1}{2}\frac{\partial Q_y}{\partial x}(dx)^2 dy$ is neglected, since it is a small quantity of higher-order. Therefore,

$$\frac{\partial M_x}{\partial x}+\frac{\partial M_{yx}}{\partial y}=Q_x, \tag{3.1-5}$$

and hence,

$$\frac{\partial^2 M_x}{\partial x^2}+\frac{\partial^2 M_{yx}}{\partial y\partial x}=\frac{\partial Q_x}{\partial x}. \tag{3.1-6}$$

Similarly, the moment equilibrium about the ***x***-axis can be written as,

$$\begin{aligned}\sum M_x=0;\quad & \left(M_y+\bar{M}_y\right)dx-(M_y+\frac{\partial M_y}{\partial y}dy+\bar{M}_y+\frac{\partial \bar{M}_y}{\partial y}dy)dx-M_{xy}dy\\ & +(M_{xy}+\frac{\partial M_{xy}}{\partial x}dx)dy+(Q_y+\frac{\partial Q_y}{\partial y}dy)\frac{dy}{2}dx+Q_y dx\frac{dy}{2}=0.\end{aligned} \tag{3.1-7}$$

After simplification, the term containing $\frac{1}{2}\frac{\partial Q_y}{\partial y}(dy)^2 dx$ is neglected, since it is a small quantity of higher-order. Therefore,

$$-\frac{\partial M_y}{\partial y}-\frac{\partial \bar{M}_y}{\partial y}+\frac{\partial M_{xy}}{\partial x}=-Q_y, \tag{3.1-8}$$

and so,

$$-\frac{\partial^2 M_y}{\partial y^2}-\frac{\partial^2 \bar{M}_y}{\partial y^2}+\frac{\partial^2 M_{xy}}{\partial x\partial y}=-\frac{\partial Q_y}{\partial y}. \tag{3.1-9}$$

where $\bar{M}_y$ is the bending moment per unit length due to the crack at the centre of the plate and this is treated later in section 3.3. Now, substituting equations (3.1-6) and (3.1-9) into equation (3.1-3), gives,

$$\frac{\partial^2 M_x}{\partial x^2} + 2\frac{\partial^2 M_{xy}}{\partial x \partial y} + \frac{\partial^2 M_y}{\partial y^2} + \frac{\partial^2 \bar{M}_y}{\partial y^2} = \rho h \frac{\partial^2 w}{\partial t^2} - P_z \qquad \textbf{(3.1-10)}$$

where M_x, M_y and M_{xy} are the bending moments per unit length along the *x* and *y* directions and can be defined as

$$M_x = \int_{-h/2}^{h/2} \sigma_x \, Z \, dz \qquad \textbf{(3.1-11)}$$

$$M_y = \int_{-h/2}^{h/2} \sigma_y \, Z \, dz \qquad \textbf{(3.1-12)}$$

and,

$$M_{xy} = \int_{-h/2}^{h/2} \tau_{xy} \, Z \, dz \qquad \textbf{(3.1-13)}$$

Also, σ_x, σ_y and τ_{xy} are the stresses along the *x* and *y* directions of the plate and these can be written as

$$\sigma_x = -\frac{EZ}{1-\upsilon^2}\left(\frac{\partial^2 w}{\partial x^2} + \upsilon \frac{\partial^2 w}{\partial y^2}\right) \qquad \textbf{(3.1-14)}$$

$$\sigma_y = -\frac{EZ}{1-\upsilon^2}\left(\frac{\partial^2 w}{\partial y^2} + \upsilon \frac{\partial^2 w}{\partial x^2}\right) \qquad \textbf{(3.1-15)}$$

and,

$$\tau_{xy} = \frac{EZ}{1-\upsilon^2}(1-\upsilon)\frac{\partial^2 w}{\partial x \partial y} \qquad \textbf{(3.1-16)}$$

Substituting the quantities σ_x, σ_y and τ_{xy} from equations (3.1-14), (3.1-15) and (3.1-16) into equations (3.1-11), (3.1-12) and (3.1-13) respectively, we get the following form of M_x, M_y and M_{xy},

$$M_x = -D\left(\frac{\partial^2 w}{\partial x^2} + \upsilon\frac{\partial^2 w}{\partial y^2}\right) \qquad \textbf{(3.1-17)}$$

$$M_y = -D\left(\frac{\partial^2 w}{\partial y^2} + \upsilon\frac{\partial^2 w}{\partial x^2}\right) \qquad \textbf{(3.1-18)}$$

and,

$$M_{xy} = -M_{yx} = -D(1-\upsilon)\frac{\partial^2 w}{\partial x \partial y} \qquad \textbf{(3.1-19)}$$

where D is the flexural rigidity and can be stated as $D = Eh^3/12(1-\upsilon^2)$; E is the modulus of elasticity, and υ is the Poisson's ratio.

Expressing the moments in terms of the curvatures, as given in equations (3.1-17), (3.1-18) and (3.1-19) to (3.1-10), leads to the following result,

$$D\left(\frac{\partial^4 w}{\partial x^4} + 2\frac{\partial^4 w}{\partial x^2 \partial y^2} + \frac{\partial^4 w}{\partial y^4}\right) = -\rho h\frac{\partial^2 w}{\partial t^2} + \frac{\partial^2 \bar{M}_y}{\partial y^2} + P_z. \qquad \textbf{(3.1-20)}$$

3.2 Addition of In-plane or Membrane Forces

In-plane forces occur when the displacements of the plate parallel to its middle surface are constrained by the supports, and we naturally assume small displacements throughout. Occasionally, membrane forces apply at the boundaries and are usually caused by temperature variations, pre-stressing and large deflection. The magnitude of the membrane forces are a function of the boundary conditions. This is easily visualised by considering two different plates, one clamped along its edges to prevent any translation or rotation and the other simply supported along its edges allowing only rotation. For equal maximum displacements, the deflected surface length of the clamped plate is greater than that of the simply supported plate, resulting in higher membrane forces.

Considering the equilibrium of the dxdy element in Figure 3-2, and given that it is subjected to in-plane forces n_x, n_y , $n_{xy} = n_{yx}$ and $\bar{n}_y$ (caused by the crack at the centre of the plate) per unit length, then since there are no body

forces, the projection of the membrane forces on the ***x***-axis leads to the following,

$$-n_x dy + (n_x + \frac{\partial n_x}{\partial x} dx)dy - n_{yx} dx + (n_{yx} + \frac{\partial n_{yx}}{\partial y} dy)dx = 0, \qquad \textbf{(3.2-1)}$$

Therefore,

$$\frac{\partial n_x}{\partial x} + \frac{\partial n_{yx}}{\partial y} = 0. \qquad \textbf{(3.2-2)}$$

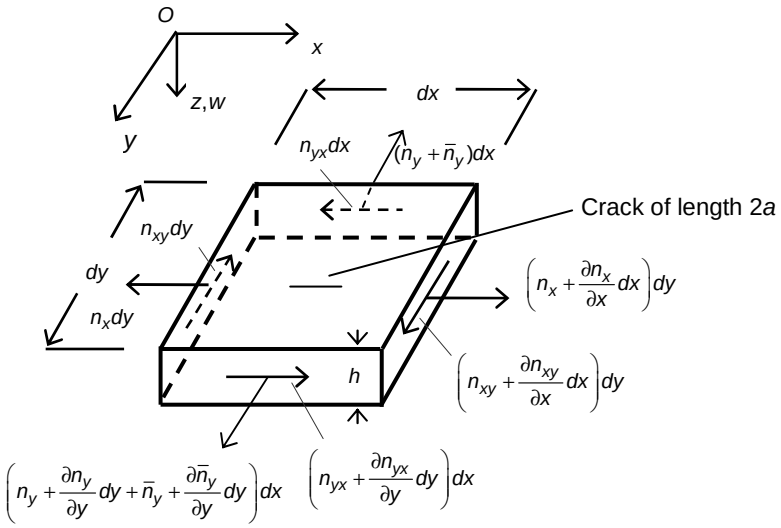

Figure 3-2: In-plane forces and a crack of length 2*a* at the centre of the plate element

Similarly, along the ***y***-axis we find that,

$$\left(-n_y - \bar{n}_y\right)dx + \left(n_y + \frac{\partial n_y}{\partial y} dy + \bar{n}_y + \frac{\partial \bar{n}_y}{\partial y} dy\right)dx - n_{xy} dy + \left(n_{xy} + \frac{\partial n_{xy}}{\partial x} dx\right)dy = 0. \qquad \textbf{(3.2-3)}$$

leading to,

$$\frac{\partial n_y}{\partial y} + \frac{\partial \bar{n}_y}{\partial y} + \frac{\partial n_{xy}}{\partial x} = 0 \qquad \textbf{(3.2-4)}$$

The equilibrium of the dxdy element in the *z* direction is considered next. It is arbitrarily assumed that the left hand and rear edges of the plate element are fixed and lie in the ***xy*** plan, as shown in Figure 3-3. Other boundary conditions are equally possible.

$$\sum F_z(x,y) = \left(n_x + \frac{\partial n_x}{\partial x}dx\right)dy\frac{\partial^2 w}{\partial x^2}dx + \left(n_y + \frac{\partial n_y}{\partial y}dy + \bar{n}_y + \frac{\partial \bar{n}_y}{\partial y}dy\right)dx\frac{\partial^2 w}{\partial y^2}dy$$
$$+\left(n_{xy} + \frac{\partial n_{xy}}{\partial x}dx\right)dy\frac{\partial^2 w}{\partial x \partial y}dx + \left(n_{yx} + \frac{\partial n_{yx}}{\partial y}dy\right)dx\frac{\partial^2 w}{\partial y \partial x}dy, \qquad \textbf{(3.2-5)}$$

So, after neglecting higher order quantities, we obtain,

$$\sum F_z(x,y) = n_x\frac{\partial^2 w}{\partial x^2} + n_y\frac{\partial^2 w}{\partial y^2} + \bar{n}_y\frac{\partial^2 w}{\partial y^2} + 2n_{xy}\frac{\partial^2 w}{\partial x \partial y}. \qquad \textbf{(3.2-6)}$$

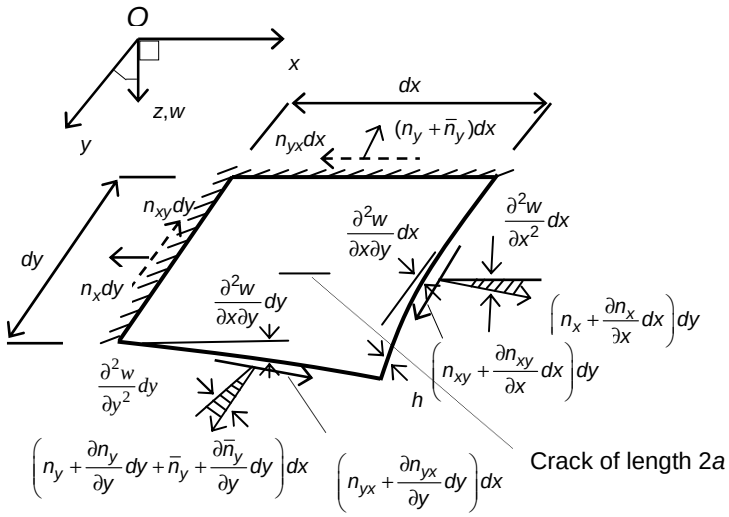

Figure 3-3: Two sided constraints and plate deformation having a part-through crack at the centre

Thus, it can be deduced from equation (3.2-6) that the effect of the membrane forces on the deflection is equivalent to an assumed lateral force, denoted here by $F_z(x,y)$. Adding this to the lateral forces in the governing equation, and noting that this force acts just in the ***x***-direction, then the terms in the ***y*** and ***xy*** directions can be neglected; leading to the final version of equation (3.1-20) which now takes the following form:

$$D\left(\frac{\partial^4 w}{\partial x^4} + 2\frac{\partial^4 w}{\partial x^2 \partial y^2} + \frac{\partial^4 w}{\partial y^4}\right) = -\rho h\frac{\partial^2 w}{\partial t^2} + n_x\frac{\partial^2 w}{\partial x^2} + \frac{\partial^2 \bar{M}_y}{\partial y^2} + \bar{n}_y\frac{\partial^2 w}{\partial y^2} + P_z. \qquad \textbf{(3.2-7)}$$

Equation (3.2-7) is the equation of motion for the cracked vibrating plate, and for the case of free vibration $P_z = 0$. The value of w should be such that it must satisfy the boundary conditions at the edges of the plate.

3.3 Crack Terms Formulation

Machines and structural components potentially require continuous monitoring for the detection of cracks and crack growth for ensuring an uninterrupted service in critical installations. Cracks can be present in structures due to various reasons such as impact, fatigue, corrosion and external and environmental factors like temperature, relative humidity, rainfall and the general properties of structures. Complex structures such as aircraft, ships, steel bridges, sea platforms etc., all use metal plates. The presence of a crack does not only cause a local variation in the stiffness, but can affect the mechanical behaviour of the entire structure to a considerable extent. Cracks present in vibrating components can lead to catastrophic failure. [Neogy and Ramamurti (1997), Ramamurti and Neogy (1998), Trendafilova (2005), Trendafilova *et al*. (2006)]. For these reasons, there is a need to understand the dynamics of cracked structures. The vibration characteristics of structures can be useful for on-line detection of cracks without actually dismantling the structure. In particular, the natural frequencies and mode shapes of cracked plates can provide insights into the extent of damage.

In the present theory, the Rice and Levy (1972) model is used for the formulation of the crack terms. This approach is based on Kirchoff's bending theory for thin plates and shells. The assumptions involved in this theory lead to important simplifications in the governing equations. Accurate values for the stress intensity factors in part-through cracked plates can be calculated, provided that the crack is not too deep. Rice and Levy, 1972, obtained an approximate relationship between nominal tensile and bending stresses at the location of the crack. These two relations are taken after some rearrangement, and then by making use of the relationships within equations (3.3-8) and (3.3-9) it can be shown that $m_{rs} = 6\sigma_{rs}$. A representation of these stresses is given in Figure 3-4.

$$\bar{\sigma}_{rs} = \frac{2a}{\left(6\alpha_{tb}^{o} + \alpha_{tt}^{o}\right)(1-\upsilon^2)h + 2a}\sigma_{rs}, \qquad \textbf{(3.3-1)}$$

and,

$$\bar{m}_{rs} = \frac{2a}{3\left(\frac{\alpha_{bt}^{o}}{6} + \alpha_{bb}^{o}\right)(3+\upsilon)(1-\upsilon)h + 2a} m_{rs}. \qquad \textbf{(3.3-2)}$$

We define $\bar{\sigma}_{rs}$ and $\bar{m}_{rs}$ as the nominal tensile and bending stresses respectively, at the crack location and on the surface of the plate, σ_{rs} and m_{rs} are the nominal tensile and bending stresses at the far sides of the plate, h is the thickness of the plate, a is the half length of the crack, and α_{bb}^{o}, α_{tt}^{o}, $\alpha_{bt}^{o} = \alpha_{tb}^{o}$ are the non-dimensional bending compliance, stretching compliance and stretching-bending compliance coefficients at the crack centre, respectively.

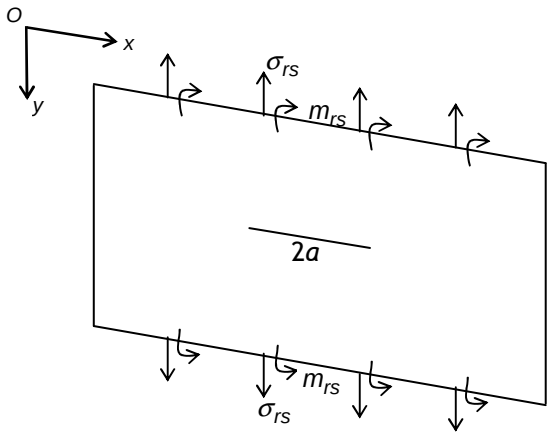

Figure 3-4: Line Spring Model (LSM) representing the bending and tensile stresses for a part-through crack of length 2*a*, after Rice and Levy, 1972

These relationships show that the nominal tensile and bending stresses at the crack location can be regarded as a function of the nominal tensile and bending stresses at the far side of the plate. It is worth noting that Okamura *et al*. (1969) and Khadem and Rezaee (2000) also restricted their analysis to the effects of bending compliance, and thus avoided the coupling effect by ignoring the stretching compliance. These three compliance coefficients depend upon the crack depth d to plate thickness h and vanish when $d = 0$. It has been shown by Rice and Levy (1972) that in general the compliance coefficient is a function of the ratio of crack depth to plate thickness, and can be calculated as:

$$\alpha_{\lambda\mu}(X) = \alpha^{o}_{\lambda\mu}\sqrt{1-X^2}\;; \quad \lambda,\mu = b,t \tag{3.3-3}$$

where $X = x_1/a$ is a dimensionless variable introduced for simple approximation. x_1 shows the values along crack length and a is the half-crack length. Also, $\lambda,\mu = b,t$ are intermediate variables proposed by Rice and Levy, 1972, for algebraic simplification. Let set $x_1 = a/2$ then the dimensionless compliance coefficient at the centre of the cracked plate takes this form,

$$\alpha^{o}_{\lambda\mu} = 1.1547\,\alpha_{\lambda\mu}, \tag{3.3-4}$$

The appropriate compliance coefficients, $\alpha_{\lambda\mu}$, may then be calculated from the following relation, noting that these equations were originally presented as being for the range $0 < \zeta = d/h < 0.7$ [Okamura *et al.* (1969), Rice and Levy (1972), and Khadem and Rezaee (2000)]. In the present analysis, we take $\zeta = 0.6$, leading to calculation of the compliance coefficients as follows:

$$\alpha_{tt} = \zeta^2\begin{pmatrix}1.98 - 0.54\zeta^1 + 18.65\zeta^2 - 33.70\zeta^3 + 99.26\zeta^4\\ -211.90\zeta^5 + 436.84\zeta^6 - 460.48\zeta^7 + 289.98\zeta^8\end{pmatrix}, \tag{3.3-5}$$

$$\alpha_{bb} = \zeta^2\begin{bmatrix}1.98 - 3.28\zeta^1 + 14.43\zeta^2 - 31.26\zeta^3 + 63.56\zeta^4\\ -103.36\zeta^5 + 147.52\zeta^6 - 127.69\zeta^7 + 61.50\zeta^8\end{bmatrix}, \tag{3.3-6}$$

and,

$$\alpha_{bt} = \alpha_{tb} = \zeta^2\begin{bmatrix}1.98 - 1.91\zeta^1 + 16.01\zeta^2 - 34.84\zeta^3 + 83.93\zeta^4\\ -153.65\zeta^5 + 256.72\zeta^6 - 244.67\zeta^7 + 133.55\zeta^8\end{bmatrix}. \tag{3.3-7}$$

This means that uniformly distributed tensile and bending stresses are at the two sides of the crack location, and these tensile and bending stresses can be expressed in term of tensile and bending force effects. Therefore, we can write the tensile and bending stresses at the far sides as, [Rice and Levy, 1972],

$$\sigma_{rs} = \frac{n_{rs}}{h} = \frac{1}{h}\int_{-h/2}^{+h/2}\tau_{rs}(x,y,z)dz, \tag{3.3-8}$$

$$m_{rs} = \frac{6}{h^2} M_{rs} = \frac{6}{h^2} \int_{-h/2}^{+h/2} z\tau_{rs}(x,y,z)dz, \qquad \textbf{(3.3-9)}$$

where $r,s = 1,2$ are intermediate variables required for algebraic simplification. n_{rs} and M_{rs} are the force and moment per unit length in the *y*-direction at the far sides of the plate, respectively, and $\tau_{rs}(x,y,z)$ is the stress state. Subsequently, the force and moment were calculated from two-dimensional plane stress plate bending theory, with the cracked section represented as a continuous line spring having its compliance matched to that of the edge cracked strip in plane strain as shown in Figure 3-4. Accordingly, we can write equations (3.3-1) and (3.3-2) in the form of force and moment as,

$$\bar{n}_{rs} = \frac{2a}{\left(6\alpha_{tb}^{o} + \alpha_{tt}^{o}\right)(1-\upsilon^2)h + 2a} n_{rs}, \qquad \textbf{(3.3-10)}$$

and,

$$\bar{M}_{rs} = \frac{2a}{3\left(\frac{\alpha_{bt}^{o}}{6} + \alpha_{bb}^{o}\right)(3+\upsilon)(1-\upsilon)h + 2a} M_{rs}, \qquad \textbf{(3.3-11)}$$

where $\bar{n}_{rs}$ and $\bar{M}_{rs}$ are the force and moment per unit length in the *y*-direction at the crack location of the plate, respectively.

It is evident from the work of Rice and Levy (1972) that when two forces are acting on the plate element to stretch and bend it, the results of their work show that the Airy stress function satisfies the compatibility condition in a region where the body force field is zero. Here, it is very useful to mention that the present theory, and the model of Rice and Levy, are both based on classical plate theory; therefore the force and moment obtained from equations (3.3-10) and (3.3-11) are the required terms and are added into the cracked plate model with a negative sign because damage causes a reduction in the overall stiffness of the plate structure, a phenomenon which can also be seen in most of the literature, such as that of Keer and Sve (1970), Stahl and Keer (1972), Solecki (1983), and Khadem and Rezaee (2000). Therefore, we can write,

$$\bar{n}_y \equiv -\bar{n}_{rs} = -\frac{2a}{\left(6\alpha_{tb}^o + \alpha_{tt}^o\right)(1-\upsilon^2)h + 2a} n_{rs}, \qquad \textbf{(3.3-12)}$$

and,

$$\bar{M}_y \equiv -\bar{M}_{rs} = -\frac{2a}{3\left(\frac{\alpha_{bt}^o}{6} + \alpha_{bb}^o\right)(3+\upsilon)(1-\upsilon)h + 2a} M_{rs}, \qquad \textbf{(3.3-13)}$$

Substituting the values of $\bar{n}_y$ and $\bar{M}_y$ from equations (3.3-12) and (3.3-13) into equation (3.2-7), so the governing equation of the plate with a crack at the centre extends to the following form,

$$D\left(\frac{\partial^4 w}{\partial x^4} + 2\frac{\partial^4 w}{\partial x^2 \partial y^2} + \frac{\partial^4 w}{\partial y^4}\right) = -\rho h \frac{\partial^2 w}{\partial t^2} + n_x \frac{\partial^2 w}{\partial x^2} + P_z - \frac{2a}{3\left(\frac{\alpha_{bt}^o}{6} + \alpha_{bb}^o\right)(3+\upsilon)(1-\upsilon)h + 2a} \frac{\partial^2 M_{rs}}{\partial y^2}$$
$$- \frac{2a}{\left(6\alpha_{tb}^o + \alpha_{tt}^o\right)(1-\upsilon^2)h + 2a} n_{rs} \frac{\partial^2 w}{\partial y^2}. \qquad \textbf{(3.3-14)}$$

As the bending stresses at the far sides of the plate are defined by,

$$M_{rs} = -D\left(\frac{\partial^2 w}{\partial y^2} + \upsilon \frac{\partial^2 w}{\partial x^2}\right), \qquad \textbf{(3.3-15)}$$

then equation (3.3-15) can be substituted into equation (3.3-14) to get the final form,

$$D\left(\frac{\partial^4 w}{\partial x^4} + 2\frac{\partial^4 w}{\partial x^2 \partial y^2} + \frac{\partial^4 w}{\partial y^4}\right) = -\rho h \frac{\partial^2 w}{\partial t^2} + n_x \frac{\partial^2 w}{\partial x^2} + P_z$$
$$+ \frac{2aD\left(\frac{\partial^4 w}{\partial y^4} + \upsilon \frac{\partial^4 w}{\partial y^2 \partial x^2}\right)}{3\left(\frac{\alpha_{bt}^o}{6} + \alpha_{bb}^o\right)(3+\upsilon)(1-\upsilon)h + 2a} - \frac{2a}{\left(6\alpha_{tb}^o + \alpha_{tt}^o\right)(1-\upsilon^2)h + 2a} n_{rs} \frac{\partial^2 w}{\partial y^2}. \qquad \textbf{(3.3-16)}$$

3.4 Galerkin's Method for a Vibrating Cracked Plate

Solutions based on linear models are considered adequate for many practical and engineering purposes although it is recognized that linearised equations

usually provide no more than a first approximation. Linearised models of vibrating systems are inadequate in cases where displacements are not small. In addition, problems treated by nonlinear theory exhibit new phenomena, for example the dependence of frequency of vibration on amplitude that cannot be predicted by means of linear theories. Moreover, an example of such a source of nonlinearity is a crack within a plate, which can lead to profound changes in the vibrational response of the system.

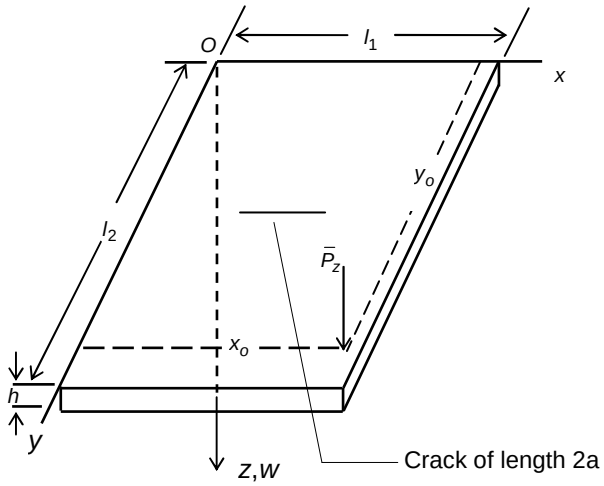

Figure 3-5: Isotropic plate loaded by arbitrary located concentrated force and small crack at the centre, and parallel to the *x*-axis

Galerkin's Method is applied to reformulate the governing equation of the cracked plate into time dependent modal coordinates by the application of given boundary conditions, and Berger's formulation is used to express formally the in-plane forces, which can then be used to transform the governing equation of the cracked plate into a nonlinear system, which is well explained in the following section. To accomplish this we consider the rectangular plate of Figure 3-5, of length l_1 in the *x*-direction and l_2 in the *y*-direction containing a crack which consists of a continuous line of length 2*a* located at the centre and parallel to the *x*-direction of the plate. A point load $\bar{P}_z$ based on the application of the appropriate delta function (in equation (3.4-8)) is introduced at the arbitrary location of (x_o, y_o).

The solution for the governing differential equation of the plate subjected to transverse loading is obtained by defining the characteristic functions

depending upon the boundary conditions of the plate. The basic model for solution is the one in which all edges are simply supported, while for other boundary conditions the principle of superposition holds [Timoshenko (1940), and Berthelot (1999)]. The most general form of the transverse deflection of the plate is,

$$w(x,y,t) = \sum_{n=1}^{\infty}\sum_{m=1}^{\infty} A_{mn} X_m Y_n \psi_{mn}(t), \qquad \textbf{(3.4-1)}$$

where X_m and Y_n are the characteristic or modal functions of the cracked rectangular plate, A_{mn} is an, as yet, arbitrary amplitude and $\psi_{mn}(t)$ is the time dependent modal coordinate.

The appropriate expressions for the characteristic or modal functions are given below and satisfy the stated boundary conditions of the plate. For all cases l_1 and l_2 are the lengths of the sides of the plate along the *x* and *y* directions respectively. Three boundary condition cases are given next. These boundary conditions have been treated by different researchers, and a few of them are as follows: The case in which two adjacent edges are clamped while the other two edges are free (CCFF) was examined by Thimoshenko (1940), Young (1950), Nagaraja and Rao (1953), in the monograph of Leissa (1993), and Berthelot (1999). The condition in which two adjacent edges are clamped while the other two edges are simply supported (CCSS) was examined by Iwato (1951), and the one in which all sides are simply supported (SSSS) was studied by Szilard (2004), and Yagiz and Sakman (2006).

Boundary Condition 1. Two adjacent edges are clamped while the other two edges are free – CCFF

$$X_m = \cos\left(\frac{\lambda_m x}{l_1}\right) - \cosh\left(\frac{\lambda_m x}{l_1}\right) - \gamma_m\left[\sin\left(\frac{\lambda_m x}{l_1}\right) - \sinh\left(\frac{\lambda_m x}{l_1}\right)\right], \qquad \textbf{(3.4-2)}$$

$$Y_n = \cos\left(\frac{\lambda_n y}{l_2}\right) - \cosh\left(\frac{\lambda_n y}{l_2}\right) - \gamma_n\left[\sin\left(\frac{\lambda_n y}{l_2}\right) - \sinh\left(\frac{\lambda_n y}{l_2}\right)\right]. \qquad \textbf{(3.4-3)}$$

The $\lambda_{m,n}$ and the $\gamma_{m,n}$ are the mode shape constants and can be found in standard reference text such as Leissa (1993), and Berthelot (1999).

Boundary Condition 2. Two adjacent edges are clamped while the other two edges are freely supported – CCSS

$$X_m = \sum_{m=1}^{\infty} \sin\frac{m\pi x}{l_1} \sin\frac{m\pi x}{2l_1} = \frac{1}{2}\sum_{m=1}^{\infty}\left(\cos\frac{m\pi x}{2l_1} - \cos\frac{3m\pi x}{2l_1}\right), \qquad \textbf{(3.4-4)}$$

$$Y_n = \sum_{n=1}^{\infty} \sin\frac{n\pi y}{l_2} \sin\frac{n\pi y}{2l_2} = \frac{1}{2}\sum_{n=1}^{\infty}\left(\cos\frac{n\pi y}{2l_2} - \cos\frac{3n\pi y}{2l_2}\right). \qquad \textbf{(3.4-5)}$$

Boundary Condition 3. All sides are simply supported – SSSS

$$X_m = \sum_{m=1}^{\infty} \sin\left(\frac{m\pi x}{l_1}\right), \qquad \textbf{(3.4-6)}$$

$$Y_n = \sum_{n=1}^{\infty} \sin\left(\frac{n\pi y}{l_2}\right). \qquad \textbf{(3.4-7)}$$

The lateral load $\bar{P}_z$ at position (x_o, y_o) can be readily expressed as follows [Fan, 2001]

$$\bar{P}_z = P_o(t)\,\delta(x - x_o)\,\delta(y - y_o). \qquad \textbf{(3.4-8)}$$

Substituting the definition of $w(x,y,t)$ from equation (3.4-1) and $\bar{P}_z$ from equation (3.4-8) into equation (3.3-16) and rearranging the terms, we get,

$$D\left(\begin{array}{l}\dfrac{\partial^4 X_m}{\partial x^4}Y_n + 2\dfrac{\partial^4 X_m Y_n}{\partial x^2 \partial y^2} + \dfrac{\partial^4 Y_n}{\partial y^4}X_m - n_x\dfrac{\partial^2 X_m}{\partial x^2}Y_n + \dfrac{2a}{\left(6\alpha_{tb}^o + \alpha_{tt}^o\right)(1-\upsilon^2)h + 2a}n_{rs}\dfrac{\partial^2 Y_n}{\partial y^2}X_m \\ -\dfrac{2a}{3\left(\dfrac{\alpha_{bt}^o}{6} + \alpha_{bb}^o\right)(3+\upsilon)(1-\upsilon)h + 2a}D\left(\dfrac{\partial^4 Y_n}{\partial y^4}X_m + \upsilon\dfrac{\partial^4 X_m Y_n}{\partial y^2 \partial x^2}\right)\end{array}\right)A_{mn}\psi(t)$$

$$= -\rho h\frac{\partial^2 \psi(t)}{\partial t^2}A_{mn}X_m Y_n + P_o(t)\,\delta(x - x_0)\,\delta(y - y_o). \qquad \textbf{(3.4-9)}$$

In 1955, Berger determined the deflection of a plate by neglecting the strain energy due to the second invariant of the middle surface strains and when the deflection is of the order of magnitude of the thickness of the plate. This can be used to obtain forms for the in-plane forces n_x and n_{rs} per unit length in the ***x*** and ***y*** direction respectively. Berger showed that this approach works well for combinations of simply supported and clamped boundary conditions. We note in passing that Wah, in 1964, and Ramachandran and Reddy, in 1972, also applied Berger's formulation efficiently for analysing the nonlinear vibrations of un-damped rectangular plates.

To derive the in-plane forces, the middle surface strains in the ***x*** and ***y*** directions can be taken as given by [Timoshenko, (1940)],

$$\varepsilon_x = \frac{\partial u}{\partial x} + \frac{1}{2}\left(\frac{\partial w}{\partial x}\right)^2, \qquad \textbf{(3.4-10)}$$

$$\varepsilon_y = \frac{\partial v}{\partial y} + \frac{1}{2}\left(\frac{\partial w}{\partial y}\right)^2, \qquad \textbf{(3.4-11)}$$

where ***u*** and ***v*** are the displacements in the ***x*** and ***y*** directions respectively.

Accordingly, we can write the in-plane forces as, [Timoshenko, (1940)],

$$n_x = \frac{Eh}{1-\upsilon^2}\left(\varepsilon_x + \upsilon\varepsilon_y\right), \qquad \textbf{(3.4-12)}$$

$$n_{rs} = \frac{Eh}{1-\upsilon^2}\left(\varepsilon_y + \upsilon\varepsilon_x\right). \qquad \textbf{(3.4-13)}$$

Substituting equations (3.4-10) and (3.4-11) into equations (3.4-12) and (3.4-13), we get,

$$\frac{n_x h^2}{12D} = \frac{\partial u}{\partial x} + \upsilon\frac{\partial v}{\partial y} + \frac{1}{2}\left(\frac{\partial w}{\partial x}\right)^2 + \frac{1}{2}\upsilon\left(\frac{\partial w}{\partial y}\right)^2, \qquad \textbf{(3.4-14)}$$

and therefore for ***y***,

$$\frac{n_{rs}h^2}{12D} = \frac{\partial v}{\partial y} + \upsilon\frac{\partial u}{\partial x} + \frac{1}{2}\left(\frac{\partial w}{\partial y}\right)^2 + \frac{1}{2}\upsilon\left(\frac{\partial w}{\partial x}\right)^2. \qquad \textbf{(3.4-15)}$$

We multiply equations (3.4-14) and (3.4-15) by dxdy and integrate over the plate area, and then impose the conditions that *u* and *v* vanish at the external boundaries and around the crack due to symmetry, leading to,

$$\frac{n_x h^2 l_1 l_2}{12D} = \frac{1}{2}\int_0^{l_1}\int_0^{l_2}\left[\left(\frac{\partial w}{\partial x}\right)^2 + \upsilon\left(\frac{\partial w}{\partial y}\right)^2\right]dxdy, \qquad \textbf{(3.4-16)}$$

and,

$$\frac{n_{rs}h^2 l_1 l_2}{12D} = \frac{1}{2}\int_0^{l_1}\int_0^{l_2}\left[\left(\frac{\partial w}{\partial y}\right)^2 + \upsilon\left(\frac{\partial w}{\partial x}\right)^2\right]dxdy. \qquad \textbf{(3.4-17)}$$

Applying the definition of $w(x,y,t)$ from equation (3.4-1) we get,

$$n_x = DF_{1mn}A_{mn}^2\psi_{mn}^2(t), \qquad \textbf{(3.4-18)}$$

where the quantity A_{mn} is a modal peak amplitude function, normalised in this case to unity,

$$F_{1mn} = \frac{6}{h^2 l_1 l_2}\sum_{n=1}^{\infty}\sum_{m=1}^{\infty}\int_0^{l_1}\int_0^{l_2}\left[\left(\frac{\partial X_m}{\partial x}\right)^2 Y_n^2 + \upsilon\left(\frac{\partial Y_n}{\partial y}\right)^2 X_m^2\right]dxdy, \qquad \textbf{(3.4-19)}$$

and,

$$n_{rs} = DF_{2mn}A_{mn}^2\psi_{mn}^2(t), \qquad \textbf{(3.4-20)}$$

where

$$F_{2mn} = \frac{6}{h^2 l_1 l_2}\sum_{n=1}^{\infty}\sum_{m=1}^{\infty}\int_0^{l_1}\int_0^{l_2}\left[\left(\frac{\partial Y_n}{\partial y}\right)^2 X_m^2 + \upsilon\left(\frac{\partial X_m}{\partial x}\right)^2 Y_n^2\right]dxdy. \qquad \textbf{(3.4-21)}$$

Substituting the in-plane forces n_x and n_{rs} from equations (3.4-18) and (3.4-20) into equation (3.4-9), multiplying each part of equation (3.4-9) by the modal function X_m and Y_n for one of the three example boundary conditions mentioned above, and then integrating over the plate area, we find that,

$$M_{mn}\ddot{\psi}_{mn}(t)+K_{mn}\psi_{mn}(t)+G_{mn}\psi^3_{mn}(t)=P_{mn}. \quad \textbf{(3.4-22)}$$

where

$$M_{mn}=\frac{\rho h}{D}\sum_{n=1}^{\infty}\sum_{m=1}^{\infty}A_{mn}\int_0^{l_1}\int_0^{l_2}X_m^2Y_n^2dxdy, \quad \textbf{(3.4-23)}$$

$$K_{mn}=\sum_{n=1}^{\infty}\sum_{m=1}^{\infty}A_{mn}\int_0^{l_1}\int_0^{l_2}\left(X_m^{iv}Y_n+2X_m''\,Y_n''+Y_n^{iv}X_m-\frac{2a\left(\upsilon X_m''\,Y_n''+Y_n^{iv}X_m\right)}{3\left(\frac{\alpha^o_{bt}}{6}+\alpha^o_{bb}\right)(3+\upsilon)(1-\upsilon)h+2a}\right)X_mY_ndxdy, \quad \textbf{(3.4-24)}$$

$$G_{mn}=\sum_{n=1}^{\infty}\sum_{m=1}^{\infty}A^3_{mn}\int_0^{l_1}\int_0^{l_2}\left(-F_{1mn}X_mX_m''Y_n^2+\frac{2aF_{2mn}X_m^2Y_nY_n''}{\left(6\alpha^o_{tb}+\alpha^o_{tt}\right)(1-\upsilon^2)h+2a}\right)dxdy, \quad \textbf{(3.4-25)}$$

The integral of the delta function is given by $\int_{-\infty}^{\infty}X_m(x)\,\delta(x-x_0)dx=X_m(x_o)$.

Therefore, the force term in equation (3.4-22) can be expressed as

$$P_{mn}=\frac{P_o(t)}{D}Q_{mn}, \quad \textbf{(3.4-26)}$$

where

$$Q_{mn}=X_m(x_0)\,Y_n(y_0). \quad \textbf{(3.4-27)}$$

Equation (3.4-22) is in the form of the well known Duffing equation containing a cubic nonlinear term, and can be re-stated as

$$\ddot{\psi}_{mn}(t)+\omega^2_{mn}\psi_{mn}(t)+\beta_{mn}\psi^3_{mn}(t)=\frac{\lambda_{mn}}{D}P_o(t), \quad \textbf{(3.4-28)}$$

where

$$\omega^2_{mn}=\frac{K_{mn}}{M_{mn}}, \quad \textbf{(3.4-29)}$$

$$\beta_{mn}=\frac{G_{mn}}{M_{mn}}, \quad \textbf{(3.4-30)}$$

$$\lambda_{mn} = \frac{Q_{mn}}{M_{mn}}, \qquad \textbf{(3.4-31)}$$

and ω_{mn} is the natural frequency of the cracked rectangular plate. β_{mn} is the nonlinear cubic term and can be either a positive (hard spring) or a negative (soft spring) depending upon the system parameters.

3.5 Linear Viscous Damping

Damping is essentially a nonlinear phenomenon. Linear viscous damping is an idealization, which provides a term proportion to velocity. Hysteretic damping, Coulomb dry friction, aerodynamic drag, etc. are examples of nonlinear damping.

Now if it is assumed that the system is attached to a nonlinear spring under the influence of weak linear viscous damping μ, then the equation of the model of the rectangular cracked plate becomes,

$$\ddot{\psi}_{mn}(t) + 2\mu\dot{\psi}_{mn}(t) + \omega_{mn}^2\psi_{mn}(t) + \beta_{mn}\psi_{mn}^3(t) = \frac{\lambda_{mn}}{D}P_o(t). \qquad \textbf{(3.5-1)}$$

Letting the load be harmonic, such that,

$$P_o(t) = p\cos\Omega_{mn}t \qquad \textbf{(3.5-2)}$$

leads to,

$$\ddot{\psi}_{mn}(t) + 2\mu\dot{\psi}_{mn}(t) + \omega_{mn}^2\psi_{mn}(t) + \beta_{mn}\psi_{mn}^3(t) = \frac{\lambda_{mn}}{D}p\cos\Omega_{mn}t. \qquad \textbf{(3.5-3)}$$

This problem is not too hard to nondimensionalise, however, physical units of the parameter are used throughout this dissertation, because there are no significant scale effects, or data complications which would otherwise require the one of formal nondimensionalisation.

3.6 Investigation of Natural Frequencies for Cracked Plate Model

Here, we consider a test plate made of aluminium alloy 5083. 5083 is an international designation used for classification. This aluminium alloy contains 5.2% magnesium, 0.1% manganese and 0.1% chromium. In the tempered condition, it is strong and retains good formability due to excellent ductility. It has high resistance to corrosion, and is used for various applications such as shipbuilding, aircrafts, rail cars, vehicle bodies, pressure vessels etc. It has low density and excellent thermal conductivity common to all aluminium alloys and has the following material properties:

Modulus of elasticity, E = 7.03 x 10^{10} N/m^2

Density, ρ = 2660 kg/m^3

Poisson's ratio, υ = 0.33

While the geometric properties of the plate are

Length along x-direction, l_1 = 0.5 m, Length along y-direction, l_2 =1 m

Half crack length, a = 0.01 – 0.025 m and thickness of the plate, h = 0.01 m

and, $p = 10$ N is the chosen load magnitude acting upon the surface of the plate at some arbitrary specified point given here by $x_0 = 0.375$ m and $y_0 = 0.75$ m, and with a damping factor of $\mu = 0.08$.

The natural frequencies without and with a crack for different boundary conditions and aspect ratios have been calculated and tabulated in Table 3-1. It may be seen from Table 3-1 that the presence of the crack at the centre of the plate significantly influences the natural frequency of the first mode of the plate, in all three cases.

First Mode Natural Frequency, ω_{mn} [rad/s] for a Half-crack Length, a = 0.01 and 0.025 [m]										
Lengths of the sides of the plate		Two adjacent edges clamped, the other two free (CCFF)			Two adjacent edges clamped, the other two simply supported (CCSS)			All edges simply supported (SSSS)		
l_1 [m]	l_2 [m]	un-cracked	cracked		un-cracked	cracked		un-cracked	cracked	
			0.01m	0.025m		0.01m	0.025m		0.01m	0.025m
1	1	80.46	77.39	74.10	445.67	432.51	418.58	77.58	75.54	73.39
0.5	1	231.06	229.95	228.80	1161.77	1154.27	1146.53	193.95	192.54	191.09
1	0.5	231.06	213.85	194.61	1161.77	1089.98	1011.04	193.95	183.18	171.42
0.5	0.5	321.85	309.54	296.38	1782.66	1730.04	1674.31	310.32	302.17	293.57

Table 3-1: Natural frequencies of the cracked plate model for different boundary conditions and aspect ratios

In the subsequent section results are plotted for the first mode and three cases of boundary conditions. The natural frequency is influenced if the geometry of the plate is changed, in particular its length and thickness, in addition to the effect of the half-crack length. Figure 3-6 shows the decrease in the natural frequency as we go on to increase the half-crack length for the same parameters as considered earlier. These changes are very small for small half-crack lengths, as one would expect.

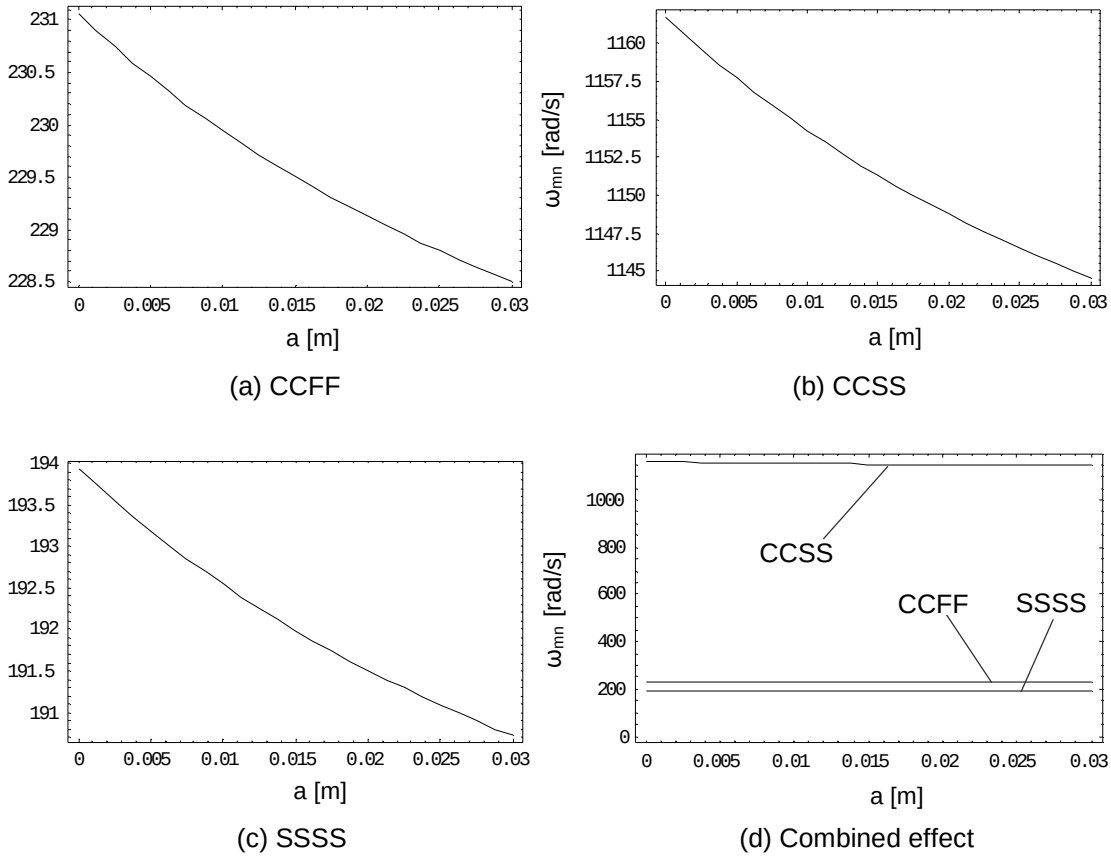

Figure 3-6: Plate first mode natural frequency of aspect ratio 0.5/1 as a function of half-crack length

Similarly, it may be seen from Figure 3-7 that by increasing the thickness of the plate the natural frequency of the first mode also increases for different values of half-crack length. This means that this natural frequency is directly related to the thickness of the plate.

The present theory can also be verified with existing linear theories as proposed by different authors, namely, Stahl and Keer (1972), Solecki (1983), Qian *et al*. (1991) , Krawczuk (1993), and Krawczuk *et al*. (1994) and (2001) for the vibration analysis of cracked plates. Let us consider a square plate of sides 0.1 m x 0.1 m made of steel having a material properties such as, young's modulus, E = 2.04×10^{11} N/m^2, Poisson's ratio, υ = 0.3, and mass density, ρ = 7860 kg/m^3. The thickness is 0.001 m and the plate is simply supported from all sides. In general, linear models are applicable only in a very restricted domain such as when the amplitude of vibration is very small as discussed in chapter 1, whereas nonlinear models capture a large range of phenomena such as jumps, modal interactions, periodic doubling and chaos. Therefore by the implication of the nonlinear model one may see all these

phenomena, and this is discussed in chapters 4 and 5 for the model of the cracked plate.

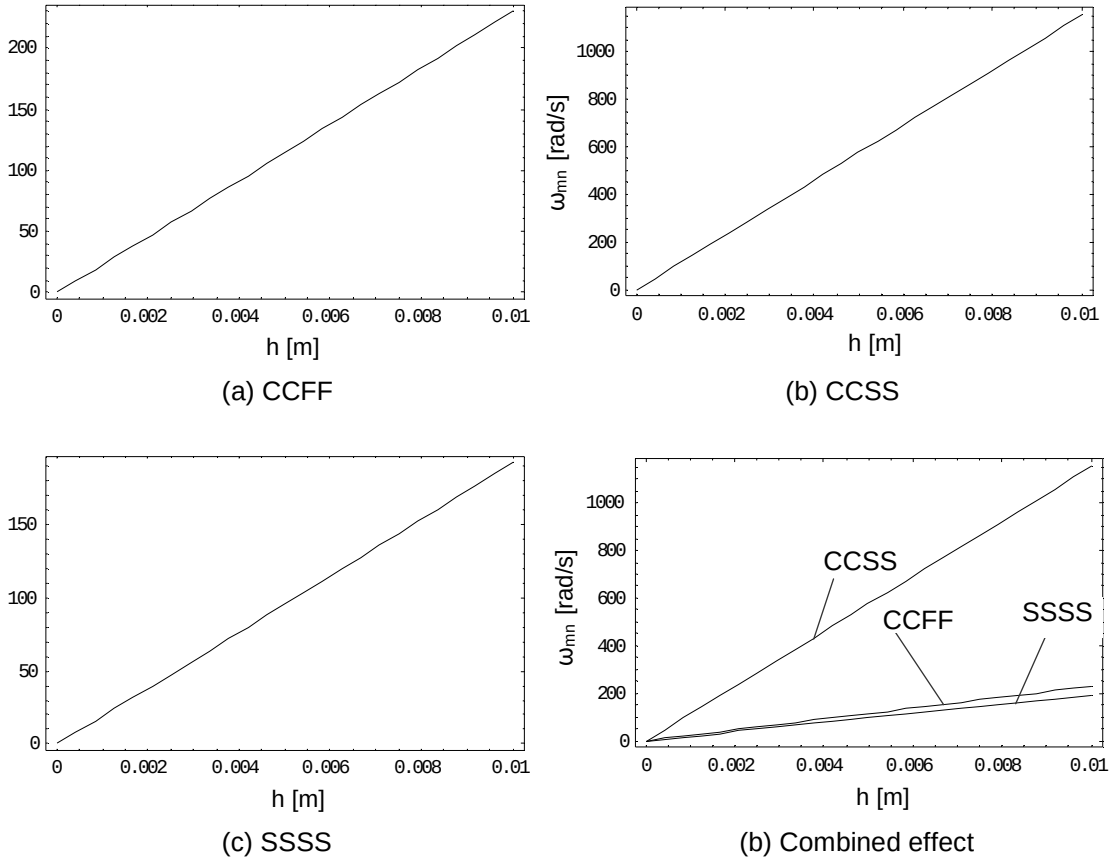

Figure 3-7: Plate first mode natural frequency as a function of the thickness of the plate for the half-crack length of 0.01 m

Table 3-2 presents a comparison of the ratio of frequencies of cracked and un-cracked plates. It shows that the percentage changes between the linear models and present nonlinear model for the range of $2a/l_1$ ratio (0.1-0.2) is approximately (1-2) %.

Linear Models	$2a/l_1$				
	0.00	0.05	0.10	0.15	0.20
Stahl & Keer (1972)	1	-	0.9940	-	0.9775
Solecki (1983)	1	-	0.9940	-	0.9780
Qian *et al.* (1991)	1	-	0.9950	-	0.9820
Krawczuk (1993)	1	0.9971	0.9942	0.9874	0.9806
Krawczuk *et al.* (1994) and (2001)	1	0.9971	0.9942	0.9874	0.9806
Present Nonlinear Model	1	0.9995	0.9992	0.9990	0.9989

Table 3-2: Relative changes of the natural frequencies of the cracked simply supported plate for the first mode only

The approximate analytical solution of the nonlinear Duffing ordinary differential equation is obtained in chapter 4 by the use of the perturbation method of multiple scales for analyzing the nonlinear behaviour of the same plate of aluminium alloy 5083.

Chapter 4

APPROXIMATE ANALYTICAL TECHNIQUES

Many exact solutions are available in the literature for the problems of linear vibration. However, for nonlinear problems, no single exact solution exists because of the general complexity of such analysis. Therefore, approximate techniques are widely used for numerical solution. We use the perturbation method of multiple scales for obtaining a close-form solution, in addition direct integration within *Mathematica*™ and a finite element analysis in ABAQUS, are also performed for the comparison of numerical solutions for the model of the cracked plate.

There are several so-called perturbation methods. Each of these techniques has its own advantages and limitations. They all rely on the same idea of splitting the co-ordinate up into successively smaller parts, in the form of a power series in terms of a small parameter, usually defined by ε. So, for the co-ordinate that we are using here is, ψ, and the expansion would have of this form

$$\psi = \psi_0 + \varepsilon\psi_1 + \varepsilon^2\psi_2 + \ldots\ldots + \varepsilon^n\psi_n \qquad \textbf{(4-1)}$$

Each term in the series is known as a perturbation. The parameter, ε, is called the perturbation parameter. If ε is small then it can be seen that the contribution to ψ which is offered by ψ_{i+1} is smaller then that offered by ψ_i. On that basis most of the solution is encoded within ψ_0, with a so-called first order correction given by ψ_1 and a second order correction given by ψ_2 and so on. In practice, if one uses a series of this sort then it is important to know where to truncate the series. This is the basis of the perturbation methods. In each method the co-ordinate or dependent variable is represented by a

suitable series, such as equation (4-1). It is also relevant to note that since $\psi = \psi(t,\varepsilon)$ then the rate of changes of ψ should also be perturbed (ideally). Simple perturbation methods do not do this, and as a result their accuracy is limited, even when higher order perturbations are included. Here, we are used the perturbation method of multiple scales to formulate the Duffing's equation (3.5-3) for the vibration analysis of a rectangular plate having a part-through crack at the centre of the plate.

4.1 The Method of Multiple Scales

The popularisation of the method of multiple scales is commonly attributed to Ali H. Nayfeh (1973), however, many other peoples have contributed to its development, and as this method is well discussed in the seminal work of Nayfeh and Mook (1979) and in the well known books of *Perturbation Methods in Applied Mathematics* by Kevorkian and Cole (1981), *Introduction to Linear, Parametric and Nonlinear Vibrations* by Cartmell (1990) and *Perturbation Theory and Methods* by Murdock (1999). We also note in passing that Cartmell *et al.*, in 2003, reviewed the multiple scales method as applied to weakly nonlinear dynamics of mechanical systems.

For the method of multiple scales, the solution of the equation (3.5-3) is approximated by a uniformly valid expansion of the form as indicated in equation (4-1),

$$\psi_{mn}(t,\varepsilon) = \psi_{0\,mn}(T_0,T_1) + \varepsilon\psi_{1mn}(T_0,T_1) + o(\varepsilon^2), \qquad \textbf{(4.1-1)}$$

where $\psi_{0\,mn}(T_0,T_1)$ and $\psi_{1mn}(T_0,T_1)$ are functions yet to be determined.

Since the highest order derivative in the equation (3.5-3) is 2, therefore, the first and the second time derivative of the function, ψ_{mn} are, $\dot{\psi}_{mn} = \frac{d\psi_{mn}}{dt}$ and $\ddot{\psi}_{mn} = \frac{d^2\psi_{mn}}{dt^2}$. The derivative perturbations rely on the notion that the real time, t, can be expressed in the form of a set of successively independent time scales, T_n, and is given by

$$T_n = \varepsilon^n t \text{ for n=0,1,2,...} \quad \textbf{(4.1-2)}$$

In equation (4.1-1), T_0 is nominally considered as fast time and T_1 as slow time, such that, $T_0 = t$ and $T_1 = \varepsilon t$ as from equation (4.1-2).

Excitation can also be expressed in term of T_0 and T_1 as

$$P_0(t) = \varepsilon p \cos\left(\omega_{mn} T_0 + \sigma_{mn} T_1\right). \quad \textbf{(4.1-3)}$$

According to that the derivatives are perturbed as follows, starting with the first time derivative

$$\frac{d}{dt} = \frac{dT_0}{dt}\frac{\partial}{\partial T_0} + \frac{dT_1}{dt}\frac{\partial}{\partial T_1} + \ldots \quad \textbf{(4.1-4)}$$

or,

$$\frac{d}{dt} = \frac{\partial}{\partial T_0} + \varepsilon\frac{\partial}{\partial T_1} + \ldots \quad \textbf{(4.1-5)}$$

It can also be written for first and second time derivative using D-operator notation for simplicity as

$$\frac{d}{dt} = D_0 + \varepsilon D_1 + \varepsilon^2 D_2 + \ldots + \varepsilon^n D_n \quad \textbf{(4.1-6)}$$

$$\frac{d^2}{dt^2} = D_0^2 + 2\varepsilon D_0 D_1 + \varepsilon^2\left(D_1^2 + 2D_0 D_2\right) + \ldots \quad \textbf{(4.1-7)}$$

Before apply this method to obtain a uniformly valid approximate solution to this problem (in case of equation (3.5-3)), it is necessary to order the cubic term, the damping, and the excitation. To accomplish this we choose to set the following to $O(\varepsilon)^1$,

$$\mu = \varepsilon\mu, \quad \beta_{mn} = \varepsilon\beta_{mn}, \quad p = \varepsilon p. \quad \textbf{(4.1-8)}$$

This philosophy is pragmatic and realistic in that it permits the pre-determined generation of linear, homogeneous generating solutions for each

co-ordinate. Moreover, instead of using the excitation frequency, Ω_{mn} as a parameter, we introduce a detuning parameter, σ_{mn}, which quantitatively describes the nearness of Ω_{mn} to ω_{mn}. This has the advantage of clarifying identification of the terms in the governing equation at first order perturbation that lead to secular terms. Accordingly we write, [Nayfeh and Mook (1979)],

$$\Omega_{mn} = \omega_{mn} + \varepsilon\sigma_{mn} \qquad \textbf{(4.1-9)}$$

where ε is an arbitrarily small perturbation parameter.

In general, equation (4.1-9) is called the primary resonance condition. After substituting equations (4.1-8) and (4.1-9) into equation (3.5-3), it becomes as follows,

$$\ddot{\psi}(t) + 2\varepsilon\mu\dot{\psi}(t) + \omega_{mn}^2\psi(t) + \varepsilon\beta_{mn}\psi^3(t) = \varepsilon\frac{\lambda_{mn}}{D}p\cos(\omega_{mn} + \varepsilon\sigma_{mn})t. \qquad \textbf{(4.1-10)}$$

This introduces damping, the cubic nonlinearity, and the excitation to first order perturbation, which is considered to be in-line with the appropriate experimental configuration, and other work on weakly nonlinear vibrating systems [Nayfeh and Mook, (1979), Kevorkian and Cole (1981), and Murdock, (1999)]. It is important to note here that for Duffing equations the coefficient of the cubic term, in this ordered case $\varepsilon\beta_{mn}$, can be numerically positive or negative, leading to overhangs of the response curve in the frequency domain to the right or left, respectively. Substituting the expansion of equation (4.1-1), the excitation term from equation (4.1-3) and the two time derivative series of equations (4.1-6) and (4.1-7) into the Ordinary Differential Equation (ODE) of the form (4.1-10), we get,

$$\begin{aligned}
&\left(D_0^2 + 2\varepsilon D_0D_1 + \varepsilon^2D_1^2\right)\psi_{0\,mn} + \varepsilon\left(D_0^2 + 2\varepsilon D_0D_1 + \varepsilon^2D_1^2\right)\psi_{1mn} + o(\varepsilon^2)\\
&+2\varepsilon\mu\left(D_0 + \varepsilon D_1\right)\psi_{0\,mn} + 2\varepsilon^2\mu\left(D_0 + \varepsilon D_1\right)\psi_{1mn} + 2\varepsilon\mu\, o(\varepsilon^2) + \omega_{mn}^2\psi_{0\,mn}\\
&+\varepsilon\omega_{mn}^2\psi_{1mn} + \omega_{mn}^2 o(\varepsilon^2) + \varepsilon\beta_{mn}\left(\psi_{0\,mn}^3 + \varepsilon\psi_{1mn}^3 + o(\varepsilon^2)\right) = \varepsilon\frac{\lambda_{mn}}{D}p\cos\left(\omega_{mn}T_0 + \sigma_{mn}T_1\right).
\end{aligned} \qquad \textbf{(4.1-11)}$$

Separating terms of like order ε yields, to order ε^o:

$$D_0^2\psi_{0\,mn} + \omega_{mn}^2\psi_{0\,mn} = 0, \qquad \textbf{(4.1-12)}$$

This is a linear, homogeneous, second order perturbation equation and can be thought of as an ordinary differential equation with respect to timescale T_0. It is usually referred to as the zeroth order perturbation equation.

and to order ε^1:

$$D_0^2\psi_{1mn} + \omega_{mn}^2\psi_{1mn} = -2D_0D_1\psi_{0\,mn} - 2\mu D_0\psi_{0\,mn} - \beta_{mn}\psi_{0\,mn}^3 + \frac{\lambda_{mn}}{D}p\cos\left(\omega_{mn}T_0 + \sigma_{mn}T_1\right). \qquad \textbf{(4.1-13)}$$

This is referred to as the first order perturbation equation. The higher orders of ε^2, ε^3 and so on, may be neglected because higher order perturbation equations will yield negligible corrections for the problem as set up here. The general solution of equation (4.1-12) can be written as

$$\psi_{0\,mn} = B(T_1)e^{i\omega_{mn}T_0} + \overline{B}(T_1)e^{-i\omega_{mn}T_0}, \qquad \textbf{(4.1-14)}$$

where B is an unknown complex amplitude, and $\overline{B}$ is the complex conjugate of B. This amplitude will be determined by eliminating the secular terms from ψ_{1mn}. Substituting the solution from equation (4.1-14) into equation (4.1-13), we get,

$$D_0^2\psi_{1mn} + \omega_{mn}^2\psi_{1mn} = -2D_0D_1\left\{B(T_1)e^{i\omega_{mn}T_0} + \overline{B}(T_1)e^{-i\omega_{mn}T_0}\right\} - 2\mu D_0\left\{B(T_1)e^{i\omega_{mn}T_0} + \overline{B}(T_1)e^{-i\omega_{mn}T_0}\right\}$$
$$-\beta_{mn}\left\{B(T_1)e^{i\omega_{mn}T_0} + \overline{B}(T_1)e^{-i\omega_{mn}T_0}\right\}^3 + \frac{\lambda_{mn}}{D}p\cos\left(\omega_{mn}T_0 + \sigma_{mn}T_1\right), \qquad \textbf{(4.1-15)}$$

which, after dropping the argument T_1 in the complex amplitudes, leads to the following,

$$D_0^2\psi_{1mn}+\omega_{mn}^2\psi_{1mn}=-2iD_1\left(\omega_{mn}Be^{i\omega_{mn}T_0}-\omega_{mn}\overline{B}e^{-i\omega_{mn}T_0}\right)-2i\mu\left(\omega_{mn}Be^{i\omega_{mn}T_0}-\omega_{mn}\overline{B}e^{-i\omega_{mn}T_0}\right)$$
$$-\beta_{mn}\left[B^3e^{3i\omega_{mn}T_0}+\overline{B}^3e^{-3i\omega_{mn}T_0}+3B\overline{B}\left(Be^{i\omega_{mn}T_0}+\overline{B}e^{-i\omega_{mn}T_0}\right)\right]+\frac{\lambda_{mn}}{D}p\cos\left(\omega_{mn}T_0+\sigma_{mn}T_1\right).$$

(4.1-16)

Expressing $\cos\left(\omega_{mn}T_0+\sigma_{mn}T_1\right)$ in complex form, and take the common factor of $e^{i\omega_{mn}T_0}$ out from the right hand side of equation (4.1-16), we get,

$$D_0^2\psi_{1mn}+\omega_{mn}^2\psi_{1mn}=\left(-2i\omega_{mn}D_1B-2i\mu\omega_{mn}B-3\beta_{mn}B^2\overline{B}+\frac{\lambda_{mn}}{2D}pe^{i\sigma_{mn}T_1}\right)e^{i\omega_{mn}T_0}-\beta_{mn}B^3e^{3i\omega_{mn}T_0}+cc,$$

(4.1-17)

where cc denotes the complex conjugate of the preceding terms.

It can be seen that some of the right hand side terms contain the term $e^{i\omega_{mn}T_0}$. The important characteristic here is that ω_{mn} is explicitly present, it means that those terms are resonant. Such terms frequently occur in perturbation analysis and are called secular terms. Now the secular terms can be identified immediately due to the removal of the common factor of $e^{i\omega_{mn}T_0}$. To eliminate the secular terms from equation (4.1-17), we must put,

$$-2i\omega_{mn}D_1B-2i\mu\omega_{mn}B-3\beta_{mn}B^2\overline{B}+\frac{\lambda_{mn}}{2D}pe^{i\sigma_{mn}T_1}=0. \qquad \textbf{(4.1-18)}$$

This means that equation (4.1-17) will be much simpler and can then be solved directly using the conventional particular integral method. In solving equation (4.1-18), it is convenient to write the complex amplitude B in the polar form,

$$B=\frac{1}{2}be^{i\alpha}, \qquad \textbf{(4.1-19)}$$

where $B=B(T_1)$, the physical reasoning behind that is to keep amplitude in a steady state or nearly so. If this is imposed then it also has to impose the conditions that real amplitude, $b=b(T_1)$ and phase, $\alpha=\alpha(T_1)$.

Substituting equation (4.1-19) into equation (4.1-18), we get,

$$\omega_{mn} b\alpha' - i\omega_{mn} b' - i\omega_{mn}\mu b - \frac{3\beta_{mn}}{8} b^3 + \frac{\lambda_{mn}}{2D} p[\cos(\sigma_{mn} T_1 - \alpha) + i\sin(\sigma_{mn} T_1 - \alpha)] = 0, \tag{4.1-20}$$

where the prime denotes the derivative with respect to T_1.

Now, separating the result into real and imaginary parts, we obtain,

$$\text{Re:} \quad b\alpha' = \frac{3\beta_{mn} b^3}{8\omega_{mn}} - \frac{\lambda_{mn}}{2\omega_{mn} D} p\cos(\sigma_{mn} T_1 - \alpha), \tag{4.1-21}$$

$$\text{Im:} \quad b' = -\mu b + \frac{\lambda_{mn}}{2\omega_{mn} D} p\sin(\sigma_{mn} T_1 - \alpha). \tag{4.1-22}$$

Equation (4.1-21) contains α', where this is the slowly varying phase angle, and equation (4.1-22) contains the slowly varying amplitude, b'.

Equations (4.1-21) and (4.1-22) can then be transformed into an autonomous system i.e. one in which T_1 does not appear explicitly, by letting,

$$\kappa = \sigma_{mn} T_1 - \alpha. \tag{4.1-23}$$

Substituting equation (4.1-23) into equations (4.1-21) and (4.1-22), we get,

$$b\kappa' = \sigma_{mn} b - \frac{3\beta_{mn} b^3}{8\omega_{mn}} + \frac{\lambda_{mn}}{2\omega_{mn} D} p\cos\kappa, \tag{4.1-24}$$

$$b' = -\mu b + \frac{\lambda_{mn}}{2\omega_{mn} D} p\sin\kappa. \tag{4.1-25}$$

In the case of steady-state motion $b' = \kappa' \approx 0$, and this corresponds to the singular points of equations (4.1-24) and (4.1-25); that is,

$$-\frac{3\beta_{mn}b^3}{8\omega_{mn}}+\sigma_{mn}b=-\frac{\lambda_{mn}}{2\omega_{mn}D}p\cos\kappa, \qquad \textbf{(4.1-26)}$$

$$\mu b=\frac{\lambda_{mn}}{2\omega_{mn}D}p\sin\kappa. \qquad \textbf{(4.1-27)}$$

Squaring and adding these equations, we obtain,

$$\left[\mu^2+\left(\sigma_{mn}-\frac{3\beta_{mn}b^2}{8\omega_{mn}}\right)^2\right]b^2=\frac{\lambda_{mn}^2}{4\omega_{mn}^2D^2}p^2. \qquad \textbf{(4.1-28)}$$

It is then possible to rearrange equation (4.1-28), we get,

$$\sigma_{mn}=\frac{3\beta_{mn}b^2}{8\omega_{mn}}\pm\sqrt{\frac{\lambda_{mn}^2}{4\omega_{mn}^2b^2D^2}p^2-\mu^2}. \qquad \textbf{(4.1-29)}$$

This is a frequency response equation which gives the modal amplitude response, b as a function of the detuning parameter, σ_{mn}, and the amplitude of the excitation, p, this being a measure of deviation from the perfect forced resonance condition. It also indicates that the peak amplitude, b_p is independent of the value of β_{mn} (cubic nonlinear term) and is given by

$$b_p=\frac{\lambda_{mn}}{2\omega_{mn}\mu D}p \qquad \textbf{(4.1-30)}$$

We can plot the linear $(\beta_{mn}=0)$ and nonlinear response curves from equation (4.1-29). The linear results are symmetric to this order of approximation and represent the solution in a very narrow band around the resonant frequency. The effect of the nonlinearity is to bend the amplitude curve left or right depending upon the negative or positive value of the cubic nonlinear term respectively.

4.2 Analytical Results

In this section, analytical results are presented based on the approximate method of multiple scales. Linear and nonlinear response curves for the three cases of boundary conditions and a half-crack length of 0.01 m, are plotted to see their effects at the resonance condition. Secondly, a detailed comparison is made between the linear and nonlinear cracked plate models. Finally, nonlinearity is also affected by changing the location of the point load, and by means of the damping factor, and these aspects are discussed next.

4.2.1 Linear and Nonlinear Response Curves

Linear and nonlinear response curves are plotted for analysing the behaviour of a model of the cracked rectangular plate. To construct such a curve, one solves for, σ_{mn} in terms of b. Figure 4-1 shows the plots of amplitude, b as a function of σ_{mn} for given μ and p in the form of a frequency-response curve for three sets of boundary conditions as discussed in section 3.4 in detail. Each point on this curve corresponds to a singular point.

Now, we consider the same mechanical and geometric properties of test aluminium plate as motioned in section 3.6 for plotting of system responses. The results are shown for the first mode only. Figures 4.1(a) and 4.1(b) are the linear and nonlinear response curves for the CCFF, CCSS and SSSS boundary conditions respectively. As shown, the nonlinearity bends the frequency-response curve away from the linear curve $(\beta_{mn} = 0)$, to the right for hard springs i.e. $\beta_{mn} > 0$ for the cases of CCSS and SSSS, and bends to the left for soft springs i.e. $\beta_{mn} < 0$ for the case of CCFF. These are shown in Figure 4-1(b), with some attendant change in the modal natural frequency, or we can say that as the amplitude of the excitation increases, the frequency response curves bend away from the $\sigma_{mn} = 0$ axis. The natural frequency is also influenced if the geometry of the plate is changed, in particular its length and thickness, in addition to the effect of the half-crack length as discussed in chapter 3 (see Figures 3-6 and 3-7 for more detail).

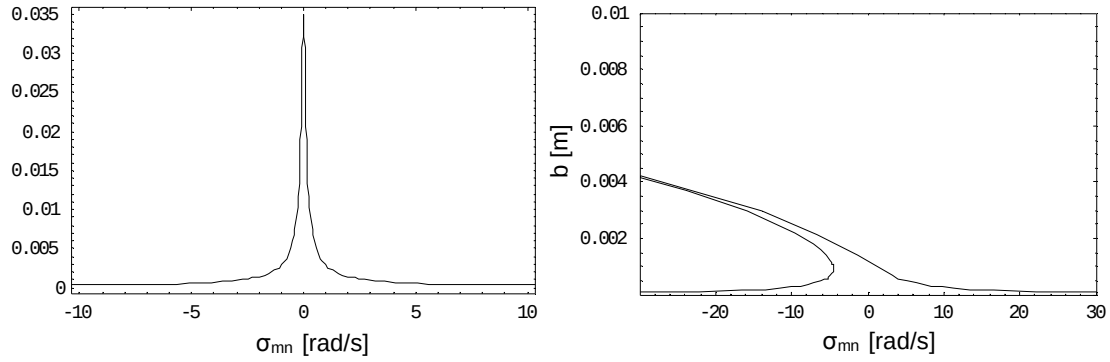

(a) Linear - CCFF (b) Nonlinear - CCFF

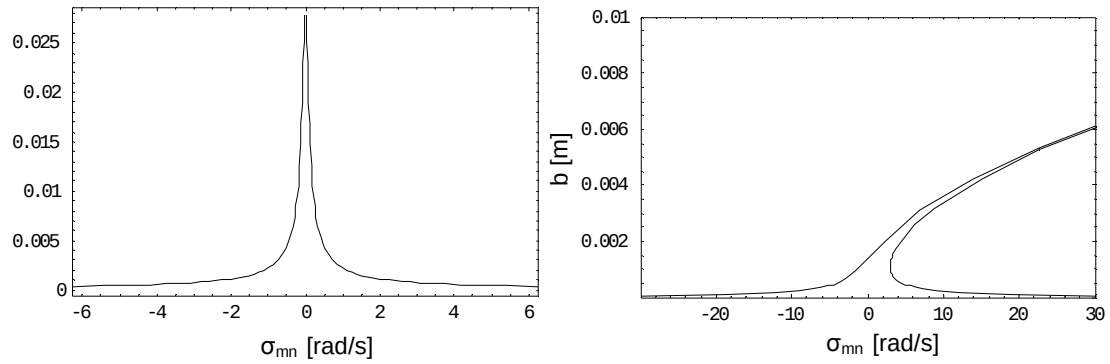

(a) Linear - CCSS (b) Nonlinear - CCSS

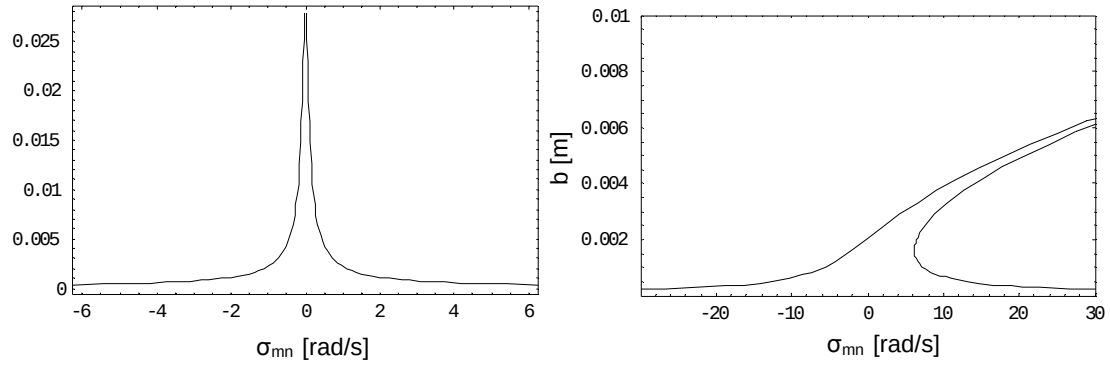

(a) Linear - SSSS (b) Nonlinear - SSSS

Figure 4-1: Linear and nonlinear response curves for three different cases of boundary conditions and half-crack length of 0.01 m

4.2.2 Comparison of Linear and Nonlinear Cracked Plate Model

If the cubic nonlinearity, β_{mn} is set to zero then the problem is linearised as discussed earlier, but in the case of the nonlinear problem the significant effect of including this term is apparent from the numerical results depicted in Figure 4-2 for the two sets of the plate aspect ratios 0.5/1 and 1/1. Figure 4-2 shows that the ratio of the linear and nonlinear solution amplitude (where β_{mn} is set to zero) is very large for negative detuning. This exactly emulates the softening nonlinear characteristic for the case of CCFF boundary

conditions as shown in Figure 4-1(b). It can also be seen that this ratio reduces close to unity for zero and positive detuning, again fully in-line with the softening characteristic observable in Figure 4-1(b) for the case of CCFF boundary condition. In addition, it can also be seen that there is a very small difference in amplitude ratio between the two aspect ratios of the plate in Figure 4-2. In the Figure 4-2, b_{NL} is the nonlinear amplitude and b_L is the corresponding linear amplitude.

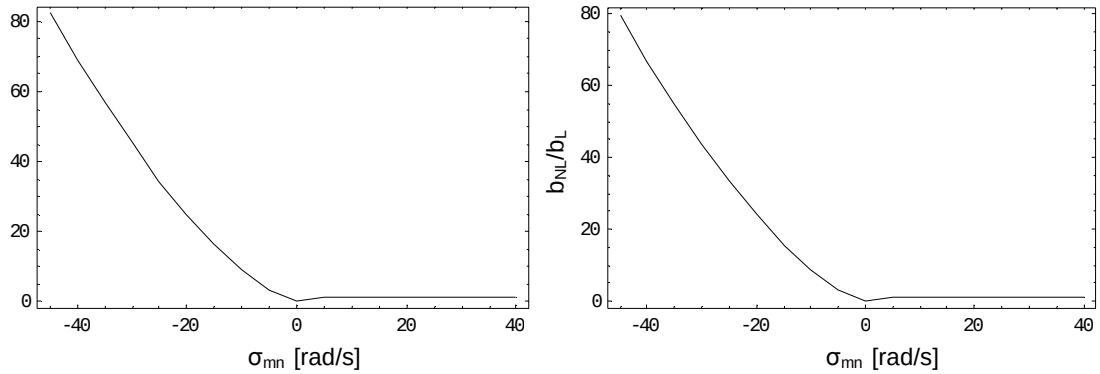

(a) Plate aspect ratio 0.5/1 (b) Plate aspect ratio 1/1

Figure 4-2: Comparison between linear and nonlinear model of the cracked rectangular plate and the boundary condition CCFF

4.2.3 Nonlinearity affects by changing the location of the Point Load

It has been observed that changing the location of the load on the plate slightly affects the global nonlinearity of the system, as shown in Figure 4-3 for the case of CCFF boundary condition and evidenced by the increasingly wide nonlinear region as the excitation location moves closer to the unsupported corner.

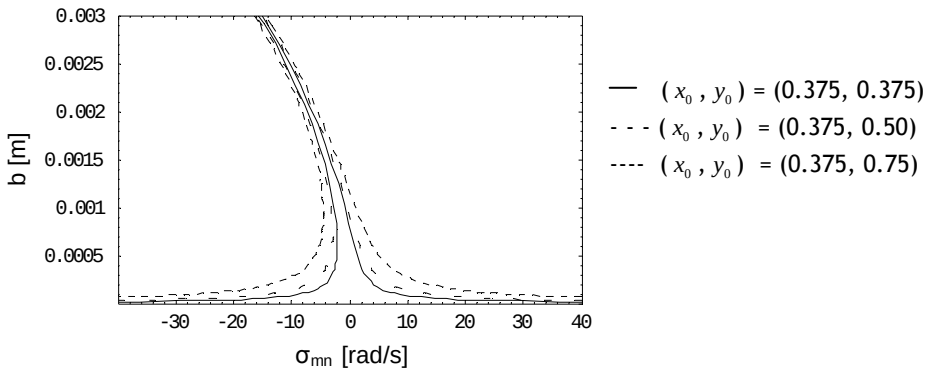

Figure 4-3: The amplitude of the response as a function of the detuning parameter, σ_{mn} [rad/s] and the point load at different locations [m] of the plate element

4.2.4 Damping Coefficient influences Nonlinearity

It is also interesting to note that the damping coefficient, μ influence the response curves. In the absence of damping, the peak amplitude is infinite, and the frequency response curve consists of two branches having as their asymptote the curve, $\sigma_{mn} = \frac{3\beta_{mn} b^2}{8\omega_{mn}}$. However, in the presence of damping, the peak amplitude is finite as in the present case.

4.2.5 Peak Amplitude

The peak amplitude, b_p as given in equation (4.1-30) for an un-cracked and cracked plate is tabulated in Table 4-1. As expected, the amplitude increases as the insertion of the crack at the centre of the plate and increases further by the increase of half-crack length from 10 mm to 25 mm.

	Boundary Conditions	Un-cracked Plate [mm]	Cracked Plate with Half-crack Lengths, *a* [mm]	
			10 mm	25 mm
Peak amplitude	CCFF	35.19	35.36	35.54
	CCSS	27.62	27.80	27.99
	SSSS	82.72	83.33	83.96

Table 4-1: Peak amplitudes for three sets of boundary conditions and two sets of half-crack length for a plate aspect ratio of 0.5/1

4.3 Direct Integration – NDSolve within *Mathematica*™

The NDSolve integrator within *Mathematica*™ (Wolfram, 1996) is used for the numerical solution of nonlinear ordinary and partial differential equations.

Special program code is developed for integrating the Duffing equation (3.5-3) for given initial conditions and is shown in Appendix A.

The results obtained are in the time domain and can be transformed into the frequency domain by running this program code as described in Appendix A several times for a range of frequency values from -40 rad/s to 40 rad/s to obtain a list of amplitude values. While going through all the data individually, one selects that portion of the amplitude values where the values are in steady state condition, and then one averages them for the plot of amplitude and frequency. These provide a basis for comparison with the approximate analytical solutions obtained from equation (4.1-29).

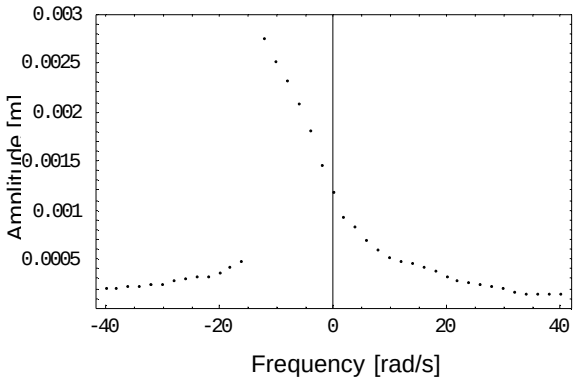

Figure 4-4: Nonlinear overhang in the form of the softening spring characteristic by the use of NDSolve within *Mathematica*™ for an aspect ratio of 0.5/1, and initial conditions zero

Figure 4-4 shows the responses of the plate obtained from direct integration by the use of NDSolve within *Mathematica*™. Reasonably close agreement can be observed, however the numerical solution does not predict the same degree of nonlinear overhang in the form of the softening spring characteristic as the approximate analytical solution. The over-prediction of the softening overhang by the multiple scales solution is undoubtedly due to an over-correction to the solution from the first order perturbation contribution, and the assumptions that necessarily went with that in order to obtain a closed-form solution.

4.4 Finite Element (FE) Technique – ABAQUS/CAE 6.7-1

ABAQUS/CAE is a general purpose finite element analysis tool with a group of engineering simulation programs capable of modelling structures under

different loading conditions. It can solve problems of relatively simple structural analysis to the most complicated linear to nonlinear analyses. In a nonlinear analysis ABAQUS/CAE automatically chooses appropriate load increments and convergence tolerances and continually adjusts them during the analysis to ensure that an accurate solution is obtained. ABAQUS/CAE consists of a widespread library of elements, wherein any type of geometry can be modelled. Apart from solving structural problems, it can also solve problems in other different areas like fracture mechanics, soil mechanics, static analysis, piezoelectric analysis, coupled thermal-electrical analyses, heat problems, and acoustics etc. The detailed description of the ABAQUS/CAE finite element program has been included in Appendix B.

In this analytical framework, ABAQUS/CAE is used for evaluating the frequencies, displacements and mode shapes of the model of a cracked plate to investigate the theoretical predictions. The required inputs for the ABAQUS/CAE finite element analysis consists of model geometry, material properties, loading, boundary conditions, and an initial crack configuration.

4.4.1 Steps Taken to Perform FE Analysis

A description of the steps taken to perform an elastic FE analysis using ABAQUS/CAE are as follows:

- Create a 3D solid model of the plate element in the ABAQUS/CAE Part module for a given geometric and mechanical properties of aluminium alloy – 5083.

- Create a part-through crack of depth 0.06 m at the centre of the plate by the use of cut feature under shape in the main menu.

- Define material properties for an aluminium plate in the Property module, including modulus of elasticity, Poisson's ratio, and density. Further, create section and section assignment of the part in the same module.

- Create partitions of the whole part for proper structural meshing in the mesh module. The partition feature can be access under tool in the main menu.

- Create an assembly of the part in the Assembly module.

- Create steps for the analysis in the step module i.e. specific output requests including field and history output requests.

- Create sets to define the boundary conditions of the part.

- Apply boundary conditions and loadings in the load module. Here, CCFF boundary condition and a concentrated force of 10 N are applied.

- Create the mesh of the part using element shape and analysis type standard, 3D stress, C3D8R - 8 node linear brick with reduced integration. Mesh and seed part instances are also required for the creation of the mesh. ABAQUS/CAE offers a number of different meshing techniques. The default meshing technique assigned to the model is indicated by the colour of the model. If ABAQUS/CAE displays the model in orange, it cannot be meshed without assistance from the user.

- When all the keywords are defined, submit the job in the job module to solve for the analysis.

- In post processing, interpret the output in the Visualisation module, including standard stress, strain and displacement distributions.

There are two basic types of dynamic analysis in ABAQUS/CAE step module; implicit and explicit. ABAQUS/Standard uses the implicit Hilber-Hughes-Taylor operator for integration of the equations of motion. This offers the use of all elements in ABAQUS, however, it can be slower than explicit, whereas ABAQUS/explicit uses the central-difference operator. In an implicit dynamical analysis the integration operator matrix is inverted and a set of nonlinear equilibrium equations are solved at each time increment. A dynamic

analysis for the cracked model is performed by employing implicit, and edits the Step module as

Basic tab Time period: 6

Incrementation tab Type: Fixed

Maximum number of increments: 6000

Increment size: 0.001

Check: Suppress half-step residual calculation

The periodic load is applied at a distance of 0.375 x 0.75 m from the fixed edges of the plate (see Figure 3-6) with a magnitude of 10 N under the resonant frequency. This can be defined in ABAQUS/CAE as Go to tools, amplitude, create, give it a name and choose periodic. The model may take a long time to run. However, it could be monitored during the runs.

4.4.2 ABAQUS/CAE Results

The results obtained from ABAQUS/CAE are shown in Figures 4-5, 4-6 and 4-7 for the nonlinear FE analysis of the plate with a part-through crack at the centre of the plate for a boundary condition of CCFF, and the aspect ratio of the plate is 0.5/1. Equally, results can readily be obtained by employing other boundary conditions, such as CCSS and SSSS.

4.4.2.1 Frequency Analysis

Figure 4-5 shows three modes of vibration for an un-cracked plate. Similarly, Figures 4-6 and 4-7 shows a decreasing trend as the inclusion of damage in the form of crack at the centre of the plate. The frequency values are tabulated in Table 4-2 for a three modes of vibration for a cracked and un-cracked plate.

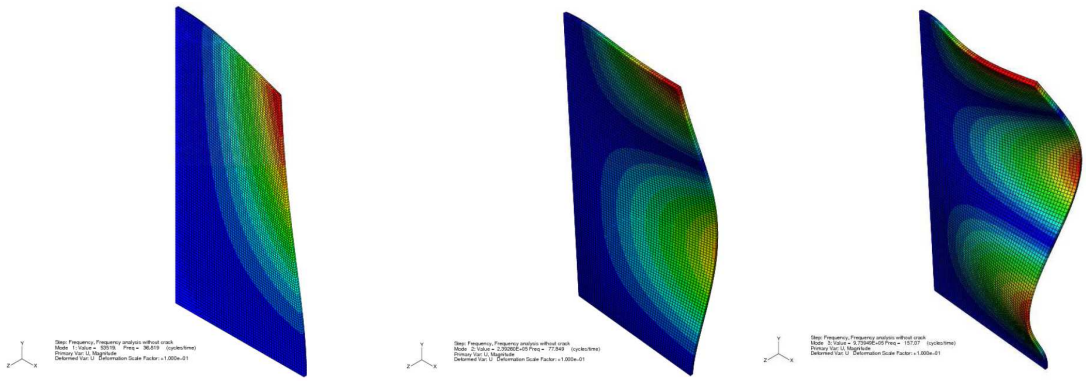

(a) Mode – I (b) Mode – II (c) Mode – III

Figure 4-5: Three modes of vibration for an aluminium plate without a crack

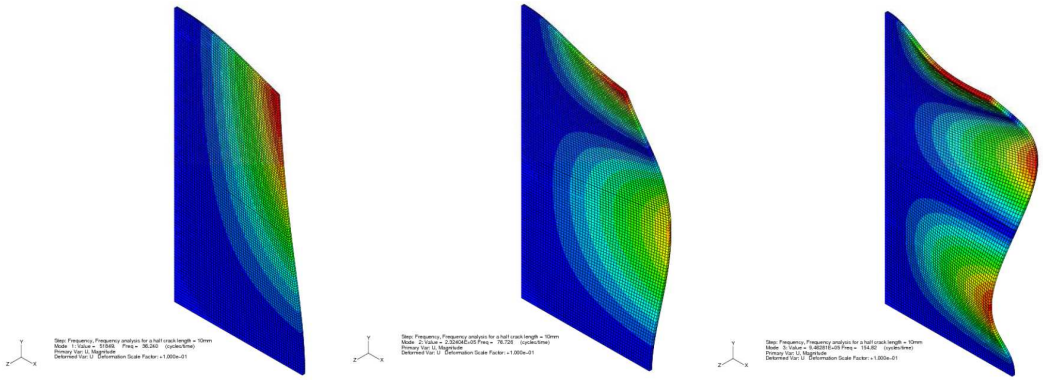

(a) Mode – I (b) Mode – II (c) Mode – III

Figure 4-6: Three modes of vibration for an aluminium plate of sides 0.5x1 m and a half-crack length of 0.01 m

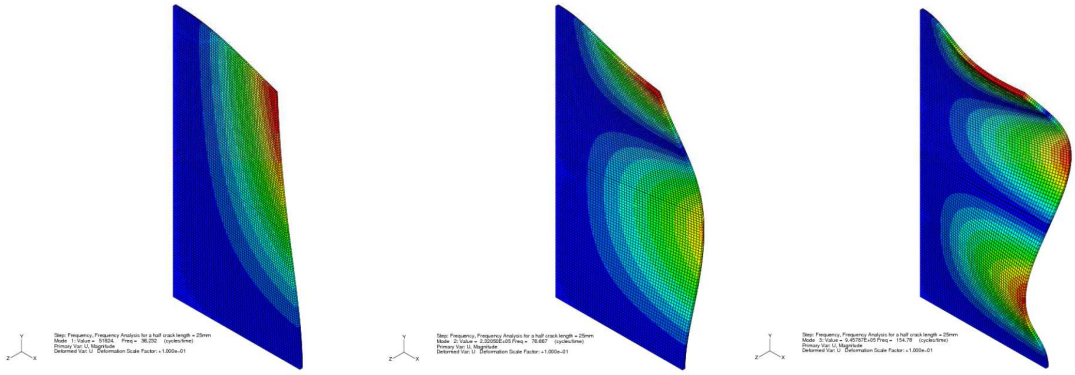

(a) Mode – I (b) Mode – II (c) Mode – III

Figure 4-7: Three modes of vibration for an aluminium plate of sides 0.5x1 m and a half-crack length of 0.025 m

4.4.2.2 Amplitude Analysis

The amplitude responses for an un-cracked and cracked plate model are obtained by employing implicit dynamic nonlinear analysis within ABAQUS/CAE. As expected, the amplitudes values increase due to the insertion of a small crack in the aluminium plate. These amplitudes values are also tabulated in Table 4-2, and the comparison is made between the theoretical model and the FEA results.

		Theoretical Results for M-1 only		FEA Results			
		Frequency [Hz]	Amplitude [mm]	Frequency [Hz]			Amplitude [mm]
				M-I	M-II	M-III	M-I only
Un-cracked Plate		36.77	1.1913	36.819	77.85	157.07	1.016
Cracked Plate	10 mm	36.60	1.1974	36.240	76.73	154.82	1.222
	25 mm	36.41	1.2045	36.232	76.67	154.78	1.386

Table 4-2: Finite element analysis results

The analytical results via the method of multiple scales can be extended for the evaluation of higher modes for the cracked plate problem. However, including higher modes makes the computation of the problem more lengthy and complex to a greater extent. As one then could see, that the general form of the transverse deflection of the plate (equation 3.4-1) will take multi-part form. It would be advantageous if this could be investigated further for the higher modes.

Chapter 5

DYNAMICAL SYSTEM ANALYSIS

In this chapter, we discuss dynamical systems theory and its application for providing an introduction to nonlinear behaviour, principally through the study of the Duffing ODE of equation (3.5-3), used as the model of the cracked rectangular plate as discussed in chapters 3 and 4. This study begins with the stability of the phase states, and the Poincaré map, and this is followed by a study of the bifurcations, that are observed from the analysis of saddle trajectories, and the calculation of the Lyapunov exponent. This lead us to the emergence of strange attractors of fractal dimension; the evolution of saddle orbits into chaos, and leads to the observation idea that in this system seemingly chaotic behaviour can emerge from perfectly deterministic origins. Chaotic behaviour might, in principle, be predicted as an outcome for a deterministic system, however, in some systems it is difficult to envisage, as the dynamics of the system are necessarily of high precision. Therefore, the understanding of the dynamics of an analytically modelled system, or a system defined by a finite element model, can be extended further by recourse to techniques based on specialised numerical investigations.

Nonlinear dynamical systems are used as models in every field of science and engineering and universal patterns of behaviour, including chaos, have been observed in many examples. Various, freely available pieces of software such as, *AUTO*[2], *XPPAUT*[3], *Matcont*[4], *Content*[5], *DynPac*[6], and *Dynamics Solver*[7] have been specifically designed for the analysis of dynamical systems, and to allow the user to compute the equilibria and limits cycles, bifurcation points and

[2] http://indy.cs.concordia.ca/auto/
[3] http://www.math.pitt.edu/~bard/bardware/tut/xppauto.html
[4] http://www.matcont.ugent.be/matcont.html
[5] http://www.enm.bris.ac.uk/staff/hinke/dss/continuation/content.html
[6] http://www.me.rochester.edu/~clark/dynpac.html
[7] http://www.enm.bris.ac.uk/staff/hinke/dss/ode/dynsolver.html

Lyapunov exponents for their own systems. In practice, it has been observed that every software package has its own specific significance, and performance, and this gives the user the choice of many. A primary function of these dynamical systems software packages is to perform numerical integration and numerical continuation. Numerical integration is an iterative technique which is applied to the majority of nonlinear systems that are not solved analytically for some reason, therefore, the trajectory is approximated by calculating a sequence of solutions over a given time span. On the other hand, numerical continuation is a technique to trace the solution path to a given system as the value of a control parameter varies, so it allows the bifurcations to be found, and stable and unstable solutions to be traced.

In this study, computational methods for the analysis of dynamical systems as system parameters varies are discussed by implementing the *Dynamics 2* dynamical system software, and also by the use of bespoke code written by the author in *Mathematica*™. In addition, these analyses are for high excitation and frequency values of the Duffing equation (3.5-3).

5.1 Dynamical System Theory

Chaos is broadly defined as a major type of irregular, unpredictable behaviour observable in deterministic nonlinear dynamic systems. In the mathematical literature, it is usually defined as a phenomenon seen in a dynamical system that has a sensitive dependence on its initial conditions. Stanisław Marcin Ulam (1909–1984) famously stated that nonlinear science is like non-elephant zoology. Chaos theory began as a field of physics and mathematics dealing with the structures of turbulence and the self-similar forms of fractal geometry. The idea that many simple nonlinear deterministic systems can behave in an apparently unpredictable and chaotic manner was first noticed by the great French mathematician Henri Poincaré (1854–1912). Other early pioneering work in the field of chaotic dynamics were found in the mathematical literature by such luminaries as Birkhoff (1844–944), Andronov (1901–1952) and his students, Littlewood (1885–1977), Kolmogorov (1903–1987), Pontryagin (1908–1988), Cartwright (1900–1998), and Smale (1930–present), amongst others. In spite of this, the importance of chaos was not

fully appreciated until the widespread availability of digital computers for numerical simulations and the demonstration of chaos in various real-time systems. This realisation has broad implications for many fields of science, and it is only within the past three decades that the field has undergone an explosive growth in such diverse disciplines as engineering, fluid mechanics, physics, biology, economics, and chemistry.

Poincaré wrote in his essay *Science and Hypothesis* (1903) that "If we knew exactly the laws of nature and the situation of the universe at the initial moment, we could predict exactly the situation of that same universe at a succeeding moment. But even if it were the case that the natural laws had no longer any secret for us, we could still only know the initial situation approximately. If that enabled us to predict the succeeding situation with the same approximation, that is all we require, and we should say that the phenomenon had been predicted, that it is governed by laws. But it is not always so; it may happen that small differences in the initial conditions produce very great ones in the final phenomena. A small error in the former will produce an enormous error in the latter. Prediction becomes impossible, and we have the fortuitous phenomenon". We can conclude from this that it is very hard to get exact predictions of any system from the initial conditions. These initial conditions can cause enormous divergence in the results, as we can see in the case of the cracked plate model in the following sections.

The book by Abrahams and Shaw, in 1982, used artistic techniques to represent phase space structures and bifurcation diagrams in three dimensions. Today the capabilities of the dynamical systems research community are far more mature, and the nomenclature of bifurcation theory is hardwired into almost all fields of scientific study. Champneys, in 2006, presented an overview of a famous book *Dynamical Systems and Bifurcations of Vector Fields* written by Guckenheimer and Holmes (1983). He pointed out that if physics was the great science of the twentieth century, then surely it will be the life sciences that increasingly dominate in the twenty-first century, to say nothing of the social sciences, economics, models of human behaviour, perception and cognition. All of these will need the insight of applied dynamical systems theory.

5.2 A Model of the Cracked Plate for Dynamical System Analysis

The model of the cracked plate in the form of the Duffing equation (3.5-3) as discussed in chapter 3 is used after some modification, to represent the behaviour of this dynamical system from nonlinear transition to chaos, by the use of *Dynamics 2* – a tool for bifurcation analysis, and by means of special bespoke code in *Mathematica*™. Therefore, we can write the Duffing equation (3.5-3) in the following form:

$$\ddot{x} + C_1\dot{x} + C_2 x + C_3 x^3 = \rho \cos(\Omega t). \qquad \textbf{(5.2-1)}$$

where

$$C_1 = 2\mu \qquad \textbf{(5.2-2)}$$

$$C_2 = \omega_{mn}^2 \qquad \textbf{(5.2-3)}$$

$$C_3 = \beta_{mn} \qquad \textbf{(5.2-4)}$$

$$\rho = \frac{P_{mn}}{M_{mn}} = \frac{\lambda_{mn}}{D} p \qquad \textbf{(5.2-5)}$$

and, $\Omega =$ Frequency of excitation

5.2.1 Nondimensionalisation

Nondimensionalisation of the timescale in equation (5.2-1) is introduced by putting $\tau = \sqrt{\omega}\, t$ in order to show realistic plots in the subsequent Figures, where ω is the natural frequency of the first mode of the cracked plate model.

Therefore,

$$\Rightarrow \quad \ddot{x} = \frac{d^2x}{dt^2} \qquad\qquad \dot{x} = \frac{dx}{dt}$$

$$= \frac{d^2x}{d\left(\frac{\tau}{\sqrt{\omega}}\right)^2} \qquad ; \qquad = \frac{dx}{d\left(\frac{\tau}{\sqrt{\omega}}\right)}$$

$$= \omega\frac{d^2x}{d\tau^2} \qquad\qquad = \sqrt{\omega}\frac{dx}{d\tau}$$

$$\ddot{x}(t) = \omega x''(\tau) \qquad\qquad \dot{x}(t) = \sqrt{\omega}x'(\tau)$$

(5.2.1-1)

In dimensionless timescale, equation (5.2-1)

$$\omega x'' + \sqrt{\omega}C_1x' + C_2x + C_3x^3 = \rho\cos\left(\frac{\Omega}{\omega}\tau\right) \qquad \textbf{(5.2.1-2)}$$

Where the prime (′) denotes differentiation with respect to dimensionless time τ.

Dividing the equation (5.2.1-2) by ω, we get

$$x'' + \frac{1}{\sqrt{\omega}}C_1x' + \frac{1}{\omega}C_2x + \frac{1}{\omega}C_3x^3 = \frac{\rho}{\omega}\cos\left(\frac{\Omega}{\omega}\tau\right) \qquad \textbf{(5.2.1-3)}$$

Let assume that $\Omega = \omega$. Therefore,

$$x'' + \frac{1}{\sqrt{\omega}}C_1x' + \frac{1}{\omega}C_2x + \frac{1}{\omega}C_3x^3 = \frac{\rho}{\omega}\cos\left(\sqrt{\omega}\tau\right) \qquad \textbf{(5.2.1-4)}$$

The 2nd order differential equation is split into two first order ordinary differential equations to make a more compact form for these types of analyses.

$$x' = y \qquad \textbf{(5.2.1-5)}$$

$$y' = -\frac{C_1}{\sqrt{\omega}}y - \frac{C_2}{\omega}x - \frac{C_3}{\omega}x^3 + \frac{\rho}{\omega}\cos\left(\sqrt{\omega}\tau\right) \qquad \textbf{(5.2.1-6)}$$

Similarly, the mechanical properties of the material used, in this case aluminium alloy 5083, are used for the calculation of system parameters, which are tabulated in Table 5-1.

System Parameters						
Boundary Conditions	Half-crack Lengths [m]	Damping, C_1 $[s^{-1}]$	Linear Stiffness, C_2 $[s^{-2}]$	Cubic Nonlinearity, C_3 $[m^{-2}s^{-2}]$	Excitation amplitude, $\rho\,[m\,s^{-2}]$	Reference Frequency, $\omega\,[rad\,s^{-1}]$
SSSS	0.01	0.16	37072.80	3.84962×10^{8}	2.56708	192.54
	0.025		36514.30	3.78199×10^{8}		191.09
CCSS	0.01		1.33234×10^{6}	2.40601×10^{9}	5.13416	1154.27
	0.025		1.31453×10^{6}	2.36375×10^{9}		1146.53
CCFF	0.01		52875.30	-1.00988×10^{9}	1.30113	229.95
	0.025		52348.10	-9.92135×10^{8}		228.80

Table 5-1: Data used for dynamical system analysis for various cases of boundary conditions and half-crack lengths

5.3 *Dynamics 2* - A Tool for Bifurcation Analysis

The *Dynamics 2* software package was developed by Nusse and Yorke in 1998 to enable the use of computational numerical investigations for investigating system dynamics. Prior to this, a previous edition, *Dynamics*, was offered by Nusse and Yorke in 1994. Several other authors have used this software for system dynamics investigations namely, Nusse *et al*. (1994), Chin *et al*. (1994) and Nusse *et al*. (1995). Lim, in 2003, used *Dynamics 2* for a preliminary investigation into the effects of nonlinear response modification within coupled oscillators and his numerical results showed that the *Dynamics 2*

software package has the capability of resolving a variety of complex nonlinear problems very efficiently.

Dynamics 2 combines different tools for visualising the dynamical systems, such as tools for plotting basins of attraction, computing saddle trajectories, automatically searching for all periodic orbits of a specified period, computation of Lyapunov exponents and plotting of bifurcation diagrams. In *Dynamics 2*, there are numerous built-in examples of maps and differential equations, particularly the Henon, Logistic, and Piecewise linear maps, amongst others, and differential equations includes Goodwin's equation, the Lorenz system, the forced-damped pendulum equation, a parametrically excited Duffing equation, the Rössler equation, and many more. Although a variety of program codes are made available in the form of maps and differential equations, it allows the user to add his/her own mathematical model within the editor menu. Figure 5-1 shows a screen dump of the program code that is created for the analysis of the Duffing system of equation (5.2-1).

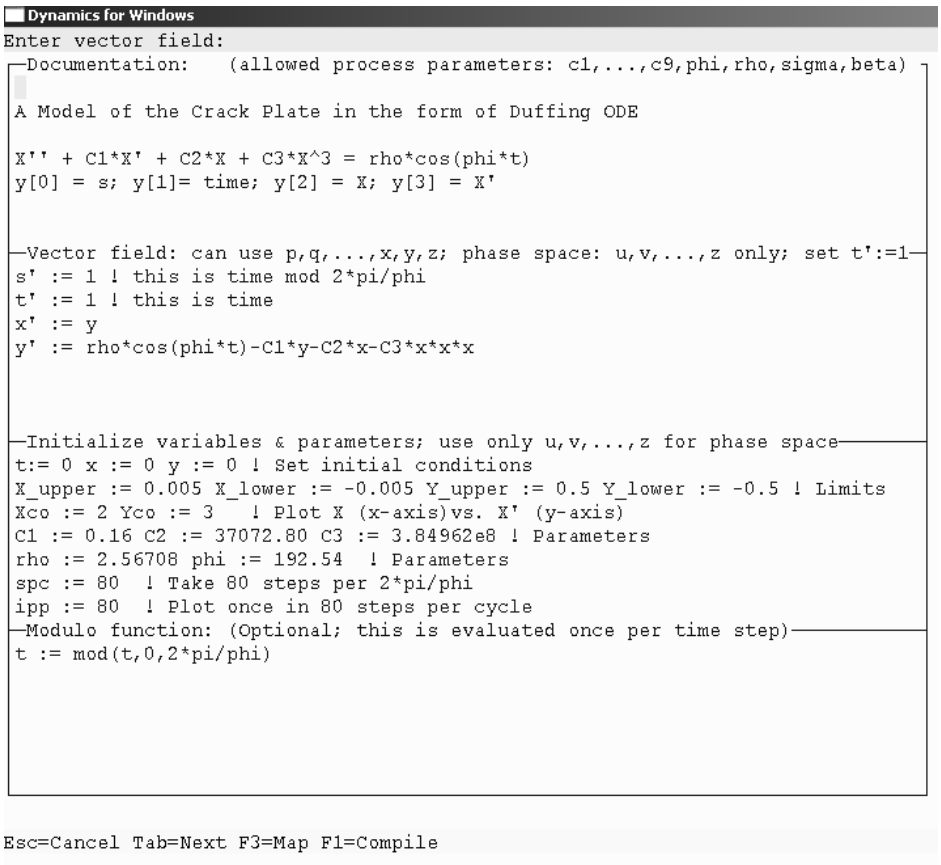

Figure 5-1: *Dynamics 2* program code for the cracked plate model and a boundary condition SSSS

5.3.1 Bifurcation Analysis

In the study of dynamical systems, a sudden qualitative or topological change can occur under the variation in a parameter of the system. These changes in the dynamics are called bifurcations, and the parameter values at which they occur are called bifurcation points. Bifurcations can take place in both continuous systems described by differential equations, and in discrete systems, described by maps. They define transitions and instabilities in the systems and are scientifically important. In the literature, there are various types of keys, defined, bifurcations, however, in the present analysis a period doubling bifurcation can mostly be observed and is analysed in the following sections in detail. A period doubling bifurcation is a bifurcation in which the system switches to new behaviour at integer multiples of the periodicity of the original response.

5.3.2 Lyapunov Exponents

Numbers that measure the exponential attraction or separation in time of two adjacent trajectories in phase space, with different initial conditions, are called Lyapunov (or Liapunov) exponents. A positive Lyapunov exponent indicates a chaotic motion in a dynamical system with bounded trajectories.

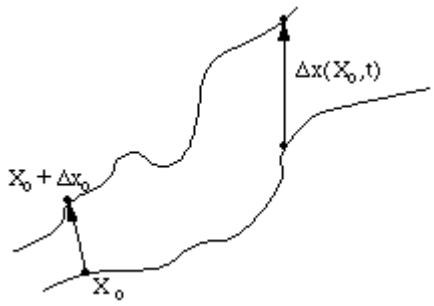

Figure 5-2: Explanation of Lyapunov exponent

By considering two points in space, X_0 and $X_0 + \Delta x_0$, and assuming an orbit in that space generated by using some equation or system of equations, then these orbits can be thought of as parametric functions of a variable like time. If one of the orbits is used as a reference orbit, then the separation between the two orbits will also be a function of time. As sensitive dependence can arise only in some portions of a system, this separation is also a function of

the location of the initial value and has the form $\Delta x(X_0, t)$. In a system with attracting fixed points or attracting periodic points, $\Delta x(X_0, t)$ diminishes asymptotically with time. If a system is unstable, then the orbits diverge exponentially for a while, however they finally settle down. For chaotic points, the function $\Delta x(X_0, t)$ behaves erratically. It is therefore appropriate to study the mean exponential rate of divergence of two initially close orbits using the formula

$$\lambda = \lim_{\substack{t\to\infty \\ |\Delta x_0|}} \frac{1}{t} \ln \frac{|\Delta x(X_o, t)|}{|\Delta x_o|} \qquad \textbf{(5.3.2-1)}$$

$\lambda < 0$ The orbit attracts to a stable fixed point, or stable periodic orbit. Negative Lyapunov exponents are characteristic of dissipative or non-conservative systems. Such systems exhibit asymptotic stability; the more negative the exponent, the greater the stability. Superstable fixed points and superstable periodic points have a Lyapunov exponent of $\lambda = -\infty$. This is something analogous to a critically damped oscillator in that the system heads towards its equilibrium point as quickly as possible.

$\lambda = 0$ The orbit is a neutral fixed point or an eventually fixed point. A Lyapunov exponent of zero indicates that the system is in some sort of steady-state mode. A physical system with this exponent is conservative. Such systems exhibit Lyapunov stability.

$\lambda > 0$ The orbit is unstable and also chaotic. Nearby points, no matter how close they are, diverge to any arbitrary separation. All neighbourhoods in the phase space are eventually visited. These points are said to be unstable. For a discrete system, the orbits would be a bit lumpy like snow. For a continuous system, the phase space would be a tangled sea of wavy lines like a pot of spaghetti.

The bifurcation behaviour of a system for the cases of the half-crack lengths of 0.01 m and 0.025 m within equation (5.2-1) is plotted next in terms of

- Amplitude of response, x, as a function of normalised excitation frequency, ω and the Lyapunov exponent.

- Amplitude of response, x, as a function of normalised excitation acceleration, and the Lyapunov exponent.

The first mode is examined in detail around the resonant region, and it is observed that at the high frequency end, a new phenomenon occurs. This could imply chaos.

All the numerical data used for these plots are tabulated in Table 5-1. Certain *Dynamics 2* commands which are necessary for the smooth plotting of all these Figures are summarised in the Table 5-2. The author has included some of the definition of these commands in Appendix C, that are necessary to get good plots. For a fuller understanding of these commands, the reader is referred *Dynamics: Numerical Explorations* by Nusse and York (1998), and the work of Lim (2003).

Commands	IPP	SPC	BIFD	BIFPI	BIFV	CON
Bifurcation diagrams	30	30	1000	1500	1000	Off
Lyapunov exponent diagrams	30	30	1000	1500	1000	On
Time plots	1	30	200	0	400	On
Phase Planes	1	30	200	0	400	On
Poincaré Maps	30	30	200	0	400	Off

Table 5-2: *Dynamics 2* command values for plotting

5.3.3 Amplitude of response, x, as a function of normalised excitation frequency, ω and the Lyapunov exponent

The following observations have been made, and summarised as follows:

- The first mode is examined around the resonant region, and it is evident that the cubic nonlinear coefficient accentuates the nonlinear effect in all three boundary conditions cases, mirroring the effect noticeable in Figures 4-1(b). Therefore, both methods show the same nonlinear trends.

- The system becomes chaotic with the increase in normalised excitation frequency. This can be observed in Figures 5-3(a) and 5-3(b), and Figures 5-4(a) and 5-4(b) for the two cases of the half-crack length. Moreover, the route to chaos can easily be seen in Lyapunov exponent plots.

- An early indication of chaos is observed, with the increase in half-crack length from 0.01 m to 0.025 m, as indicated in Figures 5-4(a) and 5-4(b).

- No indication of chaos is found in the case of the CCFF boundary condition within the normalised excitation frequency range of 0 – 30 (see Figures 5-3(c) and 5-4(c)).

- Softening characteristics can be observed for the cases of the SSSS and CCSS boundary conditions, and hardening features can be found in the CCFF case (see Figures 5-3 and 5-4).

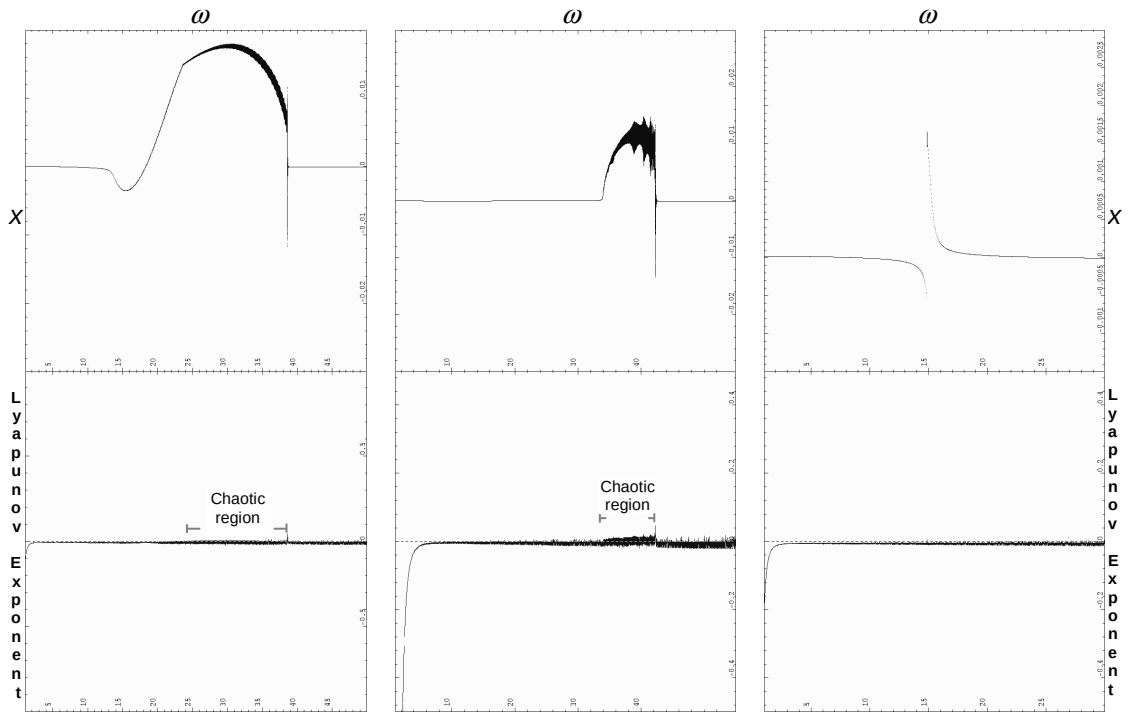

(a) SSSS (b) CCSS (c) CCFF

Figure 5-3: Bifurcation diagrams for three different cases of boundary conditions and a half-crack length of 0.01 m for the normalised control parameter, *ω*

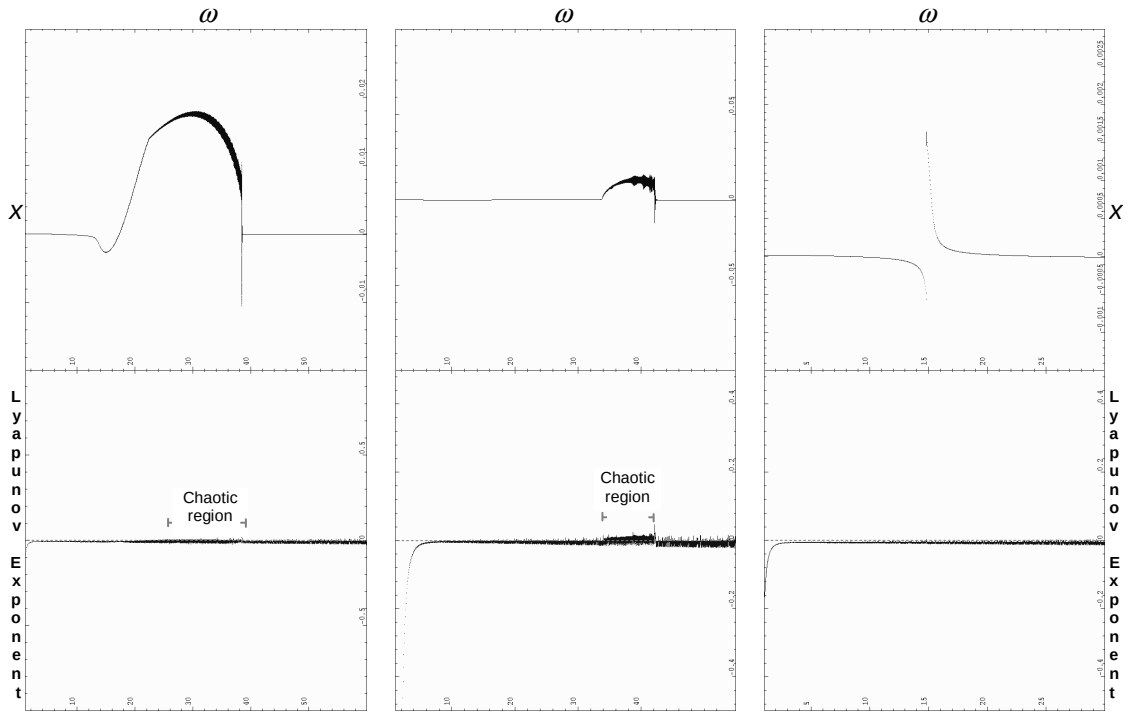

(a) SSSS (b) CCSS (c) CCFF

Figure 5-4: Bifurcation diagrams for three different cases of boundary conditions and a half-crack length of 0.025 m for the normalised control parameter, *ω*

5.3.4 Amplitude of response, *x*, as a function of normalised excitation acceleration and the Lyapunov exponent

The following are the general points observed from these analyses:

- Figures 5-5 and 5-6 show the bifurcation of *x* as controlled by the normalised excitation acceleration, and using the first mode eigenvalue, ω from Table 5-1. By increasing the normalised excitation acceleration to a very high value, the periodic response bifurcates to chaos. Positive Lyapunov exponents for these respective Figures show clear indication of chaos, while the negative Lyapunov exponents show stable motion. As the response becomes chaotic, higher normalised excitation acceleration is required in each of the three boundary conditions cases and half-crack lengths, successively.

- Period doubling bifurcation can best be observed in Figures 5-5(b), 5-5(d), 5-6(b), and 5-6(d) with the increase of normalised excitation acceleration. In the case of SSSS, period-2 and period-4 motion can be found in the region of normalised excitation acceleration 47.70 to 48.90 and 48.90 to 49.15 respectively. Similarly, further period doubling bifurcations i.e. period-8 and period-16 can be found in the same way. These period doubling bifurcations continue and lead finally to chaotic motion.

- It can be seen from these Figures that when the system bifurcates to higher multiple of periodic motion, a jump up to the zero level in the Lyapunov exponent plot occur, which is also an indication that the system moves to higher multiples of the period.

- Interesting bifurcations and period doubling routes to chaos are predicated via the Lyapunov exponent in the cases of the SSSS and CCSS boundary conditions.

- As the increase in half-crack length goes from 0.01 m to 0.025 m, the system bifurcates to period-2, -4, -8, and so on, due to the decrease in

normalised excitation frequency and cubic nonlinear coefficient (see Figures 5-5(b), 5-5(d), 5-6(b), and 5-6(d)).

- These Figures also indicate bifurcation to periodic motion after the chaos region.

- In the case of the CCFF boundary condition and for each case of the half-crack length, the *Dynamics 2* program arbitrarily depicts these as negative values, and the analysis is automatically truncated in Figure 5-5(e) due to the computational limitations of the program.

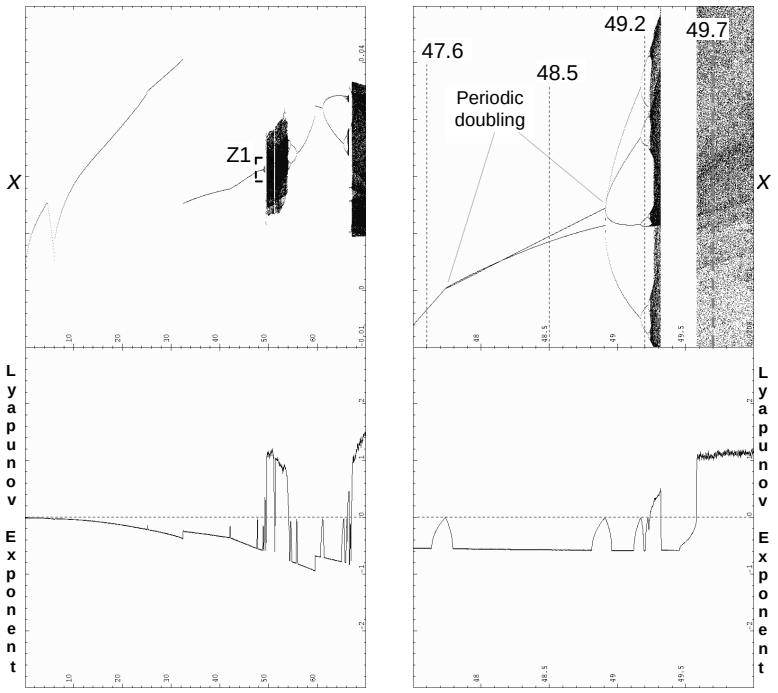

(a) SSSS (b) SSSS – Enlarged view of Z1

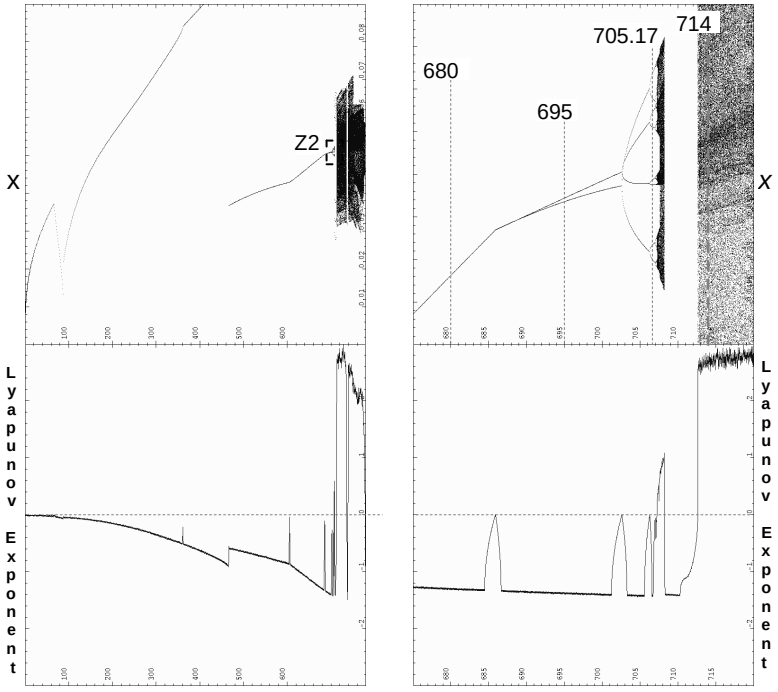

(c) CCSS (d) CCSS – Enlarged view of Z2

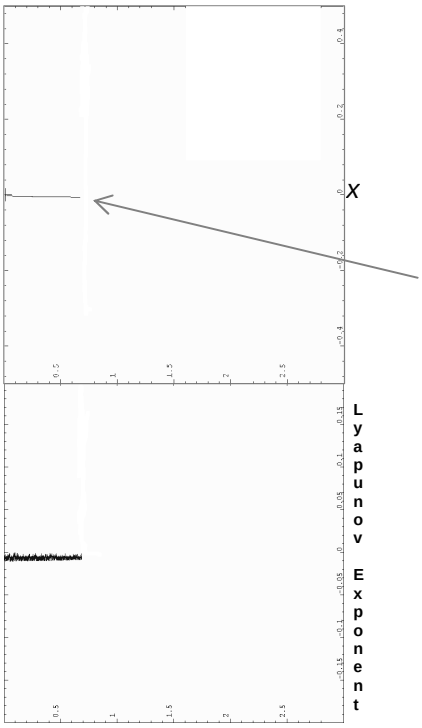

(e) CCFF

Figure 5-5: Bifurcation diagrams for three different cases of boundary conditions and a half-crack length of 0.01 m for the normalised excitation acceleration in the *x*-direction

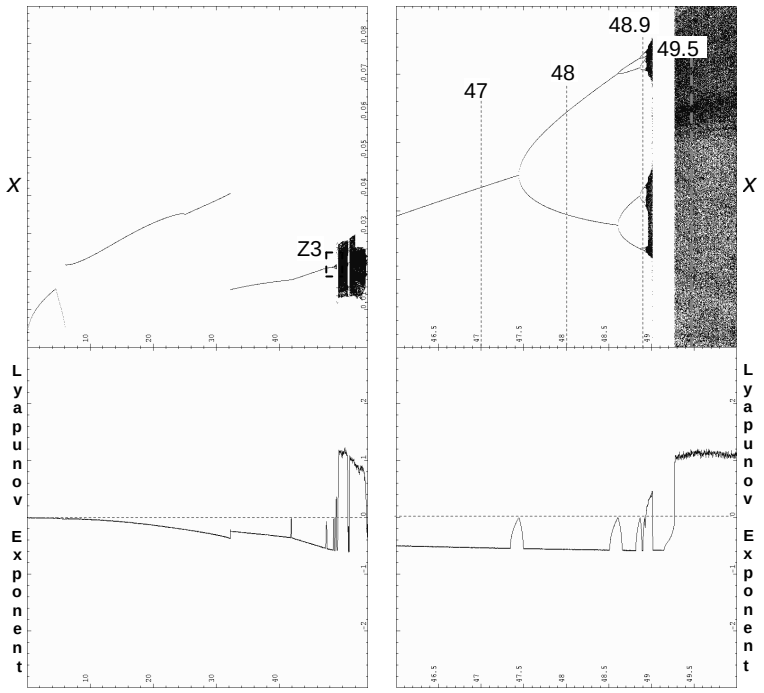

(a) SSSS (b) SSSS – Enlarged view of Z3

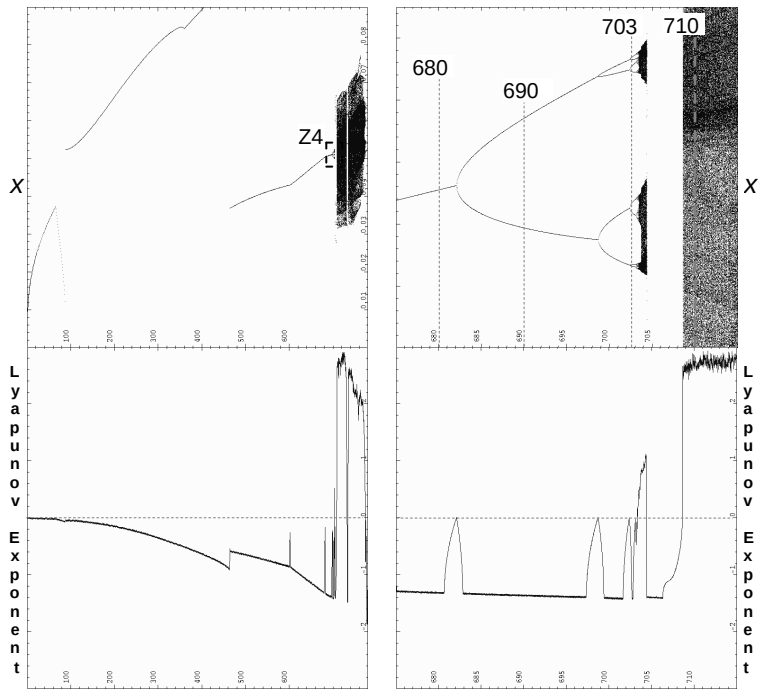

(c) CCSS (d) CCSS – Enlarged view of Z4

Figure 5-6: Bifurcation diagrams for three different cases of boundary conditions and a half-crack length of 0.025 m for the normalised excitation acceleration in the *x*-direction

Discrete normalised excitation acceleration points in Figures 5-5(b), 5-5(d), 5-6(b), and 5-6(d) are selected for the plotting of time plots, phase planes, and Poincaré maps for a more detailed understanding of the system's dynamics in the proceeding section. However, in the case of the CCFF boundary condition, the analysis of the *Dynamics 2* program automatically truncates due to the computational limitations of the program, and depicts these as negative values. Therefore, it is not currently possible to observe bifurcations in the case of the CCFF boundary condition for the cracked plate.

5.3.5 Time plots, Phase planes, and Poincaré maps

The term period(s) for a periodic motion is defined as the number of period(s) for a cycle to repeat itself. This definition is applied here and the period for these analyses is measured as $T = 2\pi/\omega$. It means that cycle repeats itself after every T sec and is called period-1 motion.

The time plots and phase planes are plotted for steady-state interval of time i.e. from 499.50 to 500 seconds. However, the Poincaré maps are plotted over the transient time, from 0 to 500 seconds as most of them converged to a periodic motion with just a point, therefore richer diagrams are preferred and so these maps converge to a point, and this is usually called a point attractor.

The break-down of the observations made for different normalised excitation acceleration values are as follows:

5.3.5.1 Figures 5-7(a) to 5-10(a)

- All the bifurcation diagrams for the two cases of the half-crack length indicate periodic and stable motion, as depicted in Figures 5-5(b), 5-5(d), 5-6(b) and 5-6(d) with negative Lyapunov exponents.

- Time plots in each boundary condition case illustrate clear evidence of a periodic response.

- In the phase planes, all the Figures show stationary and post-transient motion by the elimination of the initial part of the solutions. These

phase planes shows periodic orbits corresponding with the bifurcation diagrams.

- All the Poincaré maps converge into single points. The maps consist of a finite number of points, which implies periodic motion because there is only one point, which indicates a period-1 motion.

5.3.5.2 Figures 5-7(b) to 5-10(b)

- All the bifurcation diagrams for the two cases of the half-crack length show periodic and stable motion of period-2, with negative Lyapunov exponents.

- All the time plots depict periodic motion.

- The phase plane in each case indicates the periodic doubling phenomenon to period-2 motion, which is in-line with the bifurcation diagrams (see Figures 5-5(b), 5-5(d), 5-6(b) and 5-6(d)).

- The Poincaré maps again converge to two points, indicating period-2 motion.

5.3.5.3 Figures 5-7(c) to 5-10(c)

- The bifurcation diagrams in Figures 5-5(b), 5-5(d), 5-6(b) and 5-6(d) show a period-8 motion.

- In time plots, a careful observation show that the oscillation repeats itself after every 8 intervals of time.

- The Phase planes show complicated and rich phase plots, however, the orbit repeat itself on the same path, as the simulation time is continued.

- The Poincaré maps illustrate how the transient motion converges into 8 stationary points. These finite number of points implies period-8 motion as corresponding with the bifurcation diagrams.

5.3.5.4 Figures 5-7(d) to 5-10(d)

- The bifurcation diagrams for these cases show chaotic motion with positive Lyapunov exponents.

- In all the time plots the oscillations never repeat. This could be a qualitative visual indicator of chaotic motion.

- In the phase planes a densely filled phase plane is obtained. As the simulation is allowed to continue, the planes would be even more overlaid by repeated orbit cross-overs. No dominant single orbit is observed and so this coordinates a chaotic motion.

- The Poincaré maps show a large number of points. This describes a highly nonlinear behaviour which generally indicates chaotic motion. This conclusion is supported from the Lyapunov exponent plots of Figures 5-5(b), 5-5(d), 5-6(b) and 5-6(d).

Finally, it is concluded from these numerical results that when the system is excited at its resonant frequency, linear, nonlinear (period doubling), and chaotic responses can be obtained by changing the normalised excitation accelerations (see Figures 5-5 and 5-6). Similarly, a route to chaos can also be obtained by changing the normalised excitation frequency at a constant value of the normalised excitation acceleration (see Figures 5-3 and 5-4).

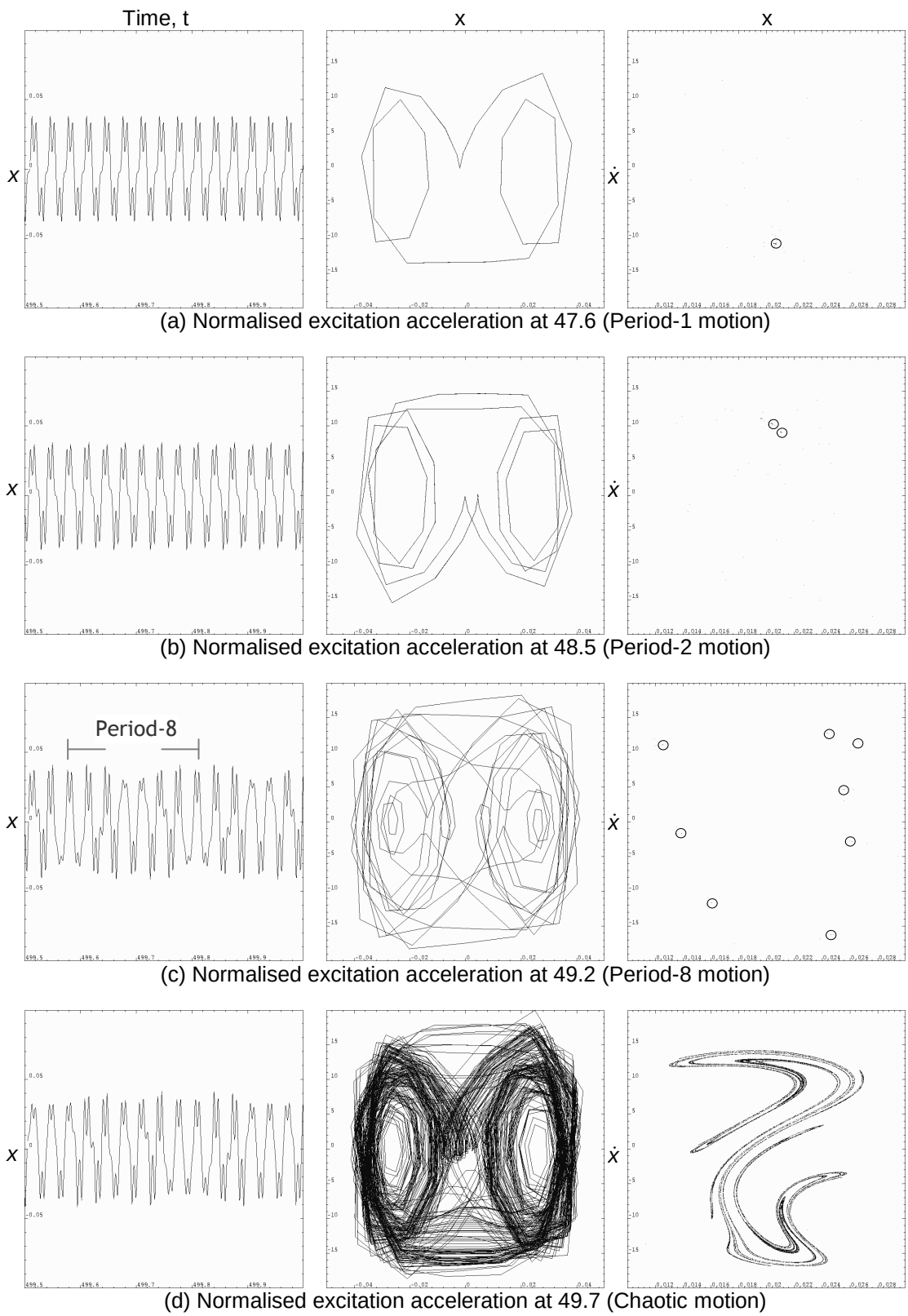

(a) Normalised excitation acceleration at 47.6 (Period-1 motion)

(b) Normalised excitation acceleration at 48.5 (Period-2 motion)

(c) Normalised excitation acceleration at 49.2 (Period-8 motion)

(d) Normalised excitation acceleration at 49.7 (Chaotic motion)

Figure 5-7: Dynamical system analysis for a half-crack length of 0.01 m and the boundary condition SSSS

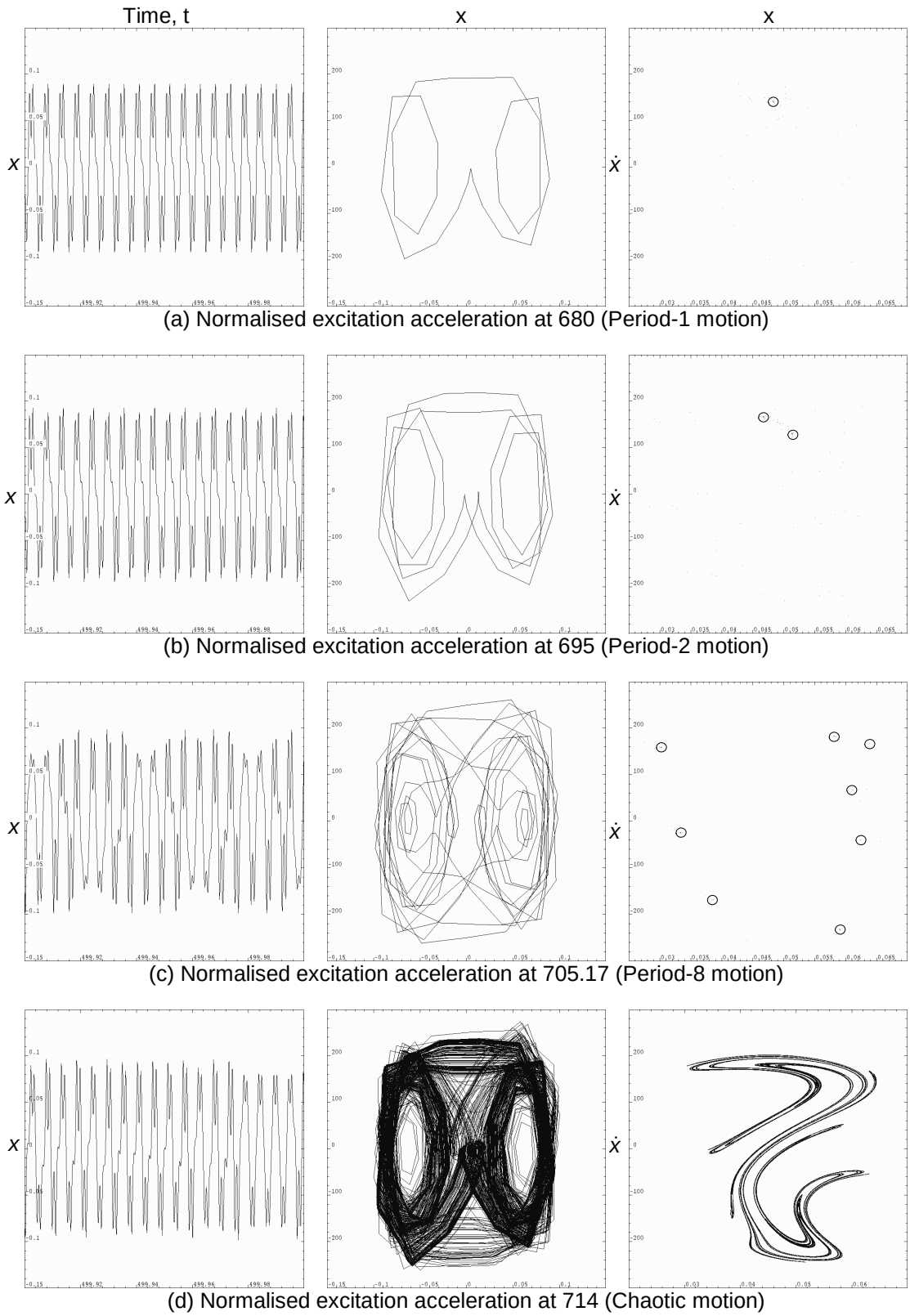

(a) Normalised excitation acceleration at 680 (Period-1 motion)

(b) Normalised excitation acceleration at 695 (Period-2 motion)

(c) Normalised excitation acceleration at 705.17 (Period-8 motion)

(d) Normalised excitation acceleration at 714 (Chaotic motion)

Figure 5-8: Dynamical system analysis for a half-crack length of 0.01 m and the boundary condition CCSS

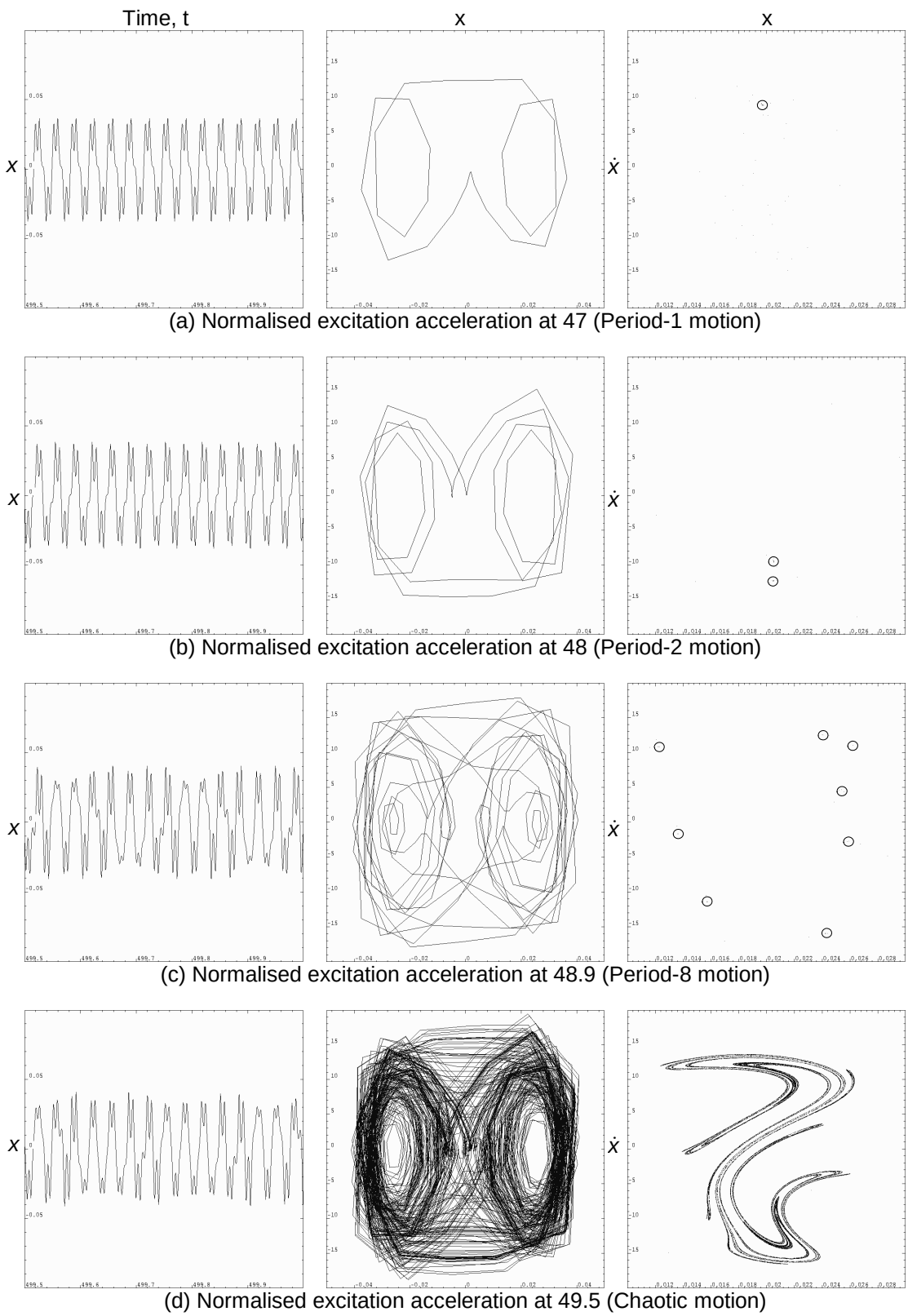

(a) Normalised excitation acceleration at 47 (Period-1 motion)

(b) Normalised excitation acceleration at 48 (Period-2 motion)

(c) Normalised excitation acceleration at 48.9 (Period-8 motion)

(d) Normalised excitation acceleration at 49.5 (Chaotic motion)

Figure 5-9: Dynamical system analysis for a half-crack length of 0.025 m and the boundary condition SSSS

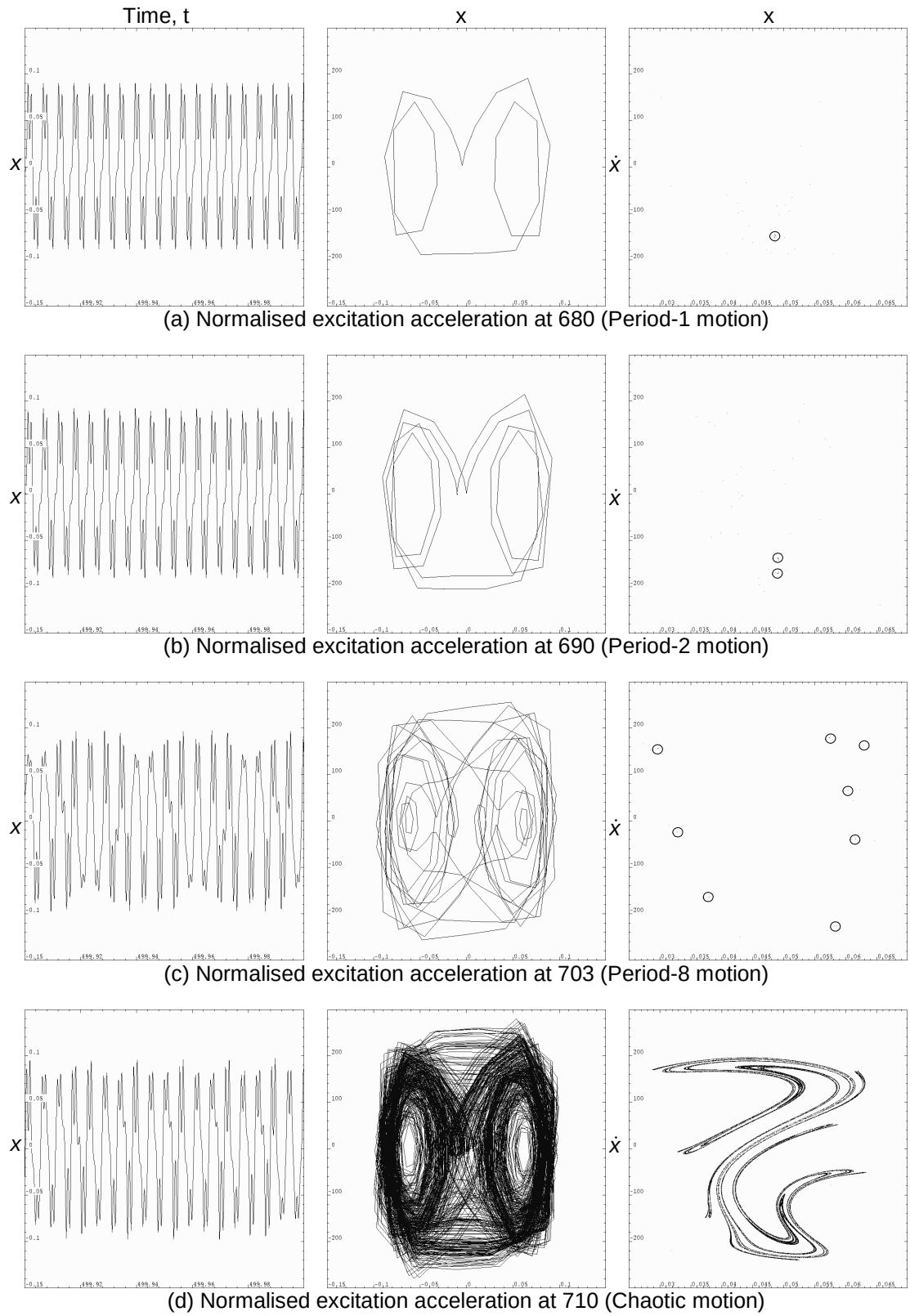

(a) Normalised excitation acceleration at 680 (Period-1 motion)

(b) Normalised excitation acceleration at 690 (Period-2 motion)

(c) Normalised excitation acceleration at 703 (Period-8 motion)

(d) Normalised excitation acceleration at 710 (Chaotic motion)

Figure 5-10: Dynamical system analysis for a half-crack length of 0.025 m and the boundary condition CCSS

5.4 Specialised Numerical Calculation Code written in *Mathematica*™

In this work the numerical nonlinear dynamical systems analysis has been performed by employing the NDSolve integrator within *Mathematica*™ for the integration and prediction of the dynamics of the cracked plate, for given initial conditions. The program code has been developed for time plots, phase planes and Poincaré maps and is presented in Appendix A. This program code is used for the prediction of chaos for the three boundary condition cases and the half-crack length of 0.01 m by using the numerical data from Table 5-1.

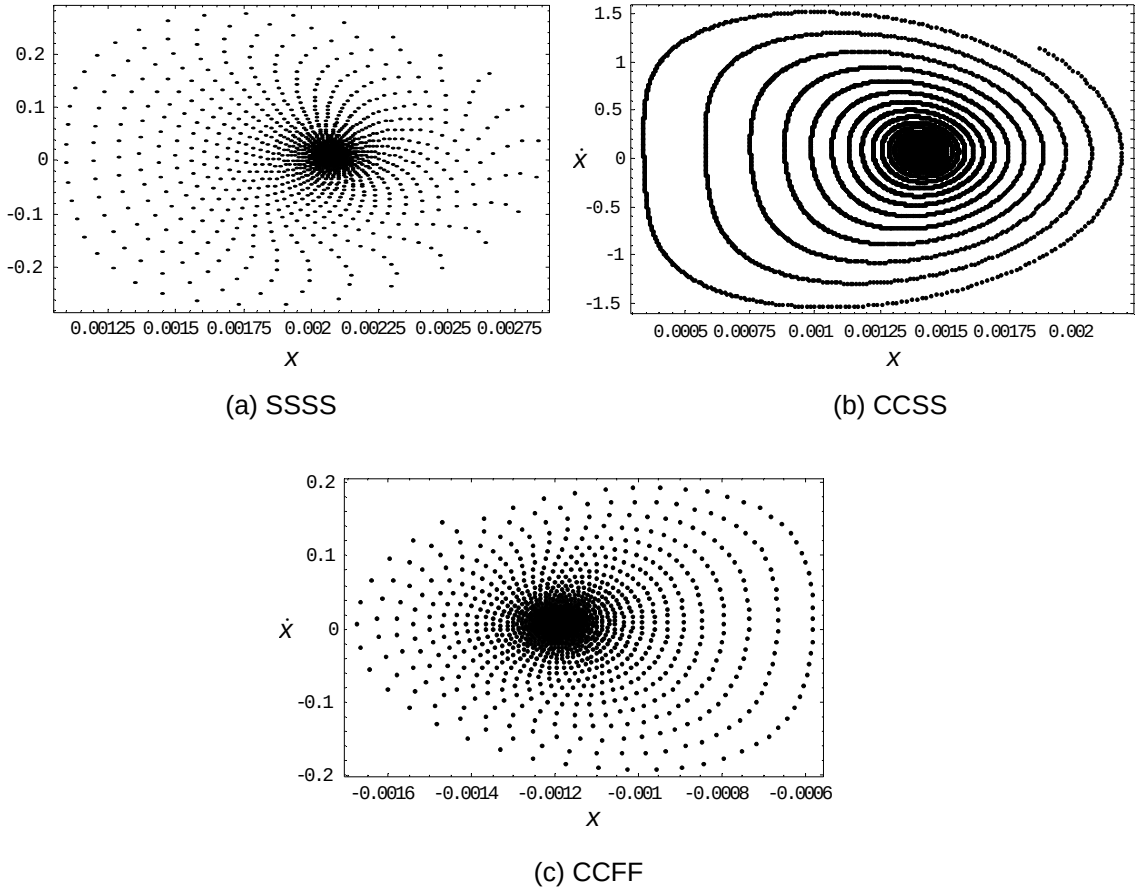

(a) SSSS

(b) CCSS

(c) CCFF

Figure 5-11: Poincaré map for the three boundary condition cases and a half-crack length of 0.01 m from the use of specialised code written in *Mathematica*™

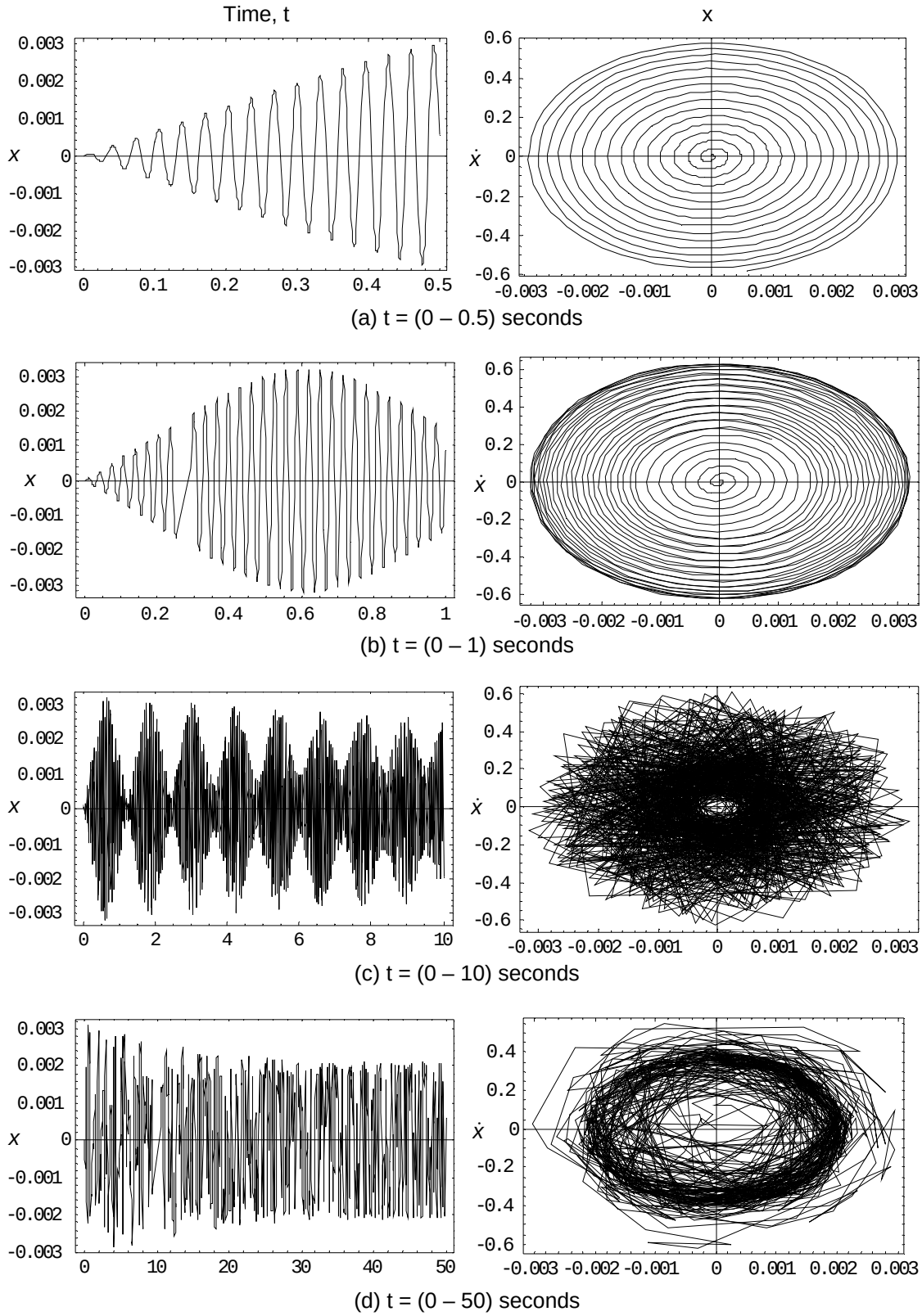

Figure 5-12: Time plots, and phase planes for a half-crack length of 0.01 m by the use of specialised code written in *Mathematica*™ and the boundary condition SSSS

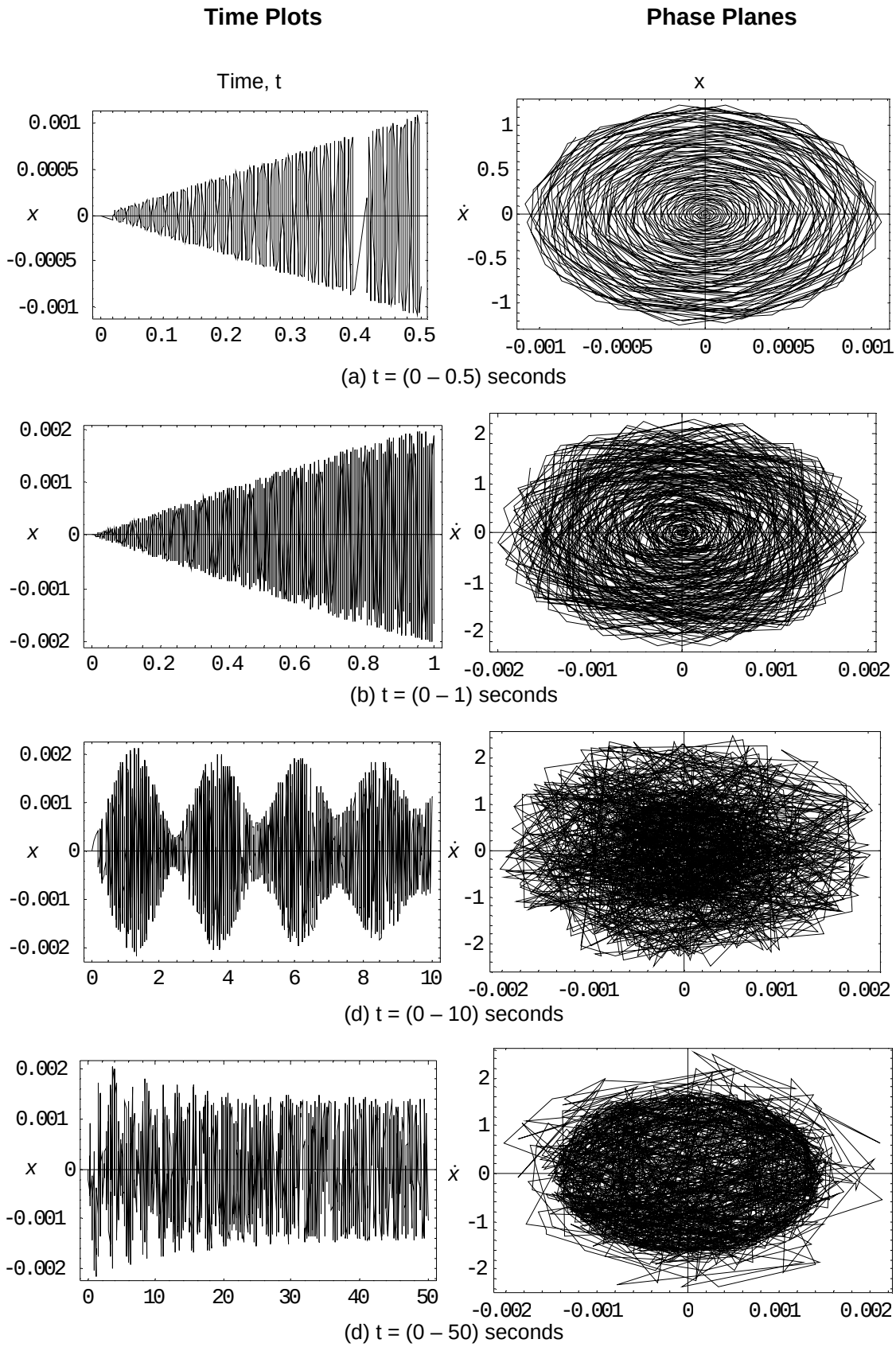

Figure 5-13: Time plots, and phase planes for a half-crack length 0.01 m by the use of specialised code written in *Mathematica*™ and the boundary condition CCSS

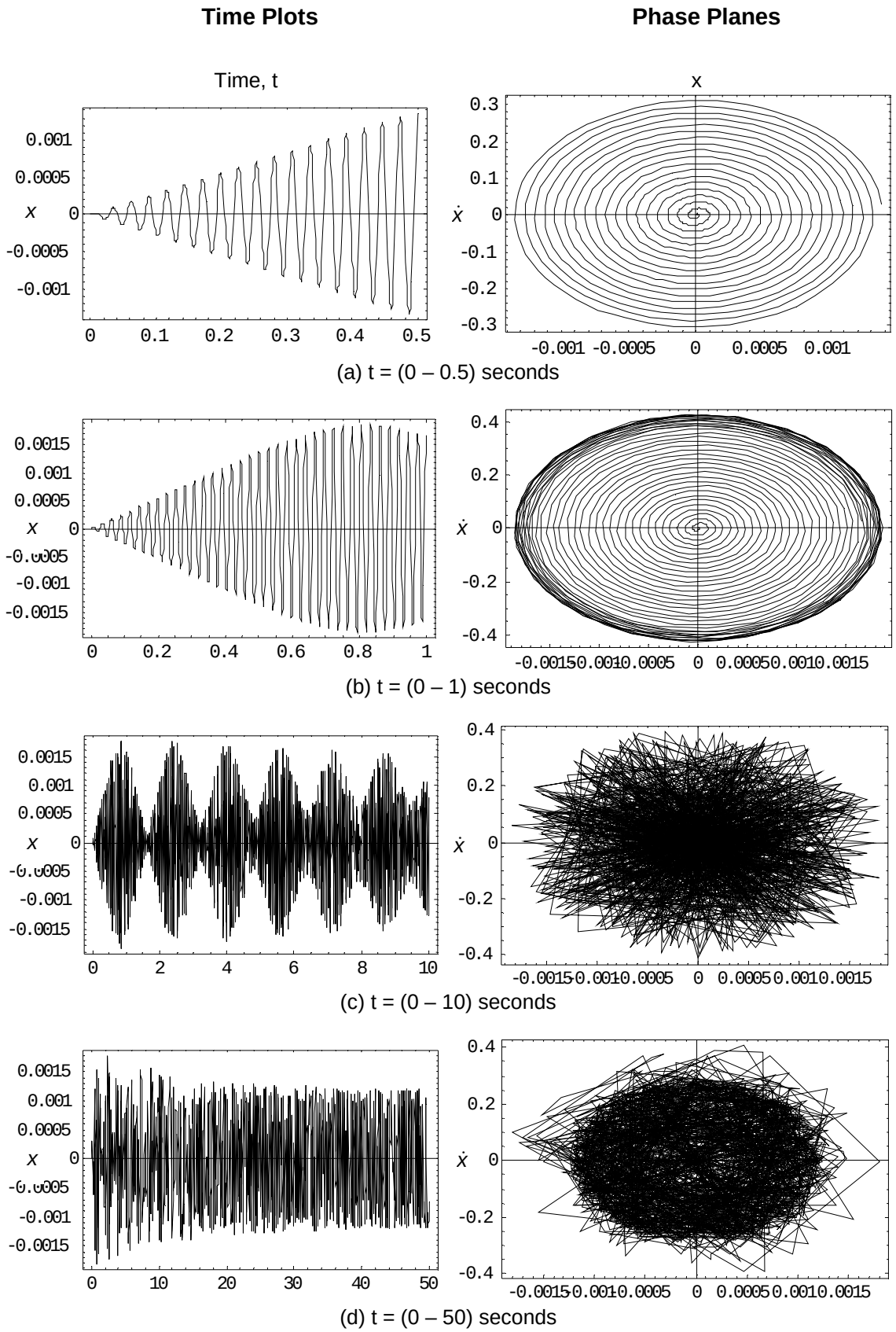

Figure 5-14: Time Plots, and phase planes for a half-crack length 0.01 m by the use of specialised code written in *Mathematica*™ and the boundary condition CCFF

All of these plots show that the system is stable and motion is periodic. The phase planes indicate periodic orbits in which system starts at the centre and moves outward in a form of circular motion. Corresponding Poincaré maps are plotted from the transient times, as most of them converge to period-1 motion with just a point, therefore, richer diagrams are preferred and so these maps converge to darker areas and finally to a point (see Figure 5-11).

Hence, it is concluded from these results that there is no clear indication of chaos in the model of the cracked plate. The *Mathematica*™ program code gives relatively good results when compared with *Dynamics 2*. *Dynamics 2* uses different command parameters such as IPP, SPC, BIFBI, BIFV, BIFD, and many more (see Appendix C) for plotting. Therefore it is very difficult to understand what happens behind the process. To avoid this complexity, a *Mathematica*™ program code was developed, which uses the powerful NDSolve function to integrate numerically the two equations of motion. The method used is as specifically stated in the code is Stiffness-Switching. This NDSolve function can potentially use a wide variety of other integration methodologies such as Adams, Gear, and RungeKutta methods. The only drawback of using this method is the computational time over *Dynamics 2*.

Chapter 6

EXPERIMENTAL INVESTIGATIONS

Many experimental studies have been carried out in the past on rectangular plates, and a variety of nonlinear phenomena has been observed. The author refers the reader to Nayfeh and Mook (1979), Chia (1980), and Sathyamoorthy (1997) for a detailed review of the nonlinear vibration of plates. However, rectangular plates with cracks have been studied by Krawczuk *et al*. (2003) and (2004), Trendafilova (2005), and Trendafilova *et al*. (2006), and by others for the vibration analysis.

In order to justify the theoretical predictions as proposed in the previous chapters, experimental measurements are carried out to verify the dependence of the cracked aluminium plate's fundamental mode shape and resonance frequency on the vibration displacement amplitude. The nonlinear resonance frequency is defined as the frequency at which the maximum vibration amplitude is observed when the excitation frequency is increased through the range of interest during a frequency response test. This definition is adopted in the plate tests and a set of measurements are carried out in which the excitation frequency is increased for a given value of force until the jump phenomenon occurs and the corresponding values of frequency and peak amplitude are noted. An interesting nonlinear dynamics phenomenon is observed in the test case of the plate with a small crack.

6.1 Instrumentation

A 500 x 1000 x 10 mm rectangular plate made of aluminium alloy 5083 is selected for the experimental investigations. The layout of the whole setup is shown in Figure 6-1. It can be noted from this Figure that the electro-dynamic exciter is driven by a function generator connected to a signal amplifier. A

vibrometer controller connected to a spectrum analyzer enables the identification of plate responses through the signal which comes from the Helium-Neon laser vibrometer. The list of the instruments used in this investigation has been included in Appendix D.

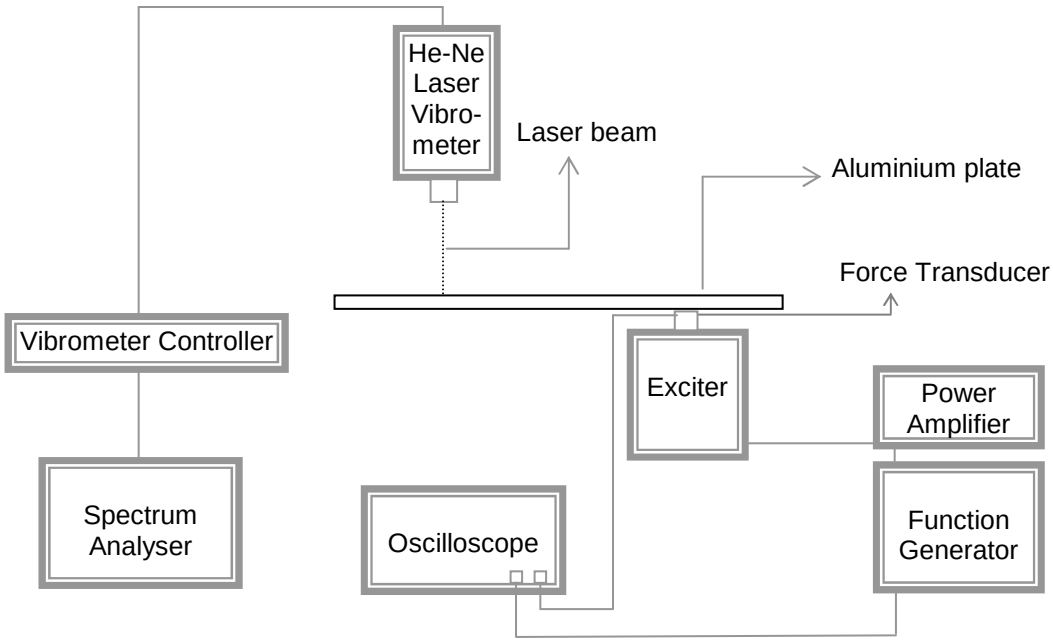

Figure 6-1: Simple layout of the experimental setup

6.2 Machining Procedure of the Crack in the Aluminium Plate

The machining of the crack can inflict additional damage on the pavement and it is desirable to use a high-precision machine that follows cracks well and produces minimal spalls or fractures. A straight part-through crack of 50 x 1 x 6 mm is required to be made at the centre and parallel to the *x*-direction of the aluminium plate by the use of an *X-Y-Z* Vertical Milling machine.

For an easy initiation of the crack machining, a scratch on the plate surface at the starting edges is required. The scratch is made using a diamond point tool. The plate is placed on the X-Y-Z coordinate table such that the desired place to be cut is below the moving cutting tool. A 2-flute solid carbide cutting tool of diameter 1 mm is used. The movement of the cutting tool is set to be 0.1 mm for each deep cut, with 40 mm per minute cutting feed in

the *X* direction and 25 mm per minute down feed in the *Z* direction. The crack propagation in the desired path is achieved by moving of the *X-Y-Z* coordinate table with the plate mounting, at a spindle speed of 2000 rpm under the moving cutting tool on the machine. The crack in the plate appears after an initial dwelling period. Figure 6-3 shows a 50 mm cut on the aluminium plate.

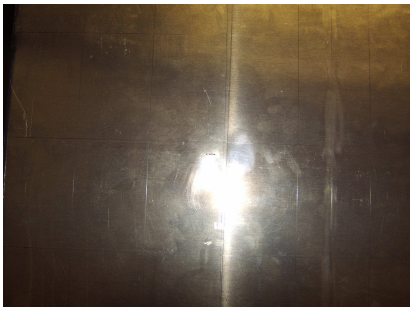

Figure 6-2: Aluminium plate with crack at the centre

Plate cutting using precision machines such as vertical milling machine gives a better profile than using a manual table. This is because of the controlled and uniform motion of the plate with the milling machine table. It is also possible to cut a repetitive profile using this milling machine procedure. This is much more difficult when it is attempted using a manual table.

6.3 Test Setup

A heavy steel rig was specifically designed for the support of the plate's ends in such a way that it could be clamped in between the clamps on the two adjacent edges of the plate, and then these clamps are tightened by a series of screws. The remaining two edges of the plate are unconstrained. A rigid guided support made of a steel frame carrying the laser vibrometer is constructed, enabling displacement measurements to be made at any point on the surface of the plate. The plate is harmonically excited by an electro-dynamic exciter which imposes no added stiffness and no additional mass on the plate. The arrangement of the two rigs and the electro-dynamic exciter is shown in Figure 6-3. The excitation of the exciter is monitored by means of a force transducer fitted into the exciter clamping fixture. This also provides a means for the control of the periodic load, as per the requirement. The excitation point is chosen to be at a distance of 37.5 x 75 mm from the fixed

ends of the plate in the *x* and *y* directions respectively. The signal from the force transducer is monitored by an oscilloscope, and the amplitude signals in terms of voltages, are monitored by the spectrum analyzer. At different points of interest over the plate's surface, the signals are recorded for further analysis. These signals are ultimately converted into mechanical amplitudes for the generation of the first mode shape of the plate at the resonance frequency. Care has to be taken to check in all tests that non-desirable vibration of the two frames and laser vibrometer occurs. The support could otherwise affect the plate displacement signals derived from the laser vibrometer. The complete instrumentation setup used in this work is illustrated in Figure 6-3.

Figure 6-3: Complete assembly of the test rig

Initially, a rough estimate of the natural frequency of the cracked and un-cracked plates is obtained using a hammer test. The plate is impacted by the hammer, and an estimate of the natural frequency is obtained from the peak in the frequency spectra. An average from multiple readings is taken for each

natural frequency. Later a sweep test around those averaged values is done to determine the exact natural frequency.

6.4 Experimental Results

Tests are carried out for the un-cracked and cracked plate of crack length 50 mm. This crack is at the centre of the plate and is parallel to the *x*-direction of the plate, so that comparisons can be made between the theoretical results and the experimental data. It is necessary initially to avoid having the excitation frequency too near to the unstable region where the jump effect could occur in the first mode. Curves show similar trends of decreasing resonance frequency with the increase of dynamic displacement amplitude for a given crack length. As may be expected the theoretical values are higher than the experimental measurements predominantly due to the inherent slip at the clamp edges, and any microscopic flaws or cracks that always exist under normal conditions at the surface, and within the interior of the body of the material. Furthermore, while developing the analytical modal, shaker-structure interaction was ignored, as was one possible nonlinear damping, and any initial geometrical distortion of the plate. It is possible that one or more of these factors could have played a significant role, and this could be further investigated.

The measured responses of the plate from repeated tests are shown in Figures 6-4 and 6-5 for an un-cracked and cracked plate of crack length 50 mm respectively, and Figure 6-6 shows the combined effect on the cracked and un-cracked plates of an excitation level of 2.5 v (This excitation level 2.5 v is equivalent to a force of 10 N approximately; this being measured from the sensitivity of the force transducer 123.78 mv/N), then as the excitation level is increased, a region of hysteresis combined with amplitude jumps and stable and unstable multivalued responses becomes evident.

Experimental investigation shows the same trend as explained in early chapters that the crack influences the excitation frequency and amplitude. In the case of the un-cracked plate an excitation frequency of 24 Hz is obtained, while it reduces to 23.6 Hz for the insertion of a crack of length 50 mm. A similarly decreasing trend in frequencies can be observed as the crack length

at the centre of the plate increases. In addition, amplitude of the vibration increases, this being summarised in Table 6-1.

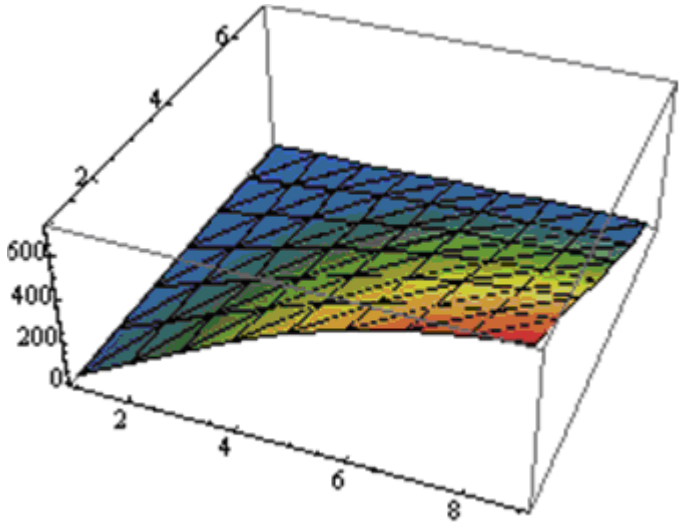

Figure 6-4: First mode shape for an un-cracked aluminium plate of aspect ratio 0.5/1

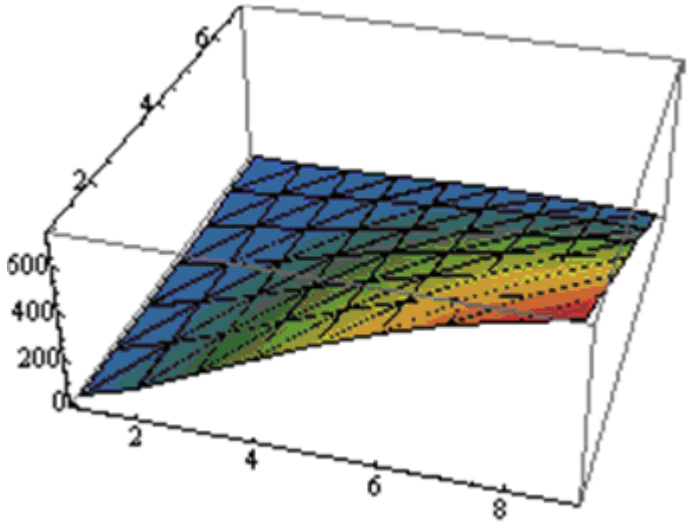

Figure 6-5: First mode shape for cracked aluminium plate of crack length 50 mm, and aspect ratio of the plate 0.5/1

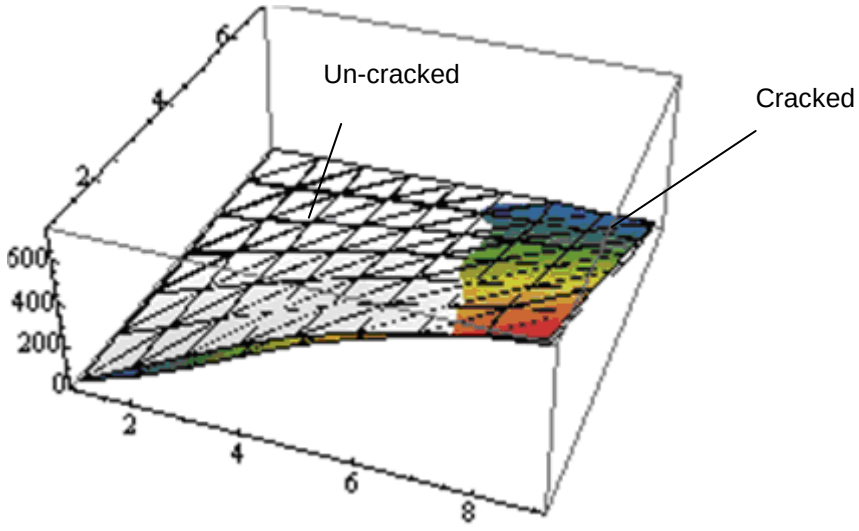

Figure 6-6: Amplitude responses (in terms of voltage signals) for first mode of an un-cracked (white mesh area) and cracked (coloured mesh area) aluminium plates of aspect ratio 0.5/1

Aluminium Plates	Frequency of excitation [Hz]	Amplitude at the tip of the free end of the aluminium plate [mm]
Un-cracked	24.0	0.90880
Cracked	23.6	0.93696

Table 6-1: Experimental results of first mode of vibration for an un-cracked and cracked aluminium plates

Chapter 7

RESULTS AND DISCUSSION

The analytical modelling of the cracked plate and their theoretical and experimental analyses have been presented in Chapters 3 to 6. The formulation of the model of the cracked plate was obtained in Chapter 3. The numerical and analytical techniques, including the method of multiple scales, direct numerical integration by the use of *Mathematica*™, and finite element analysis, were discussed in Chapter 4 for the prediction of the response of the cracked plate model as shown in Figures 3-1 to 3-3 and 3-5. A numerical study into the system's dynamics was extended into Chapter 5, where a study of the bifurcations and the stability of the solutions via time plots, phase planes and Poincaré maps, bifurcation diagrams and Lyapunov exponents were summarised. Experimental work is presented in Chapter 6 to justify the theoretical predictions.

The purpose of this chapter is to examine the results from Chapters 3 to 6, extending the discussion where appropriate, and allowing conclusions to be derived from the respective results.

7.1 Analytical Results

A new mathematical model for a cracked plate is proposed for vibration analysis. The general observations are summarised as follows:

- The natural frequency results for a cracked plate model with different aspect ratios shows that the presence of a line-crack at the centre of the plate significantly influences the natural frequency of the first mode, in all three cases of the boundary conditions investigated, which included CCFF, CCSS, SSSS (Table 3-1).

- The physical reason that cracks lower natural frequencies is due to the local flexibility in the vicinity of the crack, which in turn reduces the overall stiffness of the structure. This is intuitively discuss and clearly borne out in this research.

- In addition to the effect of the half-crack length, the natural frequency is also influenced if the geometry of the plate is changed, in particular its length and thickness (Figure 3-7).

- The results of the present nonlinear theory have been partially verified by means of existing linear models (but no such literature was found for the forced nonlinear vibration analysis of a cracked plate) as proposed by different authors, namely Stahl and Keer (1972), Solecki (1983), Qian *et al*. (1991), Krawczuk (1993) and Krawczuk *et al*. (1994) and (2001), and close agreement was found. The percentage difference between the linear models and the new nonlinear model of the cracked plate, for the chosen range of the $2a/l_1$ ratio is approximately (1-2) % (Table 3-2).

The analytical developments involved using the method of multiple scales, direct numerical integration and finite element analysis. In the following are summarised points which emerge from these studies:

- The results from the method of multiple scales given in Figures 4-1, 4-2 and 4-3 showed good conclusive results for the three cases of boundary conditions i.e. CCFF, CCSS, SSSS and one set of half-crack length of 10 mm. The effect of a crack within the plate model produced a global effect on the nonlinear response of the overall system. A hardening spring characteristic has been found in the case of CCSS and SSSS, whereas the softening spring characteristic is found in the CCFF system (Figure 4-1 for the three cases). This study can produce linear results if we set the nonlinear cubic term i.e. β_{mn} equal to zero. Comparison between the linear and nonlinear cracked plate models has also been made for the case of CCFF only, which exactly emulates the softening nonlinear characteristic as shown in Figure 4-1(b). The relative ratio of

nonlinear amplitude to linear amplitude is close to unity for zero and positive detuning, again fully in-line with the softening characteristic observable in Figure 4-1(b).

- Similarly, changing the location of the concentrated load over the plate area slightly affects the nonlinear model of the cracked plate and that is evidenced by the increasingly wide nonlinear region as the excitation location moves closer to the unsupported corner (Figure 4-3).

- The damping coefficient plays an important role, and obviously limits the finite peak amplitude. The peak amplitude shows an increasing trend with the insertion of crack into the model, as expected (see Table 4-1).

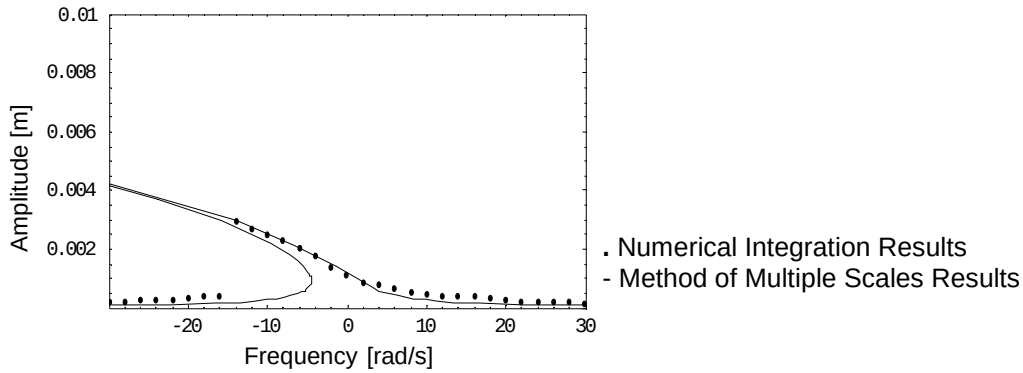

Figure 7-1: Comparison between method of multiple scales and that of numerical integration

- Numerically integrating the governing equation of motion (3.5-3) within *Mathematica*™ has produced results that corroborate those of the method of multiple scales, and are shown in Figure 7-1. The amplitudes are marginally higher in the case of numerical integration. The over-prediction of the softening overhang by the multiple scales solution is undoubtedly due to an over-correction to the solution from the first order perturbation contribution, and the assumptions that necessarily went with that in order to obtain a closed-form solution.

- The numerical integration results give the response for the first mode only whereas the method of multiple scales generates results at that

resonance condition and also around the region of perfect external tuning, by means of the detuning parameter, $\varepsilon\sigma_{mn}$ (equation 4.1-9).

The cracked plate model is investigated in ABAQUS/CAE 6.7-1, one of the tools for finite element analysis. The following are the general points observed from these results:

- The finite element analysis of the cracked plate model has produced results that corroborate those of the method of multiple scales and numerical integration for the case of CCFF only. The frequency results show a decreasing trend at the resonance condition, and similarly, the amplitude results show an increasing trend, when using a small crack, again fully in-line with the analytical model. (Figures 4-5 to 4-7, and Table 4-2). Similar results can also be obtained for other cases of the boundary conditions such as CCSS and SSSS.

- The finite element analysis results are marginally higher; this over-prediction is due to the crack geometry. In the FE analysis the crack width is taken as 1 mm, whereas it has been proposed as a continuous line spring in the derivation of the cracked plate model (chapter 3).

7.2 Numerical Results

The subsequent numerical analyses were undertaken by generating problem-specific code within the public-domain software *Dynamics 2*.

- Figures 5-3 and 5-4 give plots of the bifurcatory behaviour of amplitude response ***x*** as a function of normalised excitation frequency, ω. For the first response mode, it can be deduced that the cubic nonlinear coefficient accentuates the nonlinear effect in all the three cases of boundary conditions, mirroring the effect noticeable in the results of the method of multiple scales, numerical integrations, and finite element analysis (Figures 4-1(b), 4-4, and Table 4-2). The softening characteristic is observed for the cases of SSSS and CCSS, whereas the

response becomes more hardening in the case of CCFF, again fully in-line with the analytical model of the cracked plate.

- The calculated Lyapunov exponents support the notion that nonlinearities can generate undesirable responses, but only in cases of very high excitation level for this particular structural configuration, and damage in the form of a crack at the centre of the plate, as shown in Figures 5-3 and 5-4. As the half-crack length is increased, the system gets more chaotic, with a wider region of positive Lyapunov exponents, obviously rendering any practical system inefficient.

- Similarly, no route to chaos is indicated in the case of CCFF for the normalised excitation frequency range of 0 – 30 (Figures 5-3(c) and 5-4(c)).

- Figures 5-5 and 5-6 shows the bifurcatory behaviour of the amplitude response x as a function of normalised excitation acceleration, accompanied by its respective Lyapunov exponent. For the most linear response from Chapters 3 to 5, a periodic response for a wide range of excitation values is achieved. As the half-crack length is increased, evidence of chaos surfaces, with a higher normalised excitation acceleration that is subsequently expected.

- The results in Figures 5-5(b), 5-5(d), 5-6(b) and 5-6(d) shows period doubling bifurcations with the increase of normalised excitation acceleration. In addition, a jump up to the zero level in the Lyapunov exponent plots occurs, and indicates that the system has moved to higher period multiples.

- The *Dynamics 2* program is automatically truncated in Figure 5-5(e) due to the computational limitations of the program and arbitrarily depicts these as negative values in case of CCFF for the two sets of half-crack length.

At discrete normalised excitation acceleration points of the above bifurcations, time plots, phase planes, the Poincaré maps are given in Figure

5-7 to 5-10. The following are general observations of the cracked plate model for three set of boundary conditions.

- The periodic orbits in the phase planes move away from each other as the effect of the predominant system nonlinearity is changed, either by manipulation of the cubic nonlinear coefficient with the insertion of a small crack into the system, or by the normalised excitation acceleration. And therefore, the phenomenon behind this behaviour, as shown on the phase planes, could represent a bifurcation to chaos.

- Complicated and richer phase plots are obtained for higher normalised excitation accelerations, indicating likely chaotic motions. However, the orbits repeat themselves in the same way, as the simulation time is continued.

- Strange attractors are also obtained in the Poincaré maps for higher value of normalised excitation accelerations, again indicating chaotic motions.

Figures 5-11 to 5-14 shows the nonlinear dynamic system analysis by the use of specialised code written in *Mathematica*™. From these plots the following is concluded:

- The cracked plate model for the two sets of half-crack length is stable and the motion is periodic, in all three cases of boundary conditions.

- The Poincaré map converges to darker areas, and finally to a point, which shows a period-1 motion.

- The only drawback of using this method is the computational time when compared with *Dynamics 2*.

7.3 Experimental Results

The following results were obtained from an experimental setup carried out for the vibration analysis of the cracked plate.

- The experimental results qualitatively produce the same decreasing trend in frequencies and increasing trend in amplitudes with the insertion of a crack at the centre of the aluminium plate. However, the measured values through the experiments are significantly lower than those predicted by the theoretical calculations based on approximate techniques. This could be because of the fact that microscopic flaws or cracks that always exist under normal conditions at the surface and within the interior of the body of material, as explained by Griffith (1920).

- An experimental investigation shows that there is a local stability loss in plates with cracks under periodic loading.

7.4 Conclusions

The three methods of investigating and identifying the response behaviour of the cracked plate model, in the form of a Duffing equation (3.5-3), have all shown similar trends with regard to the effect of decreasing natural frequencies and increasing amplitude values. Dynamical system studies have also indicated that chaos is evident as the system becomes more nonlinear due to an increase in excitation acceleration. Experimental results from the tests conclude that this novel theoretical approach is practically significant.

Chapter 8

CONCLUSIONS AND FUTURE RECOMMENDATIONS

8.1 Summary

In this dissertation, a new analytical model of a cracked isotropic plate subjected to transverse harmonic excitations has been proposed, based on classical plate theory. This can be used to determine both the critical forcing amplitude as well as the jump frequencies in single mode systems such as this model depicts. This model can be applied to any single mode system with a weak cubic nonlinear geometric term, and damage in the form of a crack. This cubic nonlinear term was generated by the use of Berger's formulation, which in turn replaced the in-plane forces within the analytical model of the cracked plate, which then reduced it to the well known Duffing equation. In particular, the author studied, both experimentally and theoretically, the nonlinear behaviour, the frequency of excitation, amplitudes, and mode shapes. Three cases of boundary conditions — CCFF, CCSS and SSSS and two sets of crack length — were considered. CCFF showed negative cubic stiffness effect whereas CCSS and SSSS showed positive cubic characteristics.

In addition, the nonlinear vibration solutions of the cracked plate were investigated when it was subjected to transverse harmonic excitations, using the method of multiple scales, and the equation of motion was also numerically integrated by the use of NDsolve within *Mathematica*™. Interesting nonlinear behaviour was observed for the primary resonance condition, $\Omega_{mn} = \omega_{mn} + \varepsilon\sigma_{mn}$, where $\varepsilon\sigma_{mn}$ is the internal detuning parameter. In this study it was shown conclusively, by using a first order multiple scales approximation, that the nonlinear characteristics of the steady-state

responses are encoded within the non-autonomous modulation equations. A rectangular cross-section plate made of aluminium with a crack at the centre of the plate was considered for the numerical analysis. It was found that depending on increased crack length, the vibration frequency decreases and the amplitude increases. Furthermore, it was found that for a square CCFF plate there is an approximately 7.9 % reduction in natural frequency in the presence of a centrally located crack of length 0.05 m. However, the reduction in the value of natural frequency is lower for other plate aspect ratios, and linear and nonlinear results tend to coalesce for very low amplitude ratios (Table 3-1). There are limited references to such systems in the literature as there have not been many reported phenomena relating to nonlinear forced vibration of cracked plates to date.

Finite element analyses were performed using ABAQUS 6.7-1 for a nonlinear vibrating cracked CCFF plate. Solution of this problem was then pursued using a step-by-step procedure in conjunction with an implicit Hilber-Hughes-Taylor operator for integration. From the solution produced by this analysis a variety of information was extracted. Three dimensional profiles for various modes, deflection, and frequency of vibration were obtained (Figures 4-5, 4-6, and 4-7). It was then illustrated that these FE analyses were fully in line with the nonlinear dynamic regimes by means of comparison with the approximate analytical solution via the method of multiple scales, and numerical integration.

Further study of the bifurcations and stability of the solutions via phase planes, Poincaré maps, time plots, bifurcation diagrams and Lyapunov exponents showed that additional and highly complex dynamics could be observed, particularly in more strongly excited systems. A range of numerical results was obtained for the model of a cracked plate in the physical co-ordinate space, and these underpinned the fact that general finding of the response amplitude characteristics could be effectively achieved for different combinations of parameters.

Experimentally, the response of a rectangular, aluminium cracked plate – CCFF to transverse harmonic excitations was observed. It was found that the amplitude of vibration is a function of the crack length of the plate. The

modulation frequency, which depends on various parameters such as the amplitude and frequency of excitation, damping factors, etc., has to be near the natural frequency of the first mode. In such a case, we see a marginally increase in amplitude of the plate due to presence of crack of the first-mode component in the plate response. This is very similar to primary resonance in a structural system where the closeness of an external excitation frequency to the natural frequencies of the structure dictates the magnitude of the structure response.

The analytical model was able to predict results qualitatively similar to the experimentally observed motions, but the results differed quantitatively. Issues, such as the nonlinear damping, internal discontinuities within the plate, shaker-structure interaction, and initial curvature of the plate were ignored, when developing the analytical model. It is, therefore, possible that one or more of these factors might be playing a bigger role than expected, and this could be further investigated. Additionally, the instability region was manipulated by altering the tightness of the clamped edges of the plate. It is understood in the highly excited system that careful assembly of the system components is critical for better overall performance.

Based on the present observations, it can be concluded that conventional methods used for the reduction in frequency response in the cracked plate element, might in fact lead to an increase in the amplitude of excitation for the first mode. In other words, we can say that a loss of local stability of plates with a small crack is possible under periodic loading. As shown, a simple cracked plate under harmonic excitation could display many different nonlinear dynamic phenomena. These types of nonlinear resonances have very high excitation level to be observed. Such unusual phenomena have been observed in real engineering structures and mechanical systems, therefore there is a potential need to study such phenomena in more detail in other cracked structures. Many physical systems display nonlinear behaviour, but only a watchful eye can recognize that. Most of the time the linear perspective makes one overlook such behaviour in many practical systems. Therefore, it would be advantageous generally to model nonlinearity for overall better approximation.

Finally, this research provides some basic theory and understanding of how nonlinear plate systems can be made to be more efficient. It has also initiated an identification of the nonlinear characteristics of cracked plate structures. Engineers and scientists could be encouraged to use this new approach for prior understanding of the behaviour of damaged plates and panels. By obtaining a basic understanding, an ideal and robust system can ultimately be configured, and hence more reliable and efficient industrial systems can be constructed for a vibration based analysis methodologies, and for further development of vibration based health monitoring in cracked plate structures.

8.2 Future Recommendations

There is scope to improve and extend this cracked plate nonlinear model for a crack in arbitrary locations and orientations. Such models could then be used to explain some of the more unusual motions as described in this dissertation. Similarly, if the location of the crack is at the high-stress area, the nonlinear bend may be wider, it is therefore necessary to look into these areas for the expansion of the existing cracked plate model.

It would be interesting to see if one could introduce more than one crack and then study the influence of such cracks on the responses of the plate structures. Similarly, the study could also be extended for all-through cracks, and elliptical cracks.

Improvement of the solution technique could be pursued by implementing a second order perturbation expansion, and one could see how this affects the overall response of the system.

Finally, the solution of the cracked plate nonlinear model can further be extended for higher modes of vibration by means of approximate techniques.

LIST OF REFERENCES

Abrahams R., and Shaw C., (1982), *Dynamics: the Geometry of Behaviour*, Arial Press, Santa Cruz

Aggarwala B.D., and Ariel P.D., (1981), *Engineering Transactions*, **29**, 295-310, Vibration and Bending of a Cracked Plate.

Alhazza K. A., and Nayfeh A. H., (2001), *Proceedings of the 42nd AIAA/ASME/ASCE/AHS/ASC Structures, Structural Dynamics, and Materials Conference*, Nonlinear Vibrations of Doubly-curved Cross-ply Shallow Shells, Seattle, Washington.

Ali R., and Atwal S.J., (1980), *Computers and Structures*, **12**, 819-823, Prediction of Natural Frequencies of Vibration of Rectangular Plates with Rectangular Cutouts.

Alighanbari H., and Hashemi S.M., (2003), *AIAA-03-1206*, 36-41, Bifurcation Analysis of an Airfoil Containing a Cubic Structural Nonlinearity and subjected to Two-Dimensional Incompressible Flow.

Alwar R.S., and Nambissan K.N.R., (1983), *International Journal for Numerical Methods in Engineering*, **19**, 293-303, Three-Dimensional Finite Element Analysis of Cracked Thick Plates in Bending.

Au F.T.K., Wang M.F., (2005), *Journal of Sound and Vibration*, **281**, 1057-1075. Sound Radiation from Forced Vibration of Rectangular Orthotropic Plates under Moving Loads.

Bamnios Y., Douka E., and Trochidis A., (2002), *Journal of Sound and Vibration*, **256**(2), 287-297, Crack Identification in Beam Structures Using Mechanical Impedance.

Beidouri Z., Benamar R., and El Kadiri M., (2006), *International Journal of Non-Linear Mechanics*, **41**, 57-77, Geometrically Non-Linear Transverse Vibrations of C-S-S-S and C-S-C-S Rectangular Plates.

Benamar R., Bennouna M.M.K., and White R.G., (1990), *4th International Conference of Recent Advances in Structural Dynamics*, 749-760, The effects of Large Vibration Amplitudes on the Fundamental Mode Shape of a Fully Clamped Symmetrically Laminated Rectangular Plate.

Benamar R., Bennouna M.M.K., and White R.G., (1991), *Journal of Sound and Vibration*, **149**, 179–195, The Effects of Large Vibration Amplitudes on the Fundamental Mode Shape of Thin Elastic Structures, Part I: Simply Supported and Clamped–Clamped Beams.

Benamar R., Bennouna M.M.K., and White R.G., (1991), *Journal of Sound and Vibration*, **175**, 377-395, The Effects of Large Vibration Amplitudes on the Fundamental Mode Shape of Thin Elastic Structures, Part III: Fully clamped Rectangular Isotropic Plates--Measurements of the Mode Shape Amplitude Dependence and the Spatial Distribution of Harmonic Distortion.

Benamar R., Bennouna M.M.K., and White R.G., (1993), *Journal of Sound and Vibration*, **164**(2), 295-316, The Effects of Large Vibration Amplitudes on the Mode Shapes and Natural Frequencies of Thin Elastic Structures, Part II: Fully Clamped Rectangular Isotropic Plates.

Berger H.M., (1955), *Journal of Applied Mechanics*, **22**, 465-472, A New Approach to the Analysis of Large Deflections of Plates.

Berthelot J.M., (1999), *Dynamics of Composite Materials and Structures*, Institute for Advanced Materials and Mechanics, Springer, New York.

Bhat R.B., (1985), *Journal of Sound and Vibration*, **102**(4), 493-499, Natural Frequencies of Rectangular Plates using Characteristic Orthogonal Polynomials in Rayleigh-Ritz Method.

Bogoliubov N.N., and Mitropolski Y.A., (1961), *Asymptotic Methods in the Theory of Nonlinear Oscillations*, Gordon and Breach, New York.

Cartmell M.P., (1990), *Introduction to Linear, Parametric and Non-Linear Vibrations*, Springer, New York.

Cartmell M.P., Ziegler, S.W., Khanin, R. & Forehand, D.I.M., (2003), *Applied Mechanics Review*, **56**(5), 455-492, Multiple Scales Analysis of the Dynamics of Weakly Nonlinear Mechanical Systems.

Cawley P., and Adams R.D., (1979(a)), *Journal of Strain Analysis*, **14**(2), 49-57, The Location of Defects in Structures from Measurements of Natural Frequencies.

Cawley P., and Adams R.D., (1979(b)), *American Society of Mechanical Engineers Design Engineering Technical Conference*, St. Louis, paper 79-DET-46, Defect Location in Structures by a Vibration Technique.

Champneys A.R., (2006), *Transactions of the ASME, Journal of Computational and Nonlinear Dynamics*, **1**, 279-282, A Twenty-first Century Guidebook for Applied Dynamics Systems.

Chang C.-C., and Chen L.-W., (2004), *Applied Acoustics*, **65**, 819-832, Damage Detection of a Rectangular Plate by Spatial Wavelet Based Approach.

Chati M., Rand R., and Mukherjee S., (1997), *Journal of Sound and Vibration*, **207**(2), 249-270, Modal Analysis of a Cracked Beam.

Cheung Y.K., and Lu V.P., (1988), *Engineering Computations*, **5**, 134-140, An Implicit Implementation of Harmonic Balance Method for Nonlinear Dynamics Systems.

Chia C., (1980), *Nonlinear Analysis of Plates*, McGraw-Hill, USA.

Chin W., Ott E., Nusse H.E., and Grebogi C., (1994), *Physical Review* **E50**(6), 4427-4444, Grazing bifurcations in impact oscillators.

Chu H.N., Hermann G., (1956), *Journal of Applied Mechanics*, **23**, 532-540, Influence of Large Amplitudes on Free Flexural Vibrations of Rectangular Elastic Plates.

Cole J.D., (1968), *Perturbation Methods in Applied Mathematics,* Blaisdell, Waltham, MA.

Cole J.D., and Kevorkian J., (1963), *Nonlinear Differential Equations and Nonlinear Mechanics* (J.P.LaSalle and S. Lefschetz, eds) Academic Press, New York, 113-120, Uniformly valid Asymptotic Approximations for Certain Differential Equations.

Cordes R.D., and Joseph P.F., (1995), *International Journal of Fracture*, **68**, 287-314, Surface and Internal Cracks in a Residually Stressed Plate

Cornwell P., Doebling S.W., and Farrar C.R., (1999), *Journal of Sound and Vibration*s, **224**(2), 359-374, Application of the Strain Energy Damage Detection Method to Plate-Like Structures.

Dimarogonas A.D., (1996), *Engineering Fracture Mechanics*, **55**(5), 831-857, Vibration of Cracked Structures: A State of the Art Review.

El Bikri K., Benamar R., and Bennouna M., (2003), *Computers and Structures*, **81**, 2029-2043, Geometrically Non-linear Free Vibrations of Clamped Simply Supported Rectangular Plates. Pat I: The Effects of Large Vibration Amplitudes on the Fundamental Mode Shape.

El Kadiri M., Benamar R., (2002(b)), *Journal of Sound and Vibration*, **257**(1), 19-62, Improvement of the Semi-Analytical Method, for Determining the Geometrically Non-linear Response of Thin Straight Structures: Part II - First and Second Non-linear Mode Shapes of Fully Clamped Rectangular Plates.

El Kadiri M., Benamar R., *Journal of Sound and Vibration*, (2003), **264**(1), 1-35, Improvement of the Semi-Analytical Method, Based on Hamilton's Principle and Spectral Analysis, for Determination of the Geometrically

Non-linear Response of Thin Straight Structures. Part III: Steady State Periodic Forced Response of Rectangular Plates.

El Kadiri M., Benamar R., White R.G., (2002(a)), *Journal of Sound and Vibration*, **249**(2), 263-305, Improvement of the Semi-Analytical Method, for Determining the Geometrically Non-linear Response of Thin Straight Structures. Part I: Application to Clamped-Clamped and Simply Supported-Clamped Beams.

Emam S. A., and Nayfeh A. H., (2002), *Proceedings of the 43rd AIAA/ASME/ASCE/AHS/ASC Structures, Structural Dynamics, and Materials Conference*, Nonlinear Dynamics of a Clamped-clamped Buckled Beam, Denver, Colorado.

Epureanu B.I., and Yin S.-H., (2004), *Computers and Structures*, **82**, 2743-2751, Identification of Damage in an Aeroelastic System Based on Attractor Deformations.

Fan Z., 2001, *International Journal for Numerical Methods in Engineering*, **51**, 619-630, Transient Vibration and Sound Radiation of a Rectangular Plate with Viscoelastic Boundary Supports.

Ferri A. A., (1986), *Transactions of the ASME, Journal of Applied Mechanics*, **53**, 455-457, On the equivalence of the Incremental Harmonic Balance Method and the Harmonic Balance Newton-Raphson Method.

Fujimoto T., Wakata K., Cao F., and Nisitani H., (2003), *Materials Science Forum.*, Trans. Tech. Publications, Switzerland, **440-441**, 407-414, Vibration Analysis of a Cracked Plate Subjected to Tension using a Hybrid Method of FEM and BFM.

Goncalves J.P.M., de Castro P.M.S.T., (1999), *International Journal of Pressure Vessels and Piping*, **76**, 551-560, Application of the Line Spring Model to Some Complex Geometries, and Comparison with Three-dimensional Results.

Gorman D.G., Trendafilova I., Mulholland A., and Horàček J., (2006), *Applied Mechanics and Materials*, Trans. Tech. Publications, Switzerland, **5-6**, 323-330, Vibration of a Coupled Plate/Fluid Interacting System and its implication for Modal Analysis and Vibration Health Monitoring.

Griffith A.A., (1920), *Philosophical Transactions of the Royal Society*, London, **A221**, 162-198, The Phenomena of Rupture and Flow in Solids.

Gross B., Srawley J.E., and Brown W.F. Jr., (August 1964), NASA Technical Note D-2395, Stress-Intensity Factors for a Single-Edge-Notch Tension Specimen by Boundary Collocation of a Stress Function.

Guckenheimer J., and Holmes P.J., (1983), *Nonlinear Oscillations, Dynamical Systems, and Bifurcations of Vector Fields*, Springer-Verlag, Berlin.

Guitiérrez J.M., and Iglesias A., (1998), *Computer in Physics*, **12**(5), 508-619, *Mathematica* Package for Analysis and Control of Chaos in Nonlinear Systems.

Han W., Petyt M., (1996(a)), *Computer and Structures*, **61**(4), 713-724, Linear Vibration Analysis of Laminated Rectangular Plates using the Hierarchical Finite Element Method. I: Forced Vibration Analysis.

Han W., Petyt M., (1996(b)), *Computer and Structures*, **61**(4), 705-712, Linear Vibration Analysis of Laminated Rectangular Plates using the Hierarchical Finite Element Method I: Free Vibration Analysis.

Han W., Petyt M., (1997(a)), *Computer and Structures*, **63**(2), 295-308, Geometrically Nonlinear Vibration Analysis of Thin Rectangular Plates using the Hierarchical Finite Element Method—I: The Fundamental Mode of Isotropic Plates.

Han W., Petyt M., (1997(b)), *Computer and Structures*, **63**(2), 309-318, Geometrically Nonlinear Vibration Analysis of Thin Rectangular Plates using the Hierarchical Finite Element Method—II: 1st mode of Laminated Plates and Higher Modes of Isotropic and Laminated Plates.

Hénon M., (1976), *Commun. Mathe. Phys.*, **50**, 69-77, A Two-dimensional Mapping with a Strange Attractor.

Hirano Y., Okazaki K., (1980), *Bulletin JSME*, **23**, 732-740, Vibration of Cracked Rectangular Plates.

Holmes M.H., (1995), *Introduction to Perturbation Methods*, Springer-Verlag, New York.

Horibe T., and Watanabe K., (2006), *JSME International Journal*, **49**(3), 403-410, Crack Identification of Plates using Genetic Algorithm.

Irwin G.R., (1962), *Journal of Applied Mechanics*, **29**, 651-654, Crack Extension Force for a Part through Crack in a Plate.

Iwato (1951), *Trans JSME*, **17**(57), 30-33, Approximate Calculation for the Frequency of Natural Vibration of a Thin Rectangular Plate the two Adjacent edges of which are Clamped while the other two edges are Freely Supported. (In Japanese)

Jezequel L., Setio H.D., and Setio S., (29 Jan – 1 Feb, 1990), *Proceedings of the 8th IMAC Conference*, Orlando Florida (USA), 334-340, Nonlinear Modal Synthesis in Frequency Domain.

Jones R., and Milne B.J., (1976), *Journal of Sound and Vibration*, **45**, 309-316, Application of the Extended Kantorovich Method to the Vibration of Clamped Rectangular Plates.

Keer L.M., and Sve C., (1970), *International Journal of Solids and Structures*, **6**, 1545-1559, On the Bending of Cracked Plates.

Kerr A.D., (1968), *Quarterly of Applied Mathematics*, 26, 219-229, An Extension of the Kantorovich method.

Kevorkian J., and Cole J.D., (1981), **34**, *Perturbation Methods in Applied Mathematics*, Springer-Verlag.

Khadem S.E., and Rezaee M., (2000(a)), *Journal of Sound and Vibration*, **236**(2), 245-258, Introduction of Modified Comparison Functions for Vibration Analysis of a Rectangular Cracked Plate.

Khadem S.E., and Rezaee M., (2000(b)), *Journal of Sound and Vibration*, **230**(2), 291-308, An Analytical Approach for Obtaining the Location and Depth of an all-over Part-through Crack on Externally In-plane loaded Rectangular Plate using Vibration Analysis.

Khanin R., and Cartmell M.P., (1999), *Mathematica in Education and Research*, **8**(2), 19-26, Applying the Perturbation Method of Multiple Scales.

Khanin R., and Cartmell M.P., (2001), *Journal of Symbolic Computation*, **31**(4), 461-473, Parallelization of Perturbation Analysis: Application to Large-scale Engineering Problems.

Khanin R., Cartmell M.P., and Gilbert A., (2000), *Computer and Structures*, **76**(5), 565-575, A Computerised Implementation of the Multiple Scales Perturbation Method using *Mathematica*.

Kim Y.J., Chung K.H., Kim J.S., and Kim Y.J., (2004), *Key Engineering Materials*, Trans. Tech. Publications, Switzerland, **261-263**, 699-704, Three-dimensional Elastic-Plastic Finite Element Analysis of Biaxially Loaded Cracked Plates.

Krawczuk M., (1993), *Archive of Applied Mechanics*, **63**, 491-504, Natural Vibrations of Rectangular Plates with a Through Crack.

Krawczuk M., (1993), *Computers and Structures*, **46**(3), 487-493, A Rectangular Plate Finite Element with an Open Crack.

Krawczuk M., (1994), *Finite Elements in Analysis and Design*, **15**, 233-253, Rectangular Shell Finite Element with an Open Crack.

Krawczuk M., and Ostachowicz W.M., (1994), *Computer Methods in Applied Mechanics and Engineering*, **115**, 67-78, A Finite Plate Element for Dynamic Analysis of a Cracked Plate.

Krawczuk M., Palacz M., and Ostachowicz W., (2003), *Modern Practice in Stress and Vibration Analysis*, Materials Science Forum, **440-441**, 187-194, Spectral Plate Element for Crack Detection with the Use of Propagating Waves.

Krawczuk M., Palacz M., and Ostachowicz W., (2004), *Finite Elements in Analysis & Design*, **40**, 991-1004, Wave Propagation in Plate Structures for Crack Detection.

Krawczuk M., Żak A., and Ostachowicz W., (2001), *Computers and Structures*, **79**, 519-532, Finite Elements Model of the Plate with Elasto-platic Through Crack.

Kuzmak G.E., (1959), *Journal of Applied Mathematics and Mechanics (PMM)*, ***23***, 730-744, Asymptotic Solutions of Nonlinear Second Order Differential Equations with Variable Coefficients.

Lacarbonara W., (1999), *Journal of Sound and Vibration*, **221**, 849-866, Direct Treatment and Discretizations of Non-linear Spatially Continuous Systems.

Lau S.L., and Cheung Y.K., (1981), *Transactions of the ASME, Journal of Applied Mechanics*, **48**, 959-964, Amplitude Incremental Variational Principle for Nonlinear Vibration of Elastic Systems.

Lau S.L., Cheung T.K., Wu S.Y., (1984), *Journal of Applied Mechanics*, **51**, 837-844, Non-linear Vibrations of Thin Elastic Plates, Part I: Generalized Incremental Hamilton's Principle and Element Formulation.

Laura P.A.A., Duran R., (1975), *Journal of Sound and Vibration*, **42**(1), 129-135, A Note on Forced Vibrations of Clamped Rectangular Plate.

Lee H.E., (1992), *Computers and Structures*, **43**, 1085-1089, Fundamental Frequencies of Annular Plates with Internal Cracks.

Lee H.P., Lim S.P., and Chow S.T., (1990), *Computer and Structures*, **36**(5), 861-869, Prediction of Natural Frequencies of Rectangular Plates with Rectangular Cutouts.

Lee W.K., and Park H.D., (1999), *International Journal of Non-linear Mechanics*, **34**, 749-757, Second-order Approximation for Chaotic Responses of a Harmonically Excited Spring-pendulum System.

Leissa A.W., (1973), *Journal of Sound and Vibration*, **31**, 257-293, Free Vibrations of Rectangular Plate.

Leissa A.W., (1978), *The Shock and Vibration Digest*, **10**(12), 21-35, Recent Research in Plate Vibrations. 1973-1976: Complicating Effects.

Leissa A.W., (1984), *Proceeding of the 2nd International Conference on Structural Dynamics*: Recent Advances, Southampton, **1**, 241–260, Non-linear Analysis of Plate and Shell Vibrations.

Leissa, A.W., (1993), *Vibration of Plates*, NASA SP-160, National Acoustical and Space Administration, Washington, DC

Lele S.P., and Maiti S.K., (2002), *Journal of Sound and Vibration*, **257**(3), 559-583, Modelling of Transverse Vibration of Short Beams for Crack Detection and Measurement of Crack Extension.

Leung A.Y.T., and Zhu B., (2004), *Journal of Sound and Vibration*, **278**, 699-703, Comments on 'Free Vibration of Skew Mindlin Plates by *p*-version of F.E.M.'

Levey H.C., and Mahony J.J., (1968), *Journal of Inst. Maths Applics.*, **4**, 282-294, Resonance in almost Linear Systems.

Liew K.M., and Wang Q., (1998), *Journal of Engineering Mechanics*, **124**, 152-157, Application of Wavelet Theory for Crack Identification in Structures.

Liew K.M., Hung K.C., and Lim M.K., (1994), *Engineering Fracture Mechanics*, **48**(3), 393-404, A Solution Method for Analysis of Cracked Plates Under Vibration.

Lighthill M.J., (1949), *Philosophical Magazine*, **XL**, 1179-1201, A Technique for Rendering Approximate Solutions to Physical Problems Uniformly Valid.

Lim F.C.N., (2003), *PhD Thesis*, University of Glasgow, Glasgow, UK, A Preliminary Investigation into the Effects of Nonlinear Response Modification within Coupled Oscillators.

Lindstedt M.J., (1882), *Astron. Nachr.*, **103**, 211-220, Ueber die integration einer für die störungstheorie wichtigen differentialgleichung.

Liu G.R., and Lam K.Y., (1994), *International Journal of Solid and Structures*, **31**(21), 2965-2977, Characterization of a Horizontal Crack in Anisotropic Laminated Plates.

Liu Y., Liang L.H., Hong Q.C., and Antes H., (1999), *Engineering Fracture Mechanics*, **63**, 413-424, Non-linear Surface Crack Analysis by Three Dimensional Boundary Element with Mixed Boundary Conditions.

Lorenz H.-W., (1989), Nonlinear Dynamical Economics and Chaotic Motion, Lecture Notes in Economics and Mathematical Systems, 334, Springer-Verlag, Berlin, New York.

Lynn E.E., and Kumbasar N., (1967), *In:10th Midwestern Mechanics Conference, Fort Colins*, 911-928, Free Vibration of Thin Rectangular Plates having Narrow Cracks with Simply Supported Edges.

Mackey M.C., and Glass L., (1997), *Sciences*, **197**, 287-289, Oscillations and Chaos in Physiological Control Science.

Maestrello L., Frendi A., and Brown D.E., (1992), *AIAA Journal*, **30**, 2632-2638, Nonlinear Vibration and Radiation from a Panel with Transition to Chaos.

Malatkar P., (2003), *PhD Dissertation*, Blacksburg Virginia, Nonlinear Vibrations of Cantilever Beams and Plates.

Markström K., Storàkers B., (1980), *International Journal of Solids and Structures*, **16**, 217-229, Buckling of Cracked Members under Tension.

Mei C., (1973), *Computers and Structures*, **3**, 163-174, Finite Element Displacement Method for Large Amplitude Free Flexural Vibrations of Beams and Plates.

Mindlin R.D., (1951), *Journal of Applied Mechanics*, **18**, 31-38, Influence of Rotatory Inertia and Shear on Flexural Motions of Isotropic Elastic Plates.

Mindlin R.D., (1960), *Structural Mechanics*, Pergamon Press, 199-232, Waves and Vibrations on Isotropic Elastic Plates.

Moon F.C., (1987), *Chaotic Vibrations*, John Wiley & Sons, Inc., USA.

Morrison J.A., (1966(a)), *SIAM Rev.*, **8**, 66-85, Comparison of the Modified Method of Averaging and the two variable Expansion Procedure.

Morrison J.A., (1966(b)), *In progress in Astronautics and Aeronautics, Methods in Astrodynamics and Celestial Mechanics* (R.L. Duncombe and V.G., Szebehely, Eds.), Academic, New York, **17**, 117-138, Generalized Method of Averaging and the von Zeipel Method.

Mukhopadhyay M., (1979), *Forsch. Ing.-Wes.*, **45**(4), 111-118, A General Solution for Rectangular Plate Bending.

Murdock J.A., (1999), *Perturbations Theory and Methods*, SIAM.

Nagaraja J.V., & Rao S.S., (1953), *Journal of Aeronautical Sciences*, **20**, 855-856, Vibration of Rectangular Plates.

Nayfeh A. H., (1986), *Perturbation Methods in Nonlinear Dynamics*, 238-314, In Nonlinear Dynamics Aspects of Particle Accelerators, Jowett, J. M., Month, M., and Turner, S., eds., Springer-Verlag, Berlin, Germany.

Nayfeh A. H., (1998), *Nonlinear Dynamics*, **16**, 105-125, Reduced-order Models of Weakly Nonlinear Spatially Continuous Systems.

Nayfeh A. H., (2000), *Nonlinear Interactions*, Wiley, New York.

Nayfeh A.H. & Mook D.T., (1979), *Nonlinear Oscillations*, John Wiley & Sons, Germany.

Nayfeh A.H., (1973), *Perturbation Methods*, Wiley, New York.

Nayfeh A.H., and Arafat H.N., (2002), *Proceedings of the 43rd AIAA/ASME/ASCE/AHS/ASC Structures, Structural Dynamics, and Materials Conference*, Nonlinear Responses of Suspended Cables to Primary Resonance Excitations, Denver, Colorado.

Nayfeh A.H., and Chin C.-M., (1999), *Perturbation Methods with Mathematica™*, Dynamic Press, Virginia.

Nayfeh A.H., and Lacarbonara W., (1997), *Nonlinear Dynamics*, **13**, 203-220, On the Discretization of Distributed-parameter Systems with Quadratic and Cubic Nonlinearities.

Neogy S., and Ramamurti V., (14-17 Sep. 1997), *Proceeding of DETC'97 ASME Design Engineering Technical Conferences*, Sacramento, California, Effect of Crack on the Natural Frequency of Rotating Twisted Blades.

Nezu K., (1982), *Bulletin JSME*, **25**, 16-23, Free Vibrations of a Simple Supported Rectangular Plate with a Straight Through-notch.

Niyogi A.K., and Meyers B.L., (1981), *International Journal of Non-Linear Mechanics*, **16**(5/6), 401-408, A Perturbation Solution of Non-Linear Vibration of Rectangular Plates.

Nusee H.E., and Yorke J.A., (1994), *Dynamics: Numerical Explorations*, Springer-Verlag, New York.

Nusse H.E., Ott E., and Yorke J.A., (1995), *Physical Review Letters* **75**(13), 2482-2485, Saddle-node bifurcations on fractal basin boundaries.

Nusse H.E., York J.A., (1998), *Dynamics: Numerical Explorations*, second revised and enlarged edition, Springer, New York.

Okamura H., Liu H.W., Chu C. and Liebowitz H., (1969), *Engineering Fracture Mechanics*, **1**, 547-563, A Cracked Column under Compression.

Oliveira C.A.M., De Melo F.J.M.Q., and De Castro P.M.S.T., (1991), *Engineering Fracture Mechanics*, **39**(6), 1027-1035, The Elastic Analysis of Arbitrary thin shells having Part-through Cracks, using the Integrated Line Spring and the Semiloof Shell Elements.

Pakdemirli M., Nayfeh S.A., and Nayfeh A.H., (1995), Nonlinear Dynamics, **8**, 65-83, Analysis of One-to-One Autoparametric Resonances in Cables–Discretization vs. Direct Treatment.

Perko L.M., (July 1969), *SIAM Journal on Applied Mathematics*, **17**(4), 698-724, Higher Order Averaging and Related Methods for Perturbed Periodic and Quasi-Periodic Systems.

Petyt M., (1968), *Journal of Sound and Vibration*, **8**(3), 377-389, The Vibration Characteristics of a Tensioned Plate Containing a Fatigue Crack.

Pierre C., Dowell E.H., (1985), *Journal of Applied Mechanics*, **52**, 693-697, A Study of Dynamic Instability of Plate by an Extended Incremental Harmonic Balance Method.

Poincaré H., (1886), *Acta Math*, **8**, 295-344, Sur les intégulières des équations linéaires.

Poincare H., (1903), *Science and Hypothesis*, Dover reprint, 1952, Mineola, Dover Publications New York.

Polyzos D., Stamos A.A., and Beskos D.E., (1994), *Communications in Numerical Methods in Engineering*, **10**, 81-87, BEM Computation of DSIF in Cracked Viscoelastic Plates.

Prabhakara M.K., and Chia C.Y., (1977), *Journal of Sound and Vibration*, **52**(4), 511-518, Non-linear Flexural Vibrations of Orthotropic Rectangular Plates.

Purbolaksona J., Dirgantara T., and Aliabadi M.H., (March 2006), *Key Engineering Materials*, **306-308**, 661-666, Nonlinear Analysis of Cracked Plates.

Qian G.L., Gu S.N., and Jiang J. S., (1991), *Computers and Structures*, **39**, 483-487, A Finite Element Model of Cracked Plates Application to Vibration Problems.

Rahman Z., and Burton T.D., (1989), *Journal of Sound and Vibration*, **133**(3), 369-379, On Higher Order Methods of Multiple Scales in Non-linear Oscillators-Periodic Steady State Response.

Raju I.S., and Newman J.C.Jr., (1979), *Engineering Fracture Mechanics*, **11**, 817-829, Stress-Intensity Factors for a Wide Range of Semi-elliptical Surface Cracks in Finite-thickness Plates.

Ramachandran J. and Reddy D.V., (1972), *AIAA Journal*, **10**, 1709-1710, Nonlinear Vibrations of Rectangular Plates with Cut-outs.

Ramamurti V., and Neogy S., (1998), *Mechanics Based Design of Structures and Machines: an International Journal*, **26**(2), 131-143, Effect of Crack on the Natural Frequency of Cantilever Plates—a Rayleigh–Ritz Solution.

Rayleigh L., (1945), *Theory of Sound*. 2nd ed., Macmillan and Co. London.

Rega G., Lacarbonara W., Nayfeh A. H., and Chin C.-M., (1999), *International Journal of Non-Linear Mechanics*, **34**, 901—924, Multiple Resonances in Suspended Cables: Direct versus Reduced-order Models.

Rehfield L.W., (1973), *International Journal of Solids and Structures*, 581-590, Non-linear Free Vibrations of Elastic Structures.

Ribeiro P., Petyt M., (1999), *International Journal of Mechanical Science*, **41**(4–5), 437–459, Nonlinear Vibration of Plates by the Hierarchical Finite Element and Continuation Methods.

Ribeiro P., Petyt M., (1999), *Journal of Sound and Vibration*, **226**(5), 955–983, Geometrical Non-linear, Steady-state, Forced, Periodic Vibration of Plates: part I: Model and Convergence Studies.

Rice J.R., and Levy N., (1972), *Journal of Applied Mechanics*, **3**, 185-194, The Part Through Surface Crack in an Elastic Plate.

Rössler O.E., (1976), *Physical Letters*, **57A**, 397-398, An Equation for Continuous Chaos.

Rössler O.E., (1979), *Physical Letters*, **71A**, 155-157, An Equation for Hyperchaos.

Rossmanith H.P., (Jan. 1985), *Journal of Applied Mathematics and Physics*, **36**, 166-171, On Cracked Plates Subjected to Classical Bending.

Saavedra P.N., and Cuitino L.A., (2002), *Journal of Vibration and Control*, **8**, 51-67, Vibration Analysis of Rotor for Crack Identification.

Sathyamoorthy M., (1988), *The Shock and Vibration Digest*, 14-20, Literature Review: Recent Research in Nonlinear Plate Vibrations.

Sathyamoorthy M., (1998), *Nonlinear Analysis of Structures*, CRC, USA

Schrödinger E., (1926), *Ann. Phys.*, **80**, 437-490, Quantisierung als Eigenwertproblem.

Shawki T.G., Nakamura T., and Parks D.M., (1989), International *Journal of Fracture*, **41**, 23-38, Line-spring Analysis of Surface Flawed Plates and Shells using Deformation Theory.

Singh G., Sharma A.K., and Rao G.V., (1990), *Journal of Sound and Vibration*, **142**(1), 77–85, Large-Amplitude Free Vibrations of Beams--A Discussion on Various Formulations and Assumptions.

Smith D.R., (1985), *Singular-Perturbation Theory: An Introduction with Applications*, Cambridge University Press, London

Solecki R., (1983), *Engineering Fracture Mechanics*, **18**, 1111-1118, Bending Vibration of a Simply Supported Rectangular Plate with a Crack Parallel to one Edge.

Solecki R., (20-22 Oct. 1975), *12th Annual Meeting of the Society of Engineering Sciences*, Austin, Tex, United States, 373-380, Isotropic Finite Plates with Cracks.

Srinivasan A.V., (1965), *AIAA Journal*, **3**(10), 1951–1953, Large-amplitude Free Oscillations of Beams and Plates.

Stahl B., and Keer L.M., (1972), *International Journal of Solids and Structures*, **8**, 69-91, Vibration and Stability of Cracked Rectangular Plates.

Stanišić M.M., (1957), *Journal of Aeronautical Sciences*, **24**, 159-160, An Approximate Method Applied to the Solution of the Problem of Vibrating Rectangular Plates.

Stanišić M.M., and Payne J.G., (1968), *Archive of Applied Mechanics*, **37**(3), 189-195, A Rapidly Converging Technique for Vibration Analysis of Plates with a Discrete Mass Distribution.

Stephen W., 2005, *The Mathematica*, 5th Edition, Cambridge University Press, UK

Stokes G.G., (1843), *Trans. Camb. Philos. Soc*, **8**, 105-165, On Some Cases of Fluid Motion.

Strogatz S.H., (1994), *Nonlinear Dynamics and Chaos*, Addison-Wesley Publishing Company, USA.

Sturrock P.A., (1957), *Proc. Roy. Soc. (London)*, **A242**, 277-299, Nonlinear Effects in Electron Plasmas.

Su R.K.L., Leung A.Y.T., and Wong S.C., (1998), *Key Engineering Materials*, **145-149**, 167-172, Vibration of Cracked Kirchhoff's Plates.

Szilard R., (2004), *Theories and Applications of Plate Analysis*, John Wiley & Sons, USA.

Teng T. L., Liang C. C., and Liao C. C., (1999), *Computational Mechanics*, **23**, 1-7, 1999, Nonlinear forced vibration analysis of the rectangular plates by the Fourier series method.

Thompson J.M.T., and Stewart H.B., (1986), *Nonlinear Dynamics and Chaos*, John Wiley & Sons, UK.

Thomsen J.J., (1997), *Vibrations and Stability – Order and Chaos*, McGraw-Hill, UK

Timoshenko S., (1940), *Theory of Plates and Shells*, McGraw Hill Book Company, Inc., New York & London

Timoshenko S.P., (1921), *Philosophical Magazine*, **41**, 744-746, On the Correction for Shear of the Differential Equation for Transverse Vibrations of Prismatic Bars.

Tomotica S., (1936), Philos Magn, **21,** 745-760, The Transverse Vibration of a Square Plate Clamped at Four Edges.

Trendafilova I., (August 2005), *Applied Mechanics and Materials*, Trans. Tech. Publications, Switzerland, **3-4**, 309-314, A Study on Vibration-Based Damage Detection and Location in an Aircraft Wing Scaled Model.

Trendafilova I., (September 2005), *Key Engineering Materials*, **293-294**, 321-328, An Investigation on Vibration-based Damage Detection in an Aircraft Wing Scaled Model.

Trendafilova I., Manoach E., Cartmell M.P., Krawczuk M., Ostachowicz W.M., and Palacz M., (2006), *Modern Practice in Stress and Vibration Analysis VI*, P.Keogh, eds., Trans Tech Publications Ltd, Switzerland, **5-6**, 247-254, On the Problem for Damage Detection of Vibrating Cracked Plates.

Van der Pol B., and Van der Mark J., (1927), *Nature*, **120**, 363-364, Frequency Demultiplication.

van Dyke M., (1975), *Perturbation Methods in Fluid Mechanics*, Parabolic Press, Stanford.

Von Karman T., (1910), **IV**, 349 "Festigkeitshprobleme im Machinenbau", Encyklopadie der Mathematishen Wissenchaften.

Wah T., (1963), International *Journal of Mechanical Sciences*, **5**, 425-438, Large Amplitude Flexural Vibration of Rectangular Plates.

Wah T., (1964), *Journal of Applied Mechanics*, **31**, 139-140, The Normal Modes of Vibration of Certain Nonlinear Continuous Systems.

Wang R.-T., and Kuo N.-Y., (1999), *Structural Engineering and Mechanics*, **8**(2), 151-164, Nonlinear Vibration of Mindlin Plate Subjected to Moving Forces Including the Effect of Weight of the Plate.

Wang W.-C., Hwang C.-H., and Lin S.-Y., (August 1996), *Applied Optics*, **35**(22), 4502-4509, Vibration Measurement by the Time-averaged Electronic Speckle Pattern Interferometry Methods.

Wang Y.H., Tham L.G., Lee P.K.K., and Tsui Y., (2003), *Computers and Structures*, **81**, 2621-2630, A Boundary Collocation Method for Cracked Plates.

Wang, C., (1948), *NACA TN 1425*, Nonlinear Large-Deflection Boundary-Value problems of Rectangular Plates

Warburton G.B., (1954), *Proceeding of the Institute of Mechanical Engineering*, **168**, 371-381, The Vibration of Rectangular Plates.

Wei Z., Wen Z., and Turner K.L., (June 5-9, 2005), *Transducers 05*, Coex, Seoul Korea, **1**, 768-71, Nonlinear Dynamics of Micro Impact Oscillators in High Frequency MEMS Switch Application.

Wen Y.S and Zhixe J., (1987), *Engineering Fracture Mechanics*, **26**(1), 75-82, On the Equivalent Relation of the Line Spring Model: A Suggested Modification.

Westmann R.A., and Yang W. H., (1967), *Journal of Applied Mechanics*, **34**, 693-701, Stress Analysis of Cracked Rectangular Beams.

Whittaker E.T., (1914), *Edinburgh Math. Soc. Proc.*, **32**, 95-116, On the General Solution of Mathieu's Equation.

Wolf, Alan, Swift, Jack B., Swinny, Vastano H.L., and John A., (1985), *Physica **16D***, 285-317, Determining Lyapunov Exponents from a Time Series.

Wolfram S., (1996), *The Mathematica™ Book*, Cambridge University Press, USA

Wu G. Y., and Shih Y. S., (2005), *Computers and Structures*, **84**, 1-10, Dynamic Instability of Rectangular Plate with an Edge Crack.

Wykes C., (1982), *Optical Engineering*, **21**(3), 400-406, Use of Electronic Speckle Pattern Interferometry (ESPI) in the Measurement of Static and Dynamic Surface Displacement.

Xiao Y.-G, Fu Y.-M and Zha X.-D., (2006), *Chaos, Solitons and Fractals*, **35**, 460-465, Bifurcation and Chaos of Rectangular Moderately Thick Cracked Plates on an Elastic Foundation Subjected to Periodic Load.

Yagiz, N., and Sakman L. E., (2006), *Journal of Vibration and Control*, **12**(1), 83-98, Vibrations of a Rectangular Bridge as an Isotropic Plate under a Traveling Full Vehicle Model.

Yamaki N., (1961), *ZAMM-Journal of Applied Mathematics and Mechanics*, **41**, 501–510, Influence of Large Amplitudes on Flexural Vibrations of Elastic Plates.

Yan Y.J., and Yam L. H., (2002), *Computer and Structures*, **58**, 29-38, Online Detection of Crack Damage in Composite Plate using Embedded Piezoelectric Actuators/Sensors and Wavelet Analysis.

Yasuda K., and Torii T., (1987), *JSME International Journal*, **30**(264), 963-969, Multi-Mode Response of a Square Membrane.

Young D., (1950), *Journal of Applied Mechanics*, **17**(4), 448-453, Vibration of Rectangular Plates by the Ritz Method.

Zeng Z.-J, Dai S.-H and Yang Y.-M, (1993), *International Journal of Fracture*, **60**, 157-167, Analysis of Surface Cracks using the Line-spring Boundary Element Method and the Virtual Crack Extension Technique.

Note: Total number of references in this dissertation is 205

PUBLICATIONS

Israr A. Cartmell M.P., Krawczuk M., Ostachowicz W.M., Manoach E., Trendafilova I., Shiskina E.V., Palacz M., (2006), *Modern Practice in Stress and Vibration Analysis VI*, P.Keogh, eds., Trans Tech Publications Ltd, Switzerland, **5-6**, 315-322, On Approximate Analytical Solutions for Vibrations in Cracked Plates.

Israr A., Cartmell M.P., Manoach E., Trendafilova I., Ostachowicz W.M., Krawczuk M., Żak A., (2007), Paper accepted for publication in *ASME Journal of Applied Mechanics*, Analytical Modelling and Vibration Analysis of Partially Cracked Rectangular Plates with Different Boundary Conditions and Loading.

LIST OF FIGURES IN APPENDICES

Figure B-1: Three stages of ABAQUS/CAE analysis B-1

Figure B-2: Components of the main menu B-3

Figure B-3: The ABAQUS/CAE file environment..... B-6

Figure D-1: Schematic view of the instruments used D-2

CONTENT OF APPENDICES

LIST OF FIGURES IN APPENDICES A-1

CONTENT OF APPENDICES A-2

APPENDIX A A-3

SPECIALISED CODE WRITTEN IN *MATHEMATICA*™ A-3

A.1 Numerical Integration A-3

A.2 Plotting of Poincaré Map A-3

A.3 Plotting of Time plots and Phase planes A-4

APPENDIX B B-1

FINITE ELEMENT ANALYSIS B-1

B.1 Stages of ABAQUS/CAE B-1

B.1.1 Pre-processing B-1

B.1.2 Simulation (ABAQUS /Standard or ABAQUS /Explicit) B-2

B.1.3 Post-processing B-2

B.2 Main Components of ABAQUS/CAE B-2

B.3 The ABAQUS/CAE File Environment B-5

APPENDIX C C-1

***DYNAMICS 2* COMMANDS C-1**

C.1 Numerical Explorations Menu C-1

C.2 Plotting C-2

C.3 Storing Data C-2

C.4 Bifurcation Plotting Commands C-2

C.5 Lyapunov Commands C-2

APPENDIX D D-1

LIST OF INSTRUMENTS - EXPERIMENTAL WORK D-1

APPENDIX A

SPECIALISED CODE WRITTEN IN *MATHEMATICA*™

A.1 Numerical Integration

$$eqn = \psi''_{mn}[t] + \mu * \psi'_{mn}[t] + (\omega_{mn})^2 * \psi_{mn}[t] + \beta_{mn} * (\psi_{mn}[t])^3 - \frac{\lambda_{mn} * p * \cos[\Omega * t]}{D}$$

```
system= NDSolve[{eqn == 0, ψ[0]==0,
ψ'[0] ==0}, {ψ} ,{t,0,50),MaxSteps → Infinity,
AccuracyGoal → Automatic, PrecisionGoal → Automatic, WorkingPrecsion → 20]

Plot[Evaluate[ψ[t] /.system],{t,0,50},Frame → True,FrameTicks → Automatic,
GridLines → Automatic,FrameLabel → {Time, ψ[t] }]

Plot[Evaluate[ψ'[t] /.system],{t,0,50},Frame → True,FrameTicks → Automatic,
GridLines → Automatic,FrameLabel → {Time, ψ'[t] }]
```

A.2 Plotting of Poincaré Map

```
Poincare[Ω_,C1_,C2_,C3_,rho_,ndrop_,nplot_]:=(T=2*π/Ω;g[{xold_,yold_}]:=
{x[T],y[T]}/.NDSolve[{y'[t]==-C2*x[t]-C3*x[t]^3C1*y[t]+rho*Cos[Ω*t],x'[t]==y[t],
x[0]==xold,y[0]==yold},{x,y},{t,0,T},Method→StiffnessSwitching,
MaxSteps→Infinity,WorkingPrecision→32][[1]];

lp=ListPlot[Drop[NestList[g,{0,0},nplot+ndrop],ndrop],PlotRange→All,
Frame→True,AxesOrigin→{0.00105,-0.28},DisplayFunction→Identity]);

Show[lp,DisplayFunction→$DisplayFunction]
```

For the case of SSSS boundary condition

Poincare[192.543,0.16,37072.8,3.96872*10^8,2.56708,200,15000];

A.3 Plotting of Time plots and Phase planes

{Ω,C1,C2,C3,rho}={192.543,0.16,37072.80,3.96872*10^8,9050}

solution[tmax_]:=NDSolve[{y'[t]==-C2*x[t]-C3*x[t]^3-C1*y[t]+rho*Cos[Ω*t],
x'[t]==y[t],x[0]==0,y[0]==0},{x,y},{t,49.5,tmax},Method→StiffnessSwitching,
MaxSteps→Infinity,WorkingPrecision→32];

sol1=solution[50];

For time plots

graph1[tmin_,tmax_]:=Plot[Evaluate[x[t]/.sol1],{t,tmin,tmax},Frame→True];

graph1[49.5,50];

For phase planes

graph[tmin_,tmax_]:=ParametricPlot[Evaluate[{x[t],y[t]}/.sol1],{t,tmin,tmax}
,AxesStyle→{AbsoluteThickness[1]},Frame→True];

graph[49.5,50];

APPENDIX B

FINITE ELEMENT ANALYSIS

B.1 Stages of ABAQUS/CAE

A complete ABAQUS/CAE analysis usually consists of three distinct stages which includes pre-processing, simulation, and post-processing. These three stages are linked together by files as shown in Figure A-1.

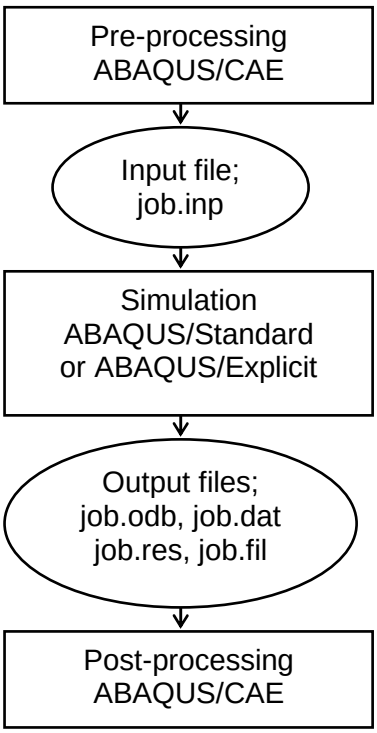

Figure B-1: Three stages of ABAQUS/CAE analysis

B.1.1 Pre-processing

In pre-processing, the model of the physical problem is defined and creates an ABAQUS input file. The model is usually created graphically using ABAQUS/CAE or another pre-processor, although the ABAQUS input file for a simple analysis can be created directly using a text editor.

B.1.2 Simulation (ABAQUS /Standard or ABAQUS /Explicit)

The simulation, which normally is run as a background process, is the stage in which ABAQUS/Standard or ABAQUS/Explicit solves the numerical problem defined in the model. Examples of output from a stress analysis include displacements and stresses that are stored in binary files ready for post-processing. Depending on the complexity of the problem being analyzed and the power of the computer being used, it may take anywhere from seconds to days to complete an analysis run.

B.1.3 Post-processing

In post-processing, the results can be evaluated once the simulation has been completed and the displacements, stresses, or other fundamental variables have been calculated. The evaluation is generally done interactively using the Visualization module of ABAQUS/CAE. The Visualisation module, which reads the neutral binary output database file, has a variety of options for displaying the results, including colour contour plots, animations, deformed shape plots, and X–Y plots.

The ABAQUS/CAE is the complete environment that provides a simple, consistent interface for creating models, interactively submitting and monitoring jobs, and evaluating results from simulations. ABAQUS/CAE is divided into modules, where each module defines a logical aspect of the modelling process, for example, defining the geometry, defining material properties, and generating a mesh. When the model is complete, ABAQUS/CAE generates an input file that is submitted to the ABAQUS analysis product. The input file can also be created manually.

B.2 Main Components of ABAQUS/CAE

Figure A-2 shows the components that appear in the main window. These components are:

Title bar — It indicates the version of ABAQUS/CAE that runs and the name of the current model database.

Menu bar

The menu bar contains all the available menus. This menu gives access to all the functionality in the product. Different menus appear in the menu bar depending on which module selected from the context bar.

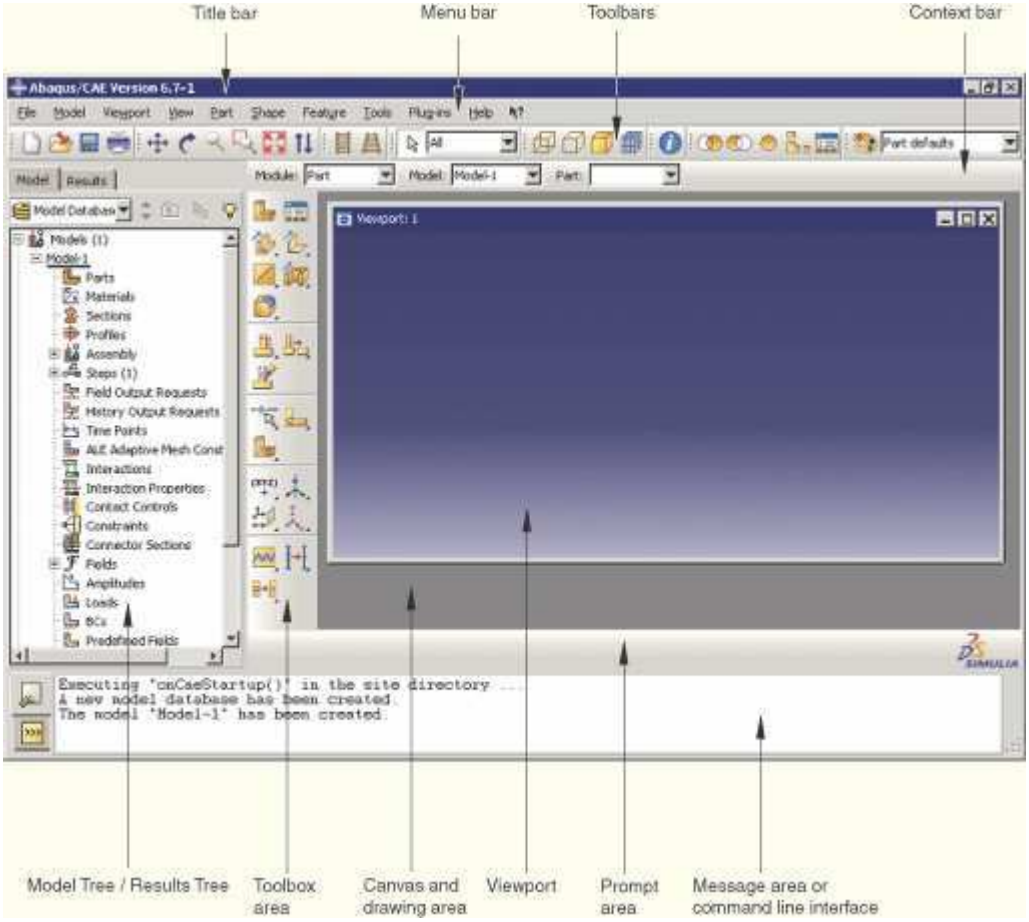

Figure B-2: Components of the main menu

Toolbars

The toolbars provide quick access to items that are also available in the menus.

Model Tree

The model tree provides with a graphical overview of the model and the objects that it contains, such as parts, materials, steps, loads, and output requests. In addition, it also provides a convenient, centralized tool for moving between modules and for managing objects. If model database contains more than one model, the model tree can

be used to move between models.

Results Tree — The results tree provides with a graphical overview of output databases and other session-specific data such as X–Y plots. If we have more than one output database open in successive session, the results tree to move between output databases.

Toolbox area — The toolbox area displays tools in the toolbox that are appropriate for that module. The toolbox allows quick access to many of the module functions that are also available from the menu bar.

Canvas and Drawing area — The canvas can be thought of as an infinite screen or bulletin board on which we post viewports. The drawing area is the visible portion of the canvas.

Viewport — Viewports are windows on the canvas in which ABAQUS/CAE displays model.

Prompt area — It displays instructions to follow during a procedure; for example, it asks to select a point in the part geometry.

Message area — It prints status information and warnings in the message area. To resize the message area, drag the top edge; to see information that has scrolled out of the message area, use the scroll bar on the right side. The message area is displayed by default, but it uses the same space occupied by the command line interface. If the command line interface has been recently used, click the tab in the bottom left corner of the main window to activate the message area.

Command line — Command line interface is used to type Python commands and

interface — evaluate mathematical expressions using the Python interpreter that is built into ABAQUS/CAE. The interface includes primary (>>>) and secondary (...) prompts to indicate when we must indent commands to comply with Python syntax. The command line interface is hidden by default, but it uses the same space occupied by the message area. Click the tab in the bottom left corner of the main window to switch from the message area to the command line interface. Click the tab to return to the message area.

A completed model contains everything that needs to start the analysis. ABAQUS/CAE uses a model database to store models. When ABAQUS/CAE starts, the Start Session dialog box allows creating a new, empty model database in memory. After the start of ABAQUS/CAE, the model database can be saved to a disk by selecting File Save from the main menu bar and for retrieving a model database from a disk, select File Open.

B.3 The ABAQUS/CAE File Environment

During execution the system creates both temporary and permanent files, the exact number of which depends upon the instructions contained in the .inp file. For nonlinear problems, the analysis is broken down into a number of steps, each of which contains a number of increments, each of which requires a number of iterations to reach a solution. The schematic view of the file environment is shown in Figure A-3.

.dat (‘dat’) — It contains the data echo, the data checking information, information about the progress of the solution and the results. The first three are switched on or off by the *PREPRINT card while the results are controlled by the *EL PRINT and *NODE PRINT cards.

.odb ('o-d-b') — It is the output database, which contains results to be read

in by the Visualisation module of ABAQUS/CAE.

.res ('res') The restart file, containing results to be read back in to ABAQUS itself to continue a nonlinear analysis from where it left off on a previous run. This .res file is generated by a *RESTART card.

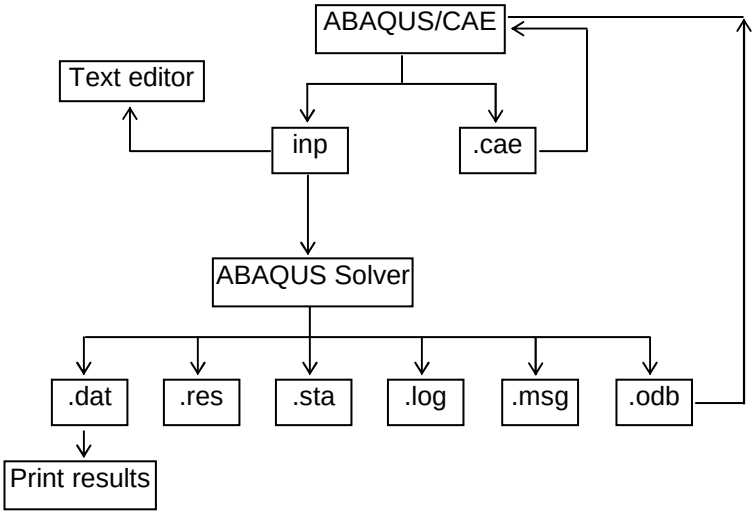

Figure B-3: The ABAQUS/CAE file environment

.sta ('status') It contains a summary of the steps and increments in a nonlinear analysis.

.log ('log') It contains a summary of the system commands invoked during the run together with CPU timing information.

.msg ('message') It contains information on the progress of the run.

The .dat, .sta, .log and .msg files are human-readable. They can be printed but are better scanned with the editor to look for errors beforehand, particularly since the .dat file can be very large. The .odb and .res files are unformatted and so aren't human-readable.

APPENDIX C

DYNAMICS 2 COMMANDS

C.1 Numerical Explorations Menu

T : plot trajectory

DYN : quit & start new map or differential equation

OWN : quit & create own process

P : pause the program

Q : quit dynamics program

BIFM : Bifurcation diagram Menu

BM : Basin of attraction Menu

DIM : Dimension Menu

FOM : Follow (periodic) Menu

LM : Lyapunov exponent Menu

POM : Periodic Orbit Menu

STM : Straddle Trajectory Menu

UM : Unstable and stable manifold Manu

C.2 Plotting

CON : connects consecutive dots

PT : plots time horizontally

SPC : number of differential equation steps in one period of the forcing period

IPP : number of iterates per plot

C.3 Storing Data

DD : Dump Data to disk

FD : retrieve picture from disk

TD : save picture to disk

C.4 Bifurcation Plotting Commands

BIFS : bifurcation plot on the screen

BIFD : number of the dots to be plotted for each parameter

BIFPI : pre-iterates for each parameter

BIFR : specifying range of parameter e.g. rho

BIFV : set number of values of parameter for better picture quality

PRM : parameter to be varied

C.5 Lyapunov Commands

L : sets number of Lyapunov exponents to be computed ($0 \le L \le 2$)

LL : current values of the Lyapunov exponents to be printed on the screen

APPENDIX D

LIST OF INSTRUMENTS - EXPERIMENTAL WORK

The list of the instruments used in this investigation and their schematic views are shown in Figure D-1.

- Power Amplifier–Model PA500L CE
- Electro-dynamic Exciter–LING ATEC Model 407
- Helium Neon Laser Vibrometer–Model Polytech OFV 303 (1 milli watt max/cw)
- Vibrometer Controller–Model Ploytech OFV3001 (100/115/230v- 50/60Hz)
- Spectrum Analyser–Model HP 3582A
- Function Generator 2Mhz–Model TG215
- Oscilloscope 20Mhz–Model ISO-Tech ISR 622
- Force Transducer IEPE – Model 8230

(a) Power Amplifier

(b) Electro-dynamics Exciter

(c) He-Ne Laser Vibrometer

(d) Vibrometer Controller

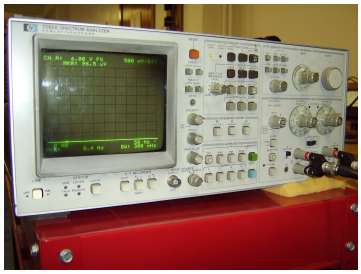

(e) Spectrum Analyser

(f) Function Generator

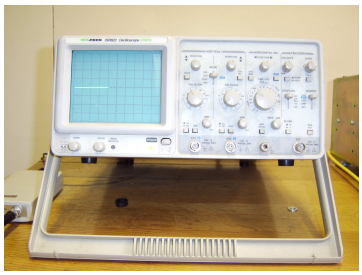

(g) Oscilloscope

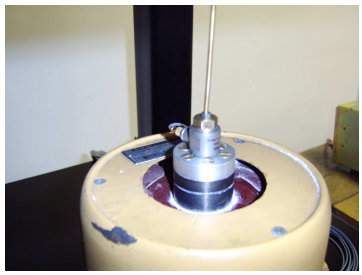

(h) Force Transducer

Figure D-1: Schematic view of the instruments used